

Department of Earth and Environmental Sciences

PhD program in Chemical, Geological and Environmental Sciences - Cycle XXXVIII

Curriculum in Terrestrial and Marine Environmental Sciences

CHARACTERIZATION OF THE ENVIRONMENTAL QUALITY OF URBAN GREEN AREAS AND ANALYSIS OF AN URBAN REGENERATION PROJECT BY MEANS OF ECOACOUSTICS

Surname: Potenza

Name: Andrea

Registration number: 816595

Tutor: Prof. Antonio Finizio

Supervisor: Prof. Giovanni Zambon

Coordinator: Prof. Marco Giovanni Malusà

ANNO ACCADEMICO / ACADEMIC YEAR 2023 / 2024

This page is intentionally left blank

Content

Abstract	pag. 4
Ch. 1: General Introduction	pag. 7
Ch. 2: Biases in Ecoacoustics Analysis: A Protocol to Equalize Audio Recorders	pag. 23
Ch 3: Preliminary Results On Audio Event Classification Applied To A University Square In Milan (Italy) Before An Urban Regeneration Project	pag. 65
Ch. 4: Ecoacoustic Monitoring of a Regenerated University Square and Two Urban Parks: a Multidisciplinary Approach Using Ecoacoustic Indices, Sound Events Classification and BirdNET	pag. 79
Thesis conclusions	pag. 145

Abstract

Noise pollution is a worldwide environmental issue and in Europe is the second cause of premature death after air pollution. In 2025, nearly 112 million people were subjected to long-term noise levels which can produce annoyance, sleep disorders and increased stress and can contribute to cardiovascular and metabolic diseases, mental health disorders and even premature deaths.

Also fauna is affected by noise pollution. It causes the same effects as on humans and in addition causes a decrease in their fitness and changes in territorial behaviours thus leading to populations' reduction and overall biodiversity decrease.

For these reasons, it is fundamental to control and reduce noise pollution and protect the few quiet areas still present. Urban green areas could serve as refugees against noise pollution and at the same time should be safeguarded against noise. In recent years, municipalities are carrying out regeneration activities increase green areas by substituting asphalt zones rethinking the cities as inhabited by people and not by vehicles. These projects are carried out to reduce the heat island effect, improve areas' quality and beauty and people's perception and use of public places. Milan (Italy) is one of the European cities where these projects are taking place.

In this changing urban environment ecoacoustics can play an important role. It is a branch of acoustics focusing on assessing the environmental quality and biodiversity of the sonic environment and monitoring ecosystems to detect changes in human presence and disturbance and faunal behaviours and presence. Ecoacoustics employs indices and machine learning techniques to describe the sonoscape.

In this thesis work, the term "sonoscape" is used to address the non-interpreted recorded acoustic information, to avoid confusion with the term "soundscape" which is acoustic environment as perceived, experienced and/or understood by a person or people, in context.

Both ecoacoustic indices and machine learning algorithms are employed in this research project to study an urban regeneration project and two green areas in Milan. In particular, ecoacoustic indices are applied considering the dynamism of the urban sonoscape, BirdNET is used to assess avian richness and a sound events classifier have been developed to

characterize the sonoscape of one of these areas. Above these studies, a method to monitor sonoscapes using different typologies of recording devices while limiting the biases introduced by different frequency responses, sensitivities and amplitude gains is developed.

The three studied areas are the square “Piazza della Scienza” of Milano-Bicocca University, the Regional Park “Parco Nord” located in the northern outskirts of Milan and the pocket park “Vivarium-Bicocca”. Specifically, Piazza della Scienza underwent an urban regeneration process consisting in the substitution of its cemented pavement with green spaces; the ecoacoustic monitoring took place before and after the intervention.

The thesis goals are: a) produce a protocol to equalize audio recordings to reduce biases in indices calculations and comparison between different devices, b) investigate the ecoacoustics changes induced by this regeneration project, which can be extended to any other urban requalification projects, c) characterize the sonoscape quality of these three areas’ to understand if the Piazza sonoscape after the intervention is similar to the one of urban parks.

The equalization protocol was developed to linearize the frequency response of audio recorders by comparing white noise recordings carried out in an anechoic chamber by Song Meter Micros, Audiomoths and Soundscape Explorer Terrestrial with a class 1 sound level meter. The bias reduction was tested by calculating and comparing the eight most common ecoacoustic indices. Statistically significant improvements were assessed on white noise recordings and in field recordings. The MATLAB script was published in an open-access journal. All the recordings carried out in this thesis were equalized following that protocol.

Seven ecoacoustic indices, a custom-made machine learning classifier and BirdNET were employed to characterize the Piazza sonoscape. Moreover, a linear mixed-effects model was employed to address the effect of species richness, birds’ and five sound classes’ presence on ACI (Acoustic Complexity Index). During the analysis, the indices parameters were calculated on the Piazza’s background noise and the minimum frequency for ADI (Acoustic Diversity Index) and AEI (Acoustic Evenness Index) and maximum frequency for H (Acoustic Entropy) and ZCR (Zero-Crossing Rate) were introduced. The machine learning classifier consisted of a Random Forest model trained using 10-fold cross-validation and default hyperparameters values; precision, recall and F1-score were used for validation. Finally, BirdNET parameters were tested to get the best precision and recall possible.

The study demonstrated that Piazza post-operam sonoscape is dissimilar to the ante-operam, being more complex and acoustically variate, with a changed contribution of sound sources (such as speech, birds, insects and road traffic) and an increased avian richness and more temporal distributed vocalization rates. The linear-regression model confirmed the change in ACI and a relationship between ACI and avian richness, birds' and human speech presence.

The equalization protocol was implemented since the monitoring of Piazza della Scienza and Vivarium-Bicocca were carried out using Song Meter Micros while Parco Nord employed Audiomoth. The three areas comparison was carried out using five ecoacoustic indices (ACI, ADI, AEI, H, ZCR) alongside BirdNET. It established that the Piazza post-operam sonoscape is similar to the urban parks' ones. In particular, the Piazza measurement sites located on the ground floor and courtyards (where the depaving and greening took place) were similar to the parks' site while the sites located at the first floor of the buildings did not change probably because of the more impact of the ventilation systems located on the building roofs and the less influence of the changed signals originated in the square. These findings prove that relatively low-impact interventions, such as pavement removal and trees and bushes increase, can significantly influence urban sonoscapes.

In conclusion, this thesis work proposes a methodology to compare ecoacoustics recordings from different devices, a topic poorly studied nowadays and which could help fill knowledge gaps in the comprehension of ecoacoustic indices and BirdNET studies. Moreover, it demonstrated the improvement of Piazza della Scienza sonoscape after the urban regeneration project and its shift towards a park-like sonoscape. In this view, ecoacoustics emerges as a monitoring tool and decision-support device for urban planning and climate adaptation policies, fostering an evidence-based dialogue between environmental science, urban design, and public governance.

Chapter 1

General introduction

1.1. Overview

In 2025, the “Environmental noise in Europe” report [1] estimates that approximately 112 million people (circa 20% of the European population) are exposed to long-term noise levels from transport sources that exceed the thresholds set by the Environmental Noise Directive [2] of 55 dBA during the day-evening-night period (Lden). According to the latest scientific research, noise-related health issues occur even at lower Lden thresholds. Thus, considering these lower levels, the estimated affected population rises to 150 million people (more than 30% of the population).

These data must be taken into consideration because noise can cause annoyance, sleep disorders and increased stress, leading to inflammation and oxidative stress, which contribute to cardiovascular and metabolic diseases, mental health disorders and even premature deaths. In 2021 in Europe, 66,000 premature deaths were linked to long-term exposure to transport noise, while 50,000 new cases of cardiovascular diseases occurred alongside 22,000 new cases of type 2 diabetes. Thus, noise pollution sets behind air pollution and temperature-related (climatic) factors in terms of environmental health threats. Furthermore, it has a higher health impact than second-hand smoke or lead exposure [1].

Noise pollution affects not only humans but also impacts biodiversity significantly, influencing behavioural, physiological, communication and sensory perception processes [1]. These effects are present because many species rely on sound for communication, navigation and detecting predators or prey, thus noise can interfere with these activities, leading to changes in foraging, mating or population distribution [3, 4, 5, 6]. Moreover, just like for humans, long term exposure to noise can induce physiological stress, causing elevated heart rates, hormonal imbalances and weakened immune responses, which can impact overall health and fitness and territorial behaviours [7, 8, 9]. On a higher scale level, alterations in species behaviour, distribution and community dynamics can produce a cascading effect on ecosystems health [10] and their biodiversity and resiliency to other types of disturbances.

On this last topic, EU legislation does not explicitly protect terrestrial ecosystems and species from noise [1]. Indeed, the Environmental Noise Directive is primarily focused on mitigating human health noise impacts and does not address the issue on wildlife. To improve people’s health and offer places with lower noise pollution, the Directive promotes

the preservation of “quiet areas” to maintain a good acoustic quality of the European soundscape. These areas can have benefits for people due to their lower noise pollution and, for this reason, they can also potentially protect terrestrial biodiversity [1]. These “quiet areas” are divided in two main groups depending on their location: “quiet area in an agglomeration” and “quiet area in open country”.

There are many definitions of “quiet area”. It can be seen as an area characterized by a pleasant soundscape and where noises are absent or non-dominant and are safe and clean and possess a pleasant view like with green space or water [1]. The Italian legislation describes the “urban quiet area” in the Decree of the Director of the Directorate-General for Environmental Assessments No. 16 of 24 March 2022 as a public use area with an extension of at least 3000 smq with an Lden not superior of 55 dB(A) and an acoustic class inferior at the IV.

When these areas will be defined, they will serve as restoring areas both for people and fauna.

1.1.1. Why green urban areas?

Generally speaking, green areas produce benefits to cities and their population and fauna.

The presence and use of green spaces by people are associated with many health benefits such as mood improvement, stress and anxiety reduction and overall mental well-being enhancement [11, 12, 13, 14, 15]. Moreover, it has been observed that exposure to natural environments improves the attention span and reduces the mental fatigue [16, 17] while blooming the sense of belonging and the aesthetic pleasure [18]. Finally, as an indirect effect on people, the presence and accessibility to green areas prevents the manifestation of chronic diseases (such as cardiovascular diseases and obesity) by encouraging outdoor physical activity [19, 20].

Focusing on fauna, green areas may serve as nesting areas, refugees and resting areas during the migration routes and generally improve cities biodiversity. Moreover, larger green space structures (such as green belts, green corridors or urban woodlands) provide a greater ecological connection between larger or fragmented areas and spread the social and recreational services to the urban communities [21].

Finally, they can reduce the water run-off by absorbing water in soil and vegetation, shading from the sun providing thermal comfort and heat diffusion through evapotranspiration [22, 23, 24], and mitigate air pollutants thanks to vegetation photosynthesis and plant-associated microbiomes [25].

These ecosystem services provided by green spaces are not linked to the acoustic classification of the area as “quiet” since the definition of “quiet area” is linked to finding spaces which can further improve human health thanks to the 55 dB(A) Lden threshold limit. Environmental benefits are always present thanks to the soil and vegetation intrinsic properties. Nonetheless, classifying a green space as a “quiet area” is useful since the classification increases the area’s importance, protection and safeguarding measures because that area generates higher benefits than a “non-quiet” area.

A problem underlined by the EEA is that quiet areas must also be uniformly distributed to allow access to all populations that should be ideally located at around 400 m walk from them. This critique can be extended also to green public spaces. To improve the accessibility, cities could protect the existing green spaces by maintaining and promoting their good acoustic quality or increasing the number of green areas within the city. Of course, in high density urban cities, the application of mitigation measures is limited due to the population being located near major noise sources [1].

1.2. Green areas in Milan

The city of Milan, Lombardy region county seat in the north of Italy, is the second city in Italy per surface (behind Rome) and presents 75 green areas (54 parks and 21 gardens) covering 13% of the city area. The most extended ones are Parco Nord (3.200.000 sqm) and Parco Forlanini (1.627.000 sqm).

The parks development in Milan is linked to the city's history [26]. The oldest park is Parco Indro Montanelli built in 1784. Sempione Park, set in the city centre beside Sforzesco Castle, was inaugurated at the end of the 19th century on the military area surrounding the Castle. Parco Pallavicino and Parco Don Giussani were constructed in the 1930s on the former railway station of Scalo Sempione. Parco Monte Stella and Collina dei Ciliegi are two hillside

parks built respectively as storage for city ruins after the World War II bombings (1950s) and for Pirelli industries demolished buildings in 2007. The second widest park, Parco Forlanini, located in the east outskirts was inaugurated in 1970 to enhance the centuries-old structure of the Lombardy countryside. The first widest park, Parco Nord, located in the north-west outskirts was established on a former military airport and Breda factory brownfield areas.

In the last five years, Milan has increased its green spaces by 340.000 sqm and 367.000 sqm of new green areas are currently being planned [27]. Some of these interventions are linked to urban regeneration strategies which are not new for the city [28, 29] but have boosted in recent times [30], leading to the publication of the Atlas of Urban Regeneration in June 2025, which contains over 100 projects of urban renewal for areas with a surface cover of more than 5'000 sqm.

The urban restoration interventions that shaped today's view of the city were carried out to mitigate the urban decay problem, improving the social network and the inclusion of vulnerable groups of people while increasing the environmental quality and the economy of those areas [31, 32]. Various strategies can be applied to reach these goals, from tactical urbanism [29, 33] to more urban-modifying actions, such as the construction of Parco Monte Stella and Collina dei Ciliegi or soil de-sealing [34, 35] and areas' renovation.

Soil de-sealing redesign the urban texture that allows many environmental benefits like an improvement in water infiltration and reduction of water run-off and risk of flooding, a reduction of the heat island effect and a promotion of biodiversity [34]. This intervention consists of removing the pavement which seals the soil making it impermeable and replacing it with more heat refractor materials or regenerating the soil profile to improve its permeability. This strategy could serve to meet the European Union targets of zero net loss of urban green space by 2030 and of total increase in urban green space coverage by 2050 [36].

1.3. Study areas

In the fertile urban-evolving environment of Milan, the MUSA (Multilayered Urban Sustainability Action) project planted roots proposing management strategies to face the environmental, social, and economic sustainability challenges of the metropolitan city of Milan. This Action promulgates a new collaboration model between the government sphere and public and private stakeholders, aiming at making it replicable at the national and international scale.

Related to the thesis, MUSA funded the regeneration of the University of Milan-Bicocca's main square (Piazza della Scienza) to reduce the heat island effect, mitigate local air pollution, improve students' life quality and the area's biodiversity. The intervention (Figure 1) consisted of de-sealing, greenery allocation and urban design improvement of the public square. In this stage, different research groups from the three main Milan universities evaluated the changes in the environmental, social and economic compartments.



Figure 1. Piazza della Scienza before (left) and after (right) the MUSA regeneration project.

Two other study areas have been considered as comparison, both near the Bicocca University campus (Figure 2): Vivarium-Bicocca, a pocket park corresponding to a former university vivarium; and Parco Nord, a regional peri-urban park located on the northern outskirts of Milan. These two areas are opposite one another since they are respectively a small park, serving as a proxy for small gardens and neighbourhood green areas, and the most extended Park in Milan.



Figure 2. Map showing the three investigated areas: Parco Nord, Vivarium-Bicocca and Piazza della Scienza.

1.4. Methodology

The thesis focuses on studying green areas and an urban regeneration project by means of ecoacoustics.

Ecoacoustics is a field of study which assesses the environmental quality of acoustic signals and monitors their ecological dynamics and complexity at multiple ecological and temporal scales [37, 38]. The monitoring can comprehend the existence, density, variability, and

diversity of biophonic and anthropophonic sounds and the study of environmental changes, such as anthropogenic impacts and effects of managing and restoring interventions [39].

The discipline employs passive automatic acoustic recordings to record the sound environment. These recordings can be analysed using ecoacoustic indices and machine learning algorithms and programs to detect the presence of soniferous species and of anthropophonies and geophonies. The sound data storage in the recordings containing unclassified acoustic signals to be later interpreted (by an operator, a software) is called sonoscape [40, 41].

Ecoacoustic indices are used as tools to summarize the recording data obtained in ecoacoustic campaigns which can be carried out using multiple recording devices and last days or weeks. These indices are calculated by analysing different sound characteristics, acoustic features, and intensity distributions on frequencies [42] of the recordings. Various indices exist nowadays to allow a comprehensive view of the recorded sonoscape [42, 43, 44, 45] but they still present many drawbacks in terms of interpretability in situ and comparison between studies [46, 47, 48, 49]. In this thesis, a possible solution to limit the biases in the use and comparison of ecoacoustic indices between study areas and scientific research is addressed (Chapter 2).

Another face of ecoacoustics is the use of machine learning software and algorithms to classify and detect the sound events stored in the sonoscape recordings. These tools can be focused on a specific macro class of sound events (biophonies, technophonies, geophonies), on a single sound event or on a broader collection of sounds. This side of ecoacoustics relies on the interpretability of the results to address important environmental and ecological challenges like the monitoring of animal presence and migratory routes [50, 51], and the presence of anthropogenic sound sources and their impact, and variation in space and time. Using machine learning algorithms that classify and detect directly the sound events, it bypasses the limits of ecoacoustic indices interpretability but it still retains some limitations, like model tuning [52, 53] and detection reliability [54, 51], and difficulties in counting sound sources [54, 55].

In this thesis, these two branches of ecoacoustics are applied to analyse their performance and usefulness on the monitoring of green urban areas. In particular, 7 ecoacoustic indices are being used alongside BirdNET and a customised sound event classifier.

1.5. Research questions

The following subsections highlight the thesis research questions and methodology applied.

The first question regards the effects of a public square regeneration project on its sonoscape in terms of ecoacoustic indices, avian biodiversity, people attendance rates and techniphones detectability. To assess people and technophonies presence, a customized machine learning classifier has been developed in collaboration with the LaSalle University of Barcelona during a 6-months abroad period.

The second question focuses on the comparison of two green areas to Piazza della Scienza to assess how similar their sonoscapes are. The areas are the pocket park Vivarium-Bicocca and the Parco Nord. The comparison involves ecoacoustic indices and BirdNET.

The third question addresses the problem of ecoacoustic indices comparability between areas and studies. The comparison between areas in this thesis is necessary to understand the effects of the MUSA regeneration project on the Piazza, thus an equalization protocol to reduce the biases between acoustic recorders have been developed.

1.6. Dissertation outline

The thesis work is arranged in a compendium of publications. Three scientific papers and a reviewed conference proceeding are used for the compendium. These papers are exposed to create a fluent workflow and answer the research questions.

Additionally, as a complementary material regarding the urban regeneration project on Piazza della Scienza, a paper regarding the analysis of the human perceived soundscape of the square before and after the regeneration project is presented at the end of the dissertation.

The dissertation is arranged in the following chapters:

Chapter 2. “Biases in Ecoacoustics Analysis: A Protocol to Equalize Audio Recorders”, addresses a gap in the ecoacoustic indices comparison literature focusing on how the use of different typologies of recorders and their non-linear frequency response can introduce a bias in the confrontation of the indices and on the sonoscape. This chapter is the first step of the dissertation because all recordings used in the thesis are equalized to get a linear frequency response curve and to allow a more stable confrontation between the three green areas and the different recorders typologies employed. This paper has been published in the journal *Sensors*.

Chapter 3. “Preliminary results on audio event classification applied to a university square in Milan (Italy) before an urban regeneration project”, show the results of the customised sound event classifier built to analyse the sonoscape of Piazza della Scienza and acquire information about sound events. This classifier has been built to bypass the aural analysis of a single measurement day and classify the whole measurement campaign. The results shown here are preliminary but the workflow and logical passages are important to understand the final classifier explained and used in Chapter 4. This chapter is a *Forum Acusticum* conference proceeding which has been reviewed and published.

Chapter 4. “Ecoacoustic monitoring of a regenerated university square and two urban parks: a multidisciplinary approach using ecoacoustic indices, sound events classification and BirdNET”, report the results of the Piazza della Scienza monitoring comparing the ante and post-opera scenarios and describing the effects and efficacy of the project on the square’s sonoscape. Moreover, the sonoscape characterization of two urban green areas (Vivarium-Bicocca and Parco Nord) and their comparison with the ante and post-opera sonoscape of Piazza della Scienza is carried out to assess the effects of the regeneration project. The analysis has been carried out employing ecoacoustic indices, the BirdNET analyser to assess avian species richness and the customized classifier to acquire people’s presence through their speech and technophonies, biophonies and geophonies presence. This article is about to be submitted.

Conclusions. Concludes the thesis dissertation by summarizing the main contributions of the work, discussing the main findings and explaining some possible future research works.

References

1. "Environmental noise in Europe 2025", Publications Office of the European Union (Luxembourg), 2025, ISBN: 978-92-9480-718-2, doi:10.2800/1181642
2. European Parliament, Council of the European Union (2002). "Directive 2002/49/EC relating to the assessment and management of environmental noise"
3. Luo, J., Siemers, B. M., & Koselj, K. (2015). How anthropogenic noise affects foraging. *Global Change Biology*, 21(9), 3278-3289.
4. Derryberry, E. P., Phillips, J. N., Derryberry, G. E., Blum, M. J., & Luther, D. (2020). Singing in a silent spring: Birds respond to a half-century soundscape reversion during the COVID-19 shutdown. *Science*, 370(6516), 575-579.
5. Bent, A. M., Ings, T. C., & Mowles, S. L. (2021). Anthropogenic noise disrupts mate choice behaviors in female *Gryllus bimaculatus*. *Behavioral Ecology*, 32(2), 201-210.
6. Chou, T. L., & Gall, M. D. (2025). I can't hear you: effects of noise on auditory processing in mixed-species flocks. *Journal of Experimental Biology*, 228(10), jeb250033.
7. Zaffaroni-Caorsi, V., Both, C., Márquez, R., Llusia, D., Narins, P., Debon, M., & Borges-Martins, M. (2023). Effects of anthropogenic noise on anuran amphibians. *Bioacoustics*, 32(1), 90-120.
8. Meillère, A., Buchanan, K. L., Eastwood, J. R., & Mariette, M. M. (2024). Pre-and postnatal noise directly impairs avian development, with fitness consequences. *Science*, 384(6694), 475-480.
9. Francis, C. D., & Barber, J. R. (2013). A framework for understanding noise impacts on wildlife: an urgent conservation priority. *Frontiers in Ecology and the Environment*, 11(6), 305-313.
10. Phillips, J. N., Termond, S. E., & Francis, C. D. (2021). Long-term noise pollution affects seedling recruitment and community composition, with negative effects persisting after removal. *Proceedings of the Royal Society B*, 288(1948), 20202906.

11. White, M. P., Alcock, I., Grellier, J., Wheeler, B. W., Hartig, T., Warber, S. L., ... & Fleming, L. E. (2019). Spending at least 120 minutes a week in nature is associated with good health and wellbeing. *Scientific reports*, 9(1), 7730.
12. Bratman, G. N., Anderson, C. B., Berman, M. G., Cochran, B., De Vries, S., Flanders, J. & Daily, G. C. (2019). Nature and mental health: An ecosystem service perspective. *Science advances*, 5(7), eaax0903.
13. Bratman, G. N., Hamilton, J. P., & Daily, G. C. (2012). The impacts of nature experience on human cognitive function and mental health. *Annals of the New York academy of sciences*, 1249(1), 118-136.
14. Hunter, M. R., Gillespie, B. W., & Chen, S. Y. P. (2019). Urban nature experiences reduce stress in the context of daily life based on salivary biomarkers. *Frontiers in psychology*, 10, 413490.
15. Bowler, D. E. (2010). Green spaces affect emotional wellbeing more than physiology. *Nursing Standard*, 25(4), 17.
16. Ohly, H., White, M. P., Wheeler, B. W., Bethel, A., Ukoumunne, O. C., Nikolaou, V., & Garside, R. (2016). Attention Restoration Theory: A systematic review of the attention restoration potential of exposure to natural environments. *Journal of Toxicology and Environmental Health, Part B*, 19(7), 305-343.
17. Berman, M. G., Jonides, J., & Kaplan, S. (2008). The cognitive benefits of interacting with nature. *Psychological science*, 19(12), 1207-1212.
18. Barragan-Jason, G., Loreau, M., de Mazancourt, C., Singer, M. C., & Parmesan, C. (2023). Psychological and physical connections with nature improve both human well-being and nature conservation: A systematic review of meta-analyses. *Biological Conservation*, 277, 109842.
19. Mytton, O. T., Townsend, N., Rutter, H., & Foster, C. (2012). Green space and physical activity: an observational study using Health Survey for England data. *Health & place*, 18(5), 1034-1041.

20. Bedimo-Rung, A. L., Mowen, A. J., & Cohen, D. A. (2005). The significance of parks to physical activity and public health: a conceptual model. *American journal of preventive medicine*, 28(2), 159-168.
21. World Health Organization. (2017). Urban green space interventions and health: A review of impacts and effectiveness. *Urban green space interventions and health: a review of impacts and effectiveness*.
22. Demuzere, M., Orru, K., Heidrich, O., Olazabal, E., Geneletti, D., Orru, H., & Faehnle, M. (2014). Mitigating and adapting to climate change: Multi-functional and multi-scale assessment of green urban infrastructure. *Journal of environmental management*, 146, 107-115.
23. Aram, F., García, E. H., Solgi, E., & Mansournia, S. (2019). Urban green space cooling effect in cities. *Heliyon*, 5(4).
24. Murtinová, V., Gallay, I., & Olah, B. (2022). Mitigating effect of urban green spaces on surface urban heat island during summer period on an example of a medium size town of Zvolen, Slovakia. *Remote Sensing*, 14(18), 4492.
25. Grimoldi, R., Gandolfi, I., Petricciuolo, M., Firrincieli, A., Federici, E., Vinciguerra, V., etruccioli, M., Crognale, S. & Franzetti, A. (2025). Biodegradation potential of Air Pollutants by Phyllosphere Microbiome in Milan urban Area (Italy). *9th European Bioremediation Conference (EBC-IX) Chania*
26. Mariani, L., Parisi, S. G., Cola, G., Laforteza, R., Colangelo, G., & Sanesi, G. (2016). Climatological analysis of the mitigating effect of vegetation on the urban heat island of Milan, Italy. *Science of the Total Environment*, 569, 762-773.
27. Municipality of Milan. (2025). *Nuovo verde urbano a Milano, dal 2021 creati 340mila metri quadrati*. Comune di Milano. Retrieved January 29, 2026, from <https://www2.comune.milano.it/web/milano-cambia-aria/-/340mila-metri-quadrati-di-nuovo-verde-urbano-creati-a-milano-dal-2021>
28. Trono, A., & Zerbi, M.C. (2002) Milan: the city of constant renewal. *GeoJournal* 58(1):65–72

29. Municipality of Milan. (2025). *Piazze Aperte*. Comune di Milano. Retrieved January 29, 2026, from <https://www.comune.milano.it/aree-tematiche/quartieri/piano-quartieri/piazze-aperte>
30. Municipality of Milan. (2025). Mappa dei progetti di Rigenerazione urbana. Retrieved January 29, 2026, from <https://www.comune.milano.it/argomenti/rigenerazione-urbana/mappa-dei-progetti-di-rigenerazione-urbana>
31. Lee, G. K., & Chan, E. H. (2008). The analytic hierarchy process (AHP) approach for assessment of urban renewal proposals. *Social indicators research*, 89(1), 155-168.
32. Chan, E. H., & Yung, E. H. (2004). Is the development control legal framework conducive to a sustainable dense urban development in Hong Kong?. *Habitat international*, 28(3), 409-426.
33. Frago, L., & Graziano, T. (2021). Public space and the green city: Conflictual narratives of the superblock programme in Poblenou, Barcelona. *Journal of Urban Regeneration & Renewal*, 15(1), 113-128.
34. Vieillard, C., Vidal-Beaudet, L., Dagois, R., Lothode, M., Vade pied, F., Gontier, M., Schwartz, C. & Ouvrard, S. (2024). Impacts of soil de-sealing practices on urban land-uses, soil functions and ecosystem services in French cities. *Geoderma Regional*, 38, e00854.
35. Maienza, A., Ungaro, F., Baronti, S., Colzi, I., Giagnoni, L., Gonnelli, C., Renella, G., Ugolini, F. & Calzolari, C. (2021). Biological restoration of urban soils after de-sealing interventions. *Agriculture*, 11(3), 190.
36. European Commission: Directorate-General for Climate Action, *Going climate-neutral by 2050 – A strategic long-term vision for a prosperous, modern, competitive and climate-neutral EU economy*, Publications Office, 2019, <https://data.europa.eu/doi/10.2834/02074>
37. Farina, A., & Reid, V. (2020). The ecological role of sound in terrestrial and aquatic landscape: theories, methods and applications of ecoacoustics. *Biodiversity*, 21(1), 1-3.
38. Sueur, J., & Farina, A. (2015). Ecoacoustics: the ecological investigation and interpretation of environmental sound. *Biosemiotics*, 8(3), 493-502.

39. Gitau, C., Kettel, E., Abrahams, C., Webala, P. W., & Uzal, A. (2025). The role of ecoacoustics in monitoring ecosystem degradation and restoration. *Restoration Ecology*, 33(8), e70168.
40. Farina, A. (2014). Soundscape ecology. *Principles, Patterns, Methods and Applications*.
41. Farina, A., Eldridge, A., & Li, P. (2021). Ecoacoustics and multispecies semiosis: Naming, semantics, semiotic characteristics, and competencies. *Biosemiotics*, 14(1), 141-165.
42. Benocci, R., Brambilla, G., Bisceglie, A., & Zambon, G. (2020). Eco-acoustic indices to evaluate soundscape degradation due to human intrusion. *Sustainability*, 12(24), 10455.
43. Sueur, J. (2018). Indices for ecoacoustics. In *Sound Analysis and Synthesis with R* (pp. 479-519). Cham: Springer International Publishing.
44. Gibb, R., Browning, E., Glover-Kapfer, P., & Jones, K. E. (2019). Emerging opportunities and challenges for passive acoustics in ecological assessment and monitoring. *Methods in Ecology and Evolution*, 10(2), 169-185.
45. Bradfer-Lawrence, T., Gardner, N., Bunnefeld, L., Bunnefeld, N., Willis, S. G., & Dent, D. H. (2019). Guidelines for the use of acoustic indices in environmental research. *Methods in Ecology and Evolution*, 10(10), 1796-1807.
46. Sethi, S. S., Bick, A., Ewers, R. M., Klinck, H., Ramesh, V., Tuanmu, M. N., & Coomes, D. A. (2023). Limits to the accurate and generalizable use of soundscapes to monitor biodiversity. *Nature Ecology & Evolution*, 7(9), 1373-1378.
47. Llusia, D. (2024). The limits of acoustic indices. *Nature Ecology & Evolution*, 8(4), 606-607.
48. Dröge, S., Martin, D. A., Andriafanomezantsoa, R., Burivalova, Z., Fulgence, T. R., Osen, K., ... & Kreft, H. (2021). Listening to a changing landscape: Acoustic indices reflect bird species richness and plot-scale vegetation structure across different land-use types in north-eastern Madagascar. *Ecological Indicators*, 120, 106929.

49. Luna-Naranjo, D., Martinez-Vargas, J. D., Sánchez-Giraldo, C., Daza, J. M., & López, J. D. (2024). Quantifying and mitigating recorder-induced variability in ecological acoustic indices. *Ecological Informatics*, 82, 102668.
50. Eldesoky, A. H., Gil, J., Kindvall, O., Stavroulaki, I., Jonasson, L., Bennett, D., Yang, W., Martinez Diaz, A.F., Lichter, R., Petrou, F. & Pont, M. B. (2025). A bird species occurrence dataset from passive audio recordings across dense urban areas in Gothenburg, Sweden. *Scientific Data*, 12(1), 1180.
51. Bick, I. A., Bakkestuen, V., Cretois, B., Hillier, B., Kålås, J. A., Pedersen, M., Raja, K., Rosten, M.C., Somveille, M., Stokke, G.B., Wiel, J. & Sethi, S. S. (2024). National-scale acoustic monitoring of avian biodiversity and phenology. *bioRxiv*, 2024-05.
52. Wood, C. M., & Kahl, S. (2024). Guidelines for appropriate use of BirdNET scores and other detector outputs. *Journal of Ornithology*, 165(3), 777-782.
53. Tseng, S., Hodder, D. P., & Otter, K. A. (2025). Setting BirdNET confidence thresholds: species-specific vs. universal approaches. *Journal of Ornithology*, 1-13.
54. Navine, A. K., Denton, T., Weldy, M. J., & Hart, P. J. (2024). All thresholds barred: direct estimation of call density in bioacoustic data. *Frontiers in Bird Science*, 3, 1380636.
55. Marques, T. A., Thomas, L., Martin, S. W., Mellinger, D. K., Ward, J. A., Moretti, D. J., Harris, D. & Tyack, P. L. (2013). Estimating animal population density using passive acoustics. *Biological reviews*, 88(2), 287-309.

Chapter 2

Biases in Ecoacoustics Analysis:

A Protocol to Equalize Audio Recorders

Andrea Potenza, Valentina Zaffaroni-Caorsi, Roberto Benocci, Giorgia Guagliumi, Jalal M. Fouani, Alessandro Bisceglie and Giovanni Zambon

Sensors, **24** (14), 4642

doi: <https://doi.org/10.3390/s24144642>

Abstract

Ecoacoustic indices allow us to rapidly evaluate habitats and ecosystems and derive information about anthropophonic impacts. However, it is proven that indices' values and trends are not comparable between studies. These incongruences may be caused by the availability on the market of recorders with different characteristics and costs. Thus, there is a need to reduce these biases and incongruences to ensure an accurate analysis and comparison between soundscape ecology studies and habitat assessments. In this study, we propose and validate an audio recording equalization protocol to reduce ecoacoustic indices' biases, by testing three soundscape recorder models: Song Meter Micro, Soundscape Explorer Terrestrial and Audiomoth. The equalization process aligns the signal amplitude and frequency response of the soundscape recorders to those of a type 1 level meter. The adjustment was made in MATLAB R2023a using a filter curve generated comparing a reference signal (white noise); the measurements were performed in an anechoic chamber using 11 audio sensors and a type 1 sound level meter (able to produce a .WAV file). The statistical validation of the procedure was performed on recordings obtained in an urban and Regional Park (Italy) assessing a significant reduction in indices' biases on the Song Meter Micro and Audiomoth.

2.1 Introduction

The production of pocket digital recorders in the past few decades allowed researchers and amateurs to record many hours of environmental noise and sounds [1]. These recorders along with mobile phones have been implemented by researchers into their work and nowadays are used in various acoustic research branches (e.g., noise mapping [2,3], soundscape assessments [4,5,6,7], bio-acoustics research and sound event detection through machine learning [8,9]).

This study focuses on an equalization procedure to reduce biases in the comparison of audio recorders which can be used in all the disciplines mentioned before. However, in this study, the evaluation of the procedure will be carried out focusing on soundscape ecology given the authors' main field of research (soundscape ecology). Therefore, the term "soundscape" will be used in the terms of this discipline from here on.

Soundscape ecology studies witnessed remarkable growth in the past few decades [10] thanks to new technologies that allowed for the production of different autonomous passive recorders [11]. These developments boosted the investigation of soundscape environments (terrestrial and maritime) and the role of anthropogenic noise on habitat degradation and biodiversity loss.

The exploration of soundscapes involves the application of passive acoustic monitoring (PAM), a method that entails deploying recording devices in the studied area and retrieving them after days or weeks. PAM serves various purposes, from monitoring a particular taxon to recording sounds in a specific environment [11]. To achieve this, researchers employ terrestrial recorders with specific characteristics like sensitivity, frequency response, dynamic range and bandwidth limits. The analysis of recordings relies mainly on ecoacoustic indices [12,13,14] which allow for summarizing the audio information and classifying soundscapes by analyzing their pitch, saturation and amplitude. This process involves confronting time steps or frequency bins to discern patterns and variations [14]. Soundscape monitoring can be carried out in different spatial designs using a regular grid of devices or arrays of sensors operating in tandem [11,15]. While the majority of studies use one to three recorders, a minority deploy more than ten instruments in the field [15,16,17,18]. Given these monitoring spatial designs, the use of all available devices, regardless of the manufacturers, is an attractive strategy to expand the study area at reduced costs.

The main challenge of this wide array of available recording instruments lies in the potential introduction of biases since recorders of different brands will mostly produce audio files with diverse properties when exposed to the same soundscape (i.e., amplitude values over the spectrum). Moreover, these biases can also be present in devices of the same brand and model due to the inherent uncertainty in sensitivity and frequency response. For these reasons, comparing sound pressure levels (SPLs) or ecoacoustic indices' values between recordings made with instruments located in different parts of a forest or different habitats can be problematic. Even when using a single-sensor model, these biases persist due to manufacturing variability, as assessed in [16] and declared by manufacturers in their user guides (i.e., sensitivity uncertainty range). The bias increases when different models are employed due to frequency response differences, wider sensitivity ranges, dynamic range and bandwidth limits. Furthermore, these biases may cause incongruities in indices' values and trends if the comparison is performed between different areas using different recorders [19,20,21]. In fact, previous studies have evidenced that differences in the frequency response led to conflicting conclusions when using indices as proxies for biodiversity or soundscape characteristics [22]. Furthermore, it is common to observe a non-correspondence between ecoacoustic indices' trends, like ACI values [19] in studies that compare ecoacoustic indices across different regions or of different habitats. In [21], Sethi and colleagues analyzed four diverse datasets (temperate forest in the USA, rainforest in Malaysia, agricultural tea landscape in Taiwan and grassland in India) investigating the correlation between acoustic features (i.e., convolutional neural network and 60 soundscape indices) and avian species richness. The calculated indices also included the acoustic complexity index (ACI), the acoustic diversity index (ADI), the bio-acoustic index (BI), the normalized difference soundscape index (NDSI) and the temporal and spectral entropy (Ht, Hf) [23]. As they reported, there was not a single ecoacoustic index correlated to avian richness across all datasets. The authors hypothesized that these incongruities may be due to comparing diverse habitats and ecosystems at different latitudes as well as using audio recorders of different brands or in different settings (i.e., spatial deployment) and conditions (i.e., rain protection bags).

To overcome these biases, it is crucial to equalize the audio files acquired from various recorders. Equalization involves processing these audio files using a curve derived from comparing two recordings of white noise: one obtained with the soundscape sensor and another with a type 1 sound level meter, which serves as reference. This process enables

the generation of soundscape recordings with a “flat” frequency response (akin to that of the sound level meter), ensuring consistent pressure levels and ecoacoustic indices across soundscape devices.

The necessity of granting an accurate comparison between recorders has been previously recognized in other papers which proposed calibration methods or pipelines to study the spectral portions in which the recordings are comparable [24,25,26].

In [24], three procedures with various accuracy to calibrate audio files were proposed. Among these, the most effective approach involves calibrating the recording using a known frequency level as a reference value. Unfortunately, the different sensitivity curves of the instruments (which are not flat) do not allow for perfect calibration, and thus, an equalization procedure is necessary.

In [25], the authors perform an equalization on one-third octave bands between 0.025 and 6.3 kHz. Their work is an initial step in facilitating accurate comparisons of soundscape recordings.

Finally, in [26], the authors proposed a pipeline to compare the ecoacoustic indices between Audiomoth and SM4 devices. In their article, Luna-Naranjo and colleagues addressed the inherent variability in these two devices mainly by selecting comparable frequency ranges between the two instruments (on which the ecoacoustic indices are calculated) and normalizing the signal amplitude.

In this study, we propose an equalization protocol aiming at mitigating biases inherent in soundscape recordings obtained from three different devices (Song Meter Micro, Audiomoth and Soundscape Explorer Terrestrial), by aligning these audio files to those captured by class 1 level meter (LD831-C), a standard reference device. This process entails adjusting the signal amplitude and frequency response of the soundscape recorders to match those of the level meter, ensuring consistency across the entire spectrum. Alongside the protocol proposal, its validation is carried out in this paper to show its efficacy. As a result, we aim to help researchers with further comparisons within and outside the study area with greater reliability and precision, enabling a more complete understanding of acoustic ecosystems and their dynamics.

This paper is structured around four key pillars, outlined as follows:

- An explanation of the equalization procedure's steps;
- Recording white noise to calculate the equalization curves;
- The application of equalization curves to the soundscape recordings;
- The validation of the procedure using three case studies.

2.2 Materials and Methods

In this section, we describe the instrumentation and steps followed for the development of the equalization process:

1. Obtaining white noise recordings to generate the equalization curves;
2. Defining the equalization procedure;
3. Validating the equalization process
 - a) On white noise measures (obtained in the lab);
 - b) In an in-field experiment placing the devices in a single measurement point;
4. Providing an example of a monitoring campaign carried out in a Regional Park using two different brands of devices.

2.2.1 Materials

For the creation of this protocol, we considered three models of different brands of soundscape recorders and a sound level meter (Figure 1):

- Song Meter Micro (Wildlife Acoustics, Inc., Maynard, MA, USA);
- Soundscape Explorer Terrestrial (Lunilettronik Coop S.p.a., Fivizzano, Italy);
- Audiomoth (Open Acoustic Devices, Oxford, UK);
- LD831-C (Larson-Davis, Depew, NY, USA).

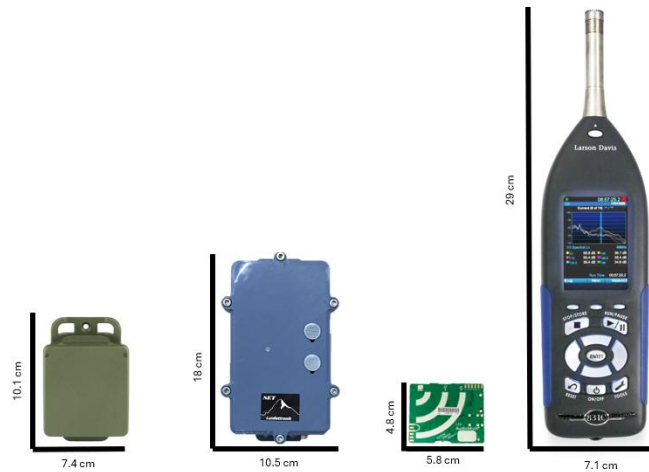


Figure 1. Devices employed in this study and relative dimensions (from left to right: Song Meter Micro, Soundscape Explorer Terrestrial, Audiomoth and LD831-C).

These models were chosen given their diffusion in the soundscape ecology community, their relative economical cost and the different sensitivity curves. We used a class 1 level meter to obtain the best input result.

The Song Meter Micro (SMM hereafter) is a passive recorder with a maximum sampling rate of 96 kHz. The sensitivity of the whole signal transmission chain (i.e., microphone, gain and analog-to-digital converter) is $2 \text{ dBV} \pm 4 \text{ dBV}$ relative to 1 Pa at 1 kHz Full-Scale, measured using a gain of +18 dB. The sensitivity curve is not linear with frequency (Figure 2). It generates output files in wave format, 16-bit and not compressed. The maximum recording length is 60 min. It works using three AA batteries. The model tested here is the first version of the Song Meter Micro series.

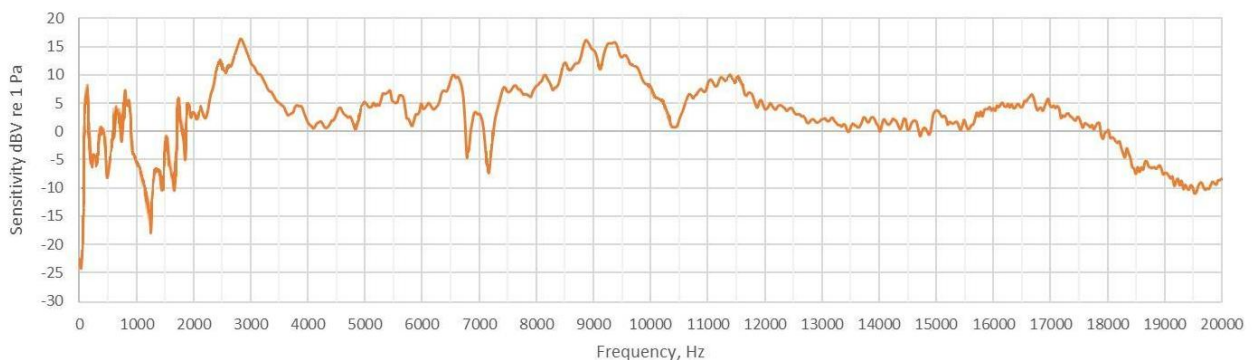


Figure 2. Sensitivity curve for Song Meter Micro. The sensitivity curve is referred to the whole signal transmission chain (provided by Wildlife Acoustic Support Team).

The Soundscape Explorer Terrestrial (SET hereafter) is a programmable recorder equipped with two microphones (with a sampling rate of 48 and 192 kHz, respectively) and environmental sensors (for humidity, temperature, light and atmospheric pressure). The microphone has a sensitivity of $-28 \text{ dBV} \pm 3 \text{ dBV}$ relative to 1 Pa at 1 kHz; its frequency response is almost flat up to 6 kHz (Figure 3). It generates output files in wave format, 16-bit and not compressed. It works using eight AA batteries.

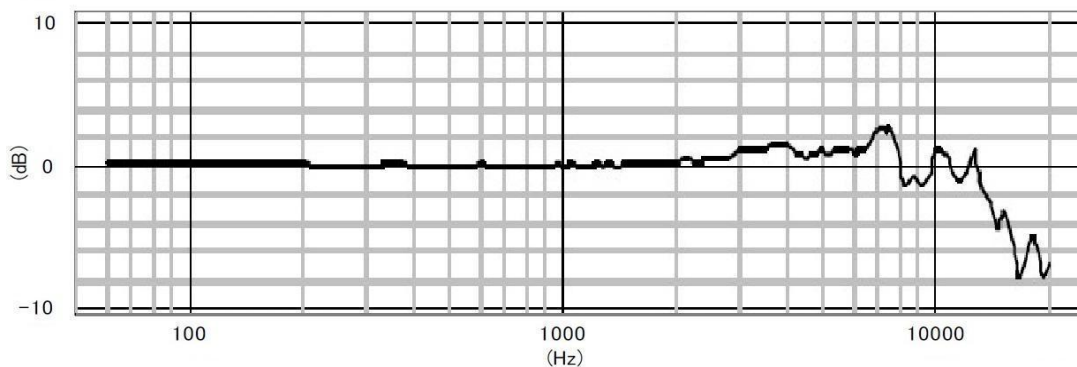


Figure 3. Microphone sensitivity curve for Soundscape Explorer Terrestrial (Adapted from the Microphone technical data by PRIMO Co., Ltd., Tokyo, Japan, installed on the SET).

The Audiomoth 1.2.0 (AM hereafter) is a programmable, low-cost recorder equipped with an analog MEMS (Micro Electrical–Mechanical System) microphone with a maximum sampling rate of 384 kHz. The sensitivity of the microphone is $-38 \text{ dBV} \pm 6 \text{ dBV}$ relative to 1 Pa at 1 kHz, and its frequency response is almost flat (without the waterproof case) (Figure 4). An analysis of the response with and without the waterproof case is carried out. Its output files are .wav, 16-bit and not compressed. It runs using three AA batteries.

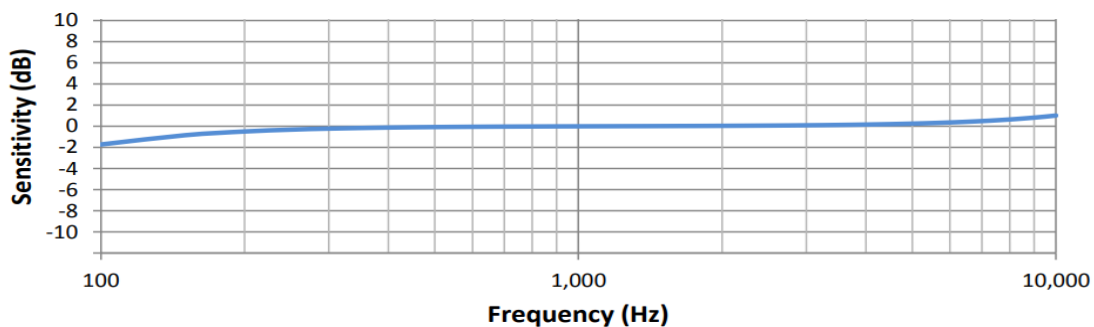


Figure 4. Microphone sensitivity curve for Audiomoth 1.2.0 (Adapted from RevSpace).

Finally, we used as a reference device the sound level meter of class “A” LD-831C (831 hereafter) produced by Larson-Davis. It is equipped with a class A microphone, calibrated in a certified laboratory, with a sensitivity of -26.19 dBV relative to 1 Pa at 251.2 Hz. Moreover, it has a flat response over all frequencies in the interval 0–20 kHz. This level meter can produce an uncompressed .wav file, 16-bit.

2.2.2 Methods

Recording White Noise in the Anechoic Chamber

The first step of the equalization process involves acquiring white noise recordings using the soundscape devices and the level meter simultaneously.

These measurements were carried out in an anechoic chamber, 4×4 m and 2.8 m high, configured to operate in “full anechoic” mode. The chamber can also operate in the “semi-anechoic” configuration (walkable floor without pyramid absorbers), but the “full anechoic” mode ensures an optimal background noise level of 10 dBA for precise recordings. Finally, the cut-off frequencies are around 120 Hz due to the size of the chamber and of the sound-absorbing elements.

The reference signal (white noise) was built using Audacity 3.0.2 [27] with a sample rate of 48 kHz, RMS value of -18.74 dBFS and a duration of 20 s. To reproduce the signal in the anechoic chamber, we employed the loudspeaker TD508 Mk3 of the Eclipse series (Denso Ten, Kobe, Japan) (Figure 5). This speaker has a sensitivity of 82 dB/W/m, emitting between 52 Hz and 27 kHz with an angular coverage of $+15/-10^\circ$.

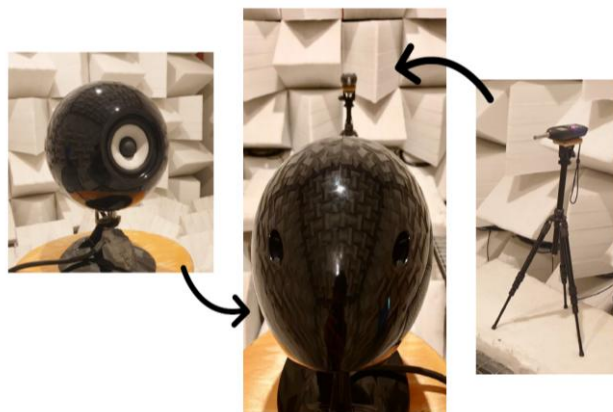


Figure 5. White noise measurements in the anechoic chamber with a loudspeaker and LD831-C.

Measurements were performed by placing one device at a time in the same position: 1 m from the loudspeaker, with the microphone facing the sound source and vertically centered in the middle of the woofer (Figure 5).

The appropriate functioning and frequency response of the loudspeaker were tested previous to the measurements. The results showed that the white noise emitted by the device was not flat (Figure 6). For this reason, the loudspeaker output was recorded with the level meter and equalized to generate a new output in the range 24–15 kHz that was perfectly flat when measured with the level meter. The equalization of the loudspeaker was performed using the white noise generated with Audacity and the signal recorded with the level meter when emitted by the loudspeaker.

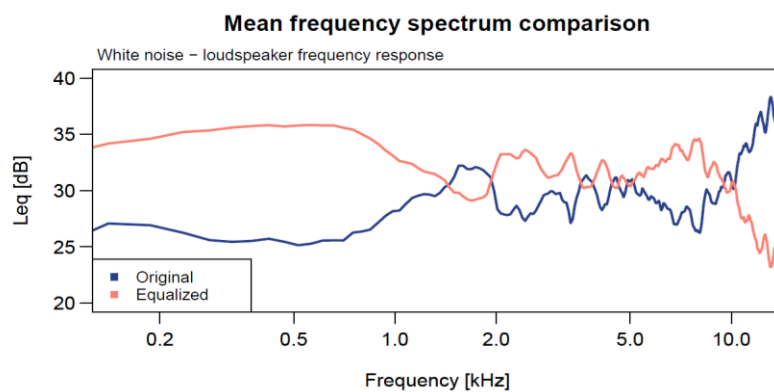


Figure 6. White noise mean frequency spectrum showing the original frequency response of the loudspeaker (blue) and equalized (orange) to obtain a white noise signal measured by LD831-C.

The following settings were used to measure the white noise with the soundscape recorders (Table 1). To understand intra-model variability, we tested all the devices available in our laboratory and some kindly lent to us by Professor Guarnaccia of the Università degli Studi di Salerno; the devices were set as usually employed in the field by the research groups. All devices were set with parameter values used by our group during in-field monitoring [13,16,28,29]. The sampling frequency was set at 48 kHz to correctly sample all birds' vocalizations. The amplitude gains were set for SMM at +18 dB since this is the default value suggested by Wildlife Acoustic, for SET, two values were analyzed due to in-field choices performed by the group during the years and the AM was set at "medium" (+15 dB) since it is the nearest value to the other device's amplitude gains. The level meter gain was set to +0 dB since the device choice is between 0 or +20 dB. Finally, the level meter was employed

without the windproof cap since the measurement was performed in a closed environment, while the AM was analyzed with and without the waterproof case to better understand its effect on the sensitivity curve.

Table 1. Parameters set for each device in the anechoic chamber.

Parameters	831	SMM	SET 18dB	SET 20dB	AM
Sampling rate	48 kHz	48 kHz	48 kHz	48 kHz	48 kHz
Amplitude gain	+ 0 dB	+ 18 dB	+ 18 dB	+ 20 dB	+ 15 dB
Number of devices	1	7	2	1	2
Other characteristics	No windproof cap				With and without the waterproof case by Audiomoth

Equalization procedure

The equalization procedure consists of calculating an equalization curve using the white noise measures and then applying it to in-field recordings. The process is carried out in the MATLAB environment.

Calculating the Equalization Curve

The process to generate the equalization curves is summarized in Figure 7, and the MATLAB script is available in the Supplementary Materials Section. This procedure is an amended version of the one conducted in [30] for the aim of this study and to be able to run it through MATLAB R2023a [31].

The curve is used to generate a filter in the frequency domain which is applied to the in-field recordings.

The first step consists of calculating the power spectral density (PSD) of the level meter and soundscape white noise recordings, which describes the frequency distribution of the signal's power [32].

These vectors are compared by dividing the PSD of the level meter by the soundscape device one.

The curve is finally calculated using the “fir2” function. This function returns an nth-order filter with frequency–magnitude characteristics by interpolating the desired frequency response onto a dense grid and then using the inverse Fourier transform and a Hamming window. The input parameters are the ratio between the PSDs, the number of FFT points and the frequency vector.

The equalization curve is calculated for each device since the frequency response is diverse even between recorders of the same brand.

Furthermore, considering that the soundscape devices have amplitude gain ([Table 1](#)), the white noise recorded by the 831 was amplified to +18 dB before computing the equalization curves. This gain was applied to avoid altering the gains set in the soundscape devices which are optimized to record distant sound events such as birds’ vocalizations. This operation was implemented using Audacity 3.0.2, and a rapid evaluation showed that the gain was linearly applied on all frequencies without any distortion on the recordings. To ensure an accurate comparison of the devices after the equalization, the calculation of the curves was performed on a single white noise 831 recording amplified at +18 dB.

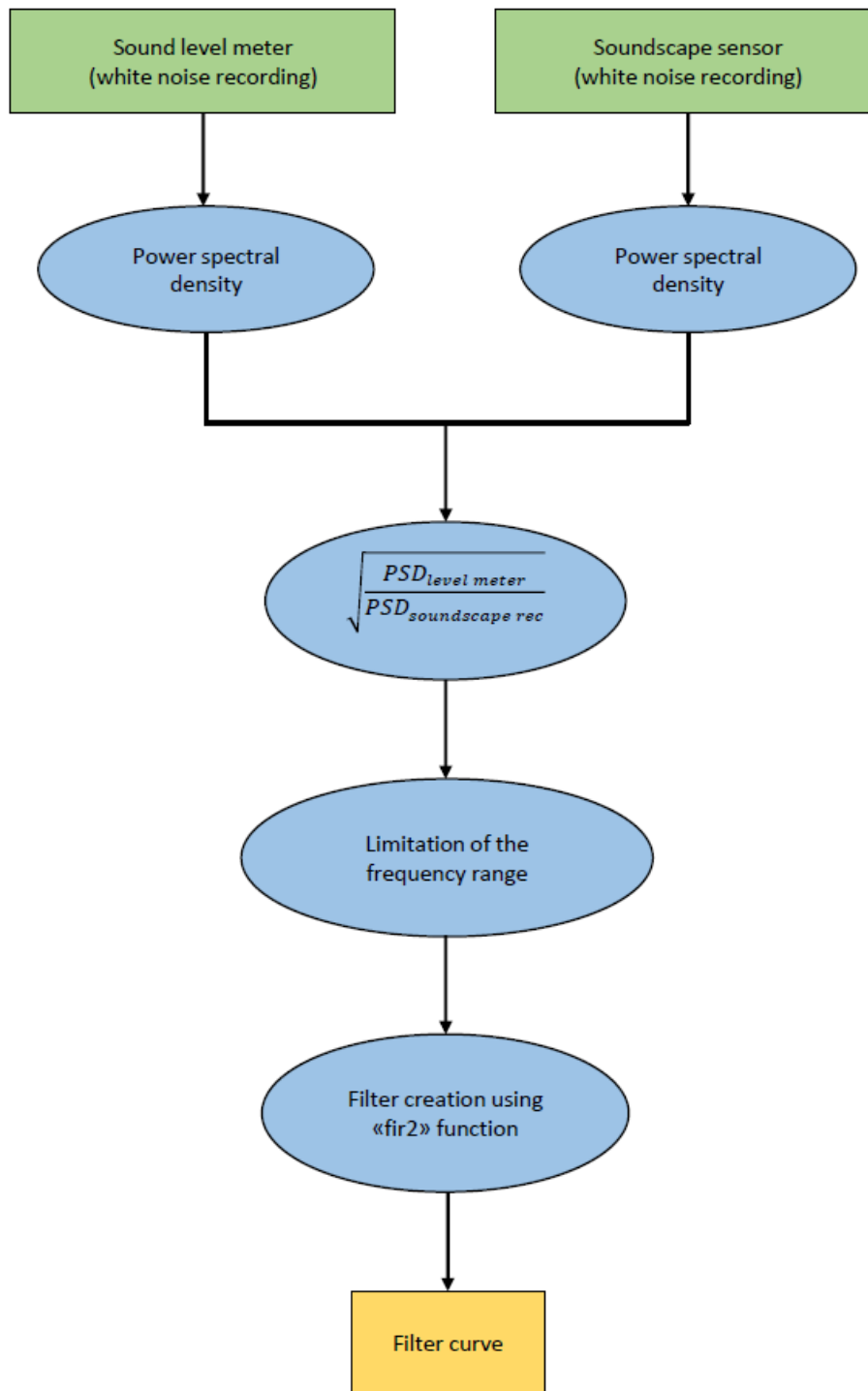


Figure 7. A scheme illustrating the steps to calculate the equalization curves.

Equalization of In-Field Recordings

After the implementation of the equalization, the curves were applied to the in-field recordings (using a MATLAB script available in the Supplementary Materials Section) following the scheme described in Figure 8.

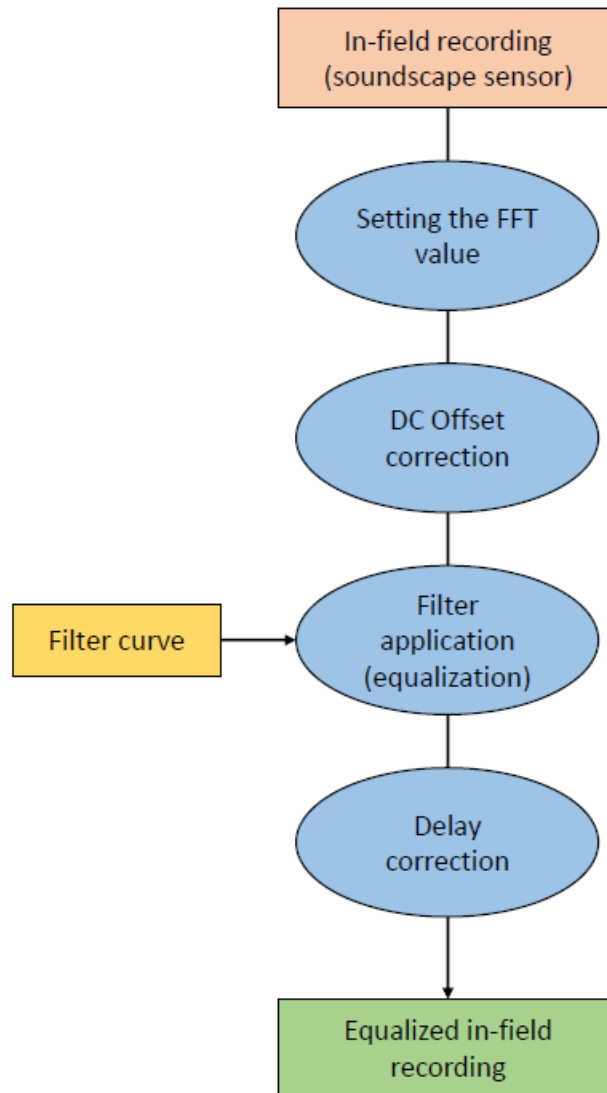


Figure 8. A scheme illustrating the equalization of an in-field recording.

The first step consists of the correction of the possible presence of the DC offset. This fixed voltage offset present in the audio chain of the device is visible as a shift of the waveform from the 0.0 horizontal center. It affects the calculation of the ecoacoustic indices since it alters the frequency domain (being a direct current, it manifests as an intensity peak in the

first frequency bin of the signal). The removal of the DC offset is conducted by subtracting the offset to the signal; the offset value is determined utilizing the mean estimation method, wherein it corresponds to the mean value of the audio signal [33].

The second passage is the application of the equalization curve to the field recording. It is performed using a rational transfer function (“filter”) defined by the numerator and denominator coefficients; the numerator is set to 1, while the denominator is the result of the “fir2” function, in other words, the equalization curve.

Finally, since filtering a signal introduces a delay (i.e., the output signal is shifted in time), the delay is calculated using the “grpdelay” function and then corrected. This function calculates the delay of a narrow-band “group” of sinusoidal components; if the filter has a linear phase response, the group delay and phase delay are identical [34].

The equalized recording is finally saved in .wav format.

Parameters Set in the Equalization Script

In the calculation of the equalization curve script, the number of FFT points was given in input to calculate the power spectral density. The number of FFT points was also applied to implement the curve using the “fir2” function; in particular, it was set as the filter’s order value. After analyzing their frequency response vector and angular frequency vector (Figure 9), we validated the equalization procedure using values of 512, 1024 and 16,384, since they allowed for good accuracy without excessive phase changes. This choice allowed us to obtain three calculated curves for each device.

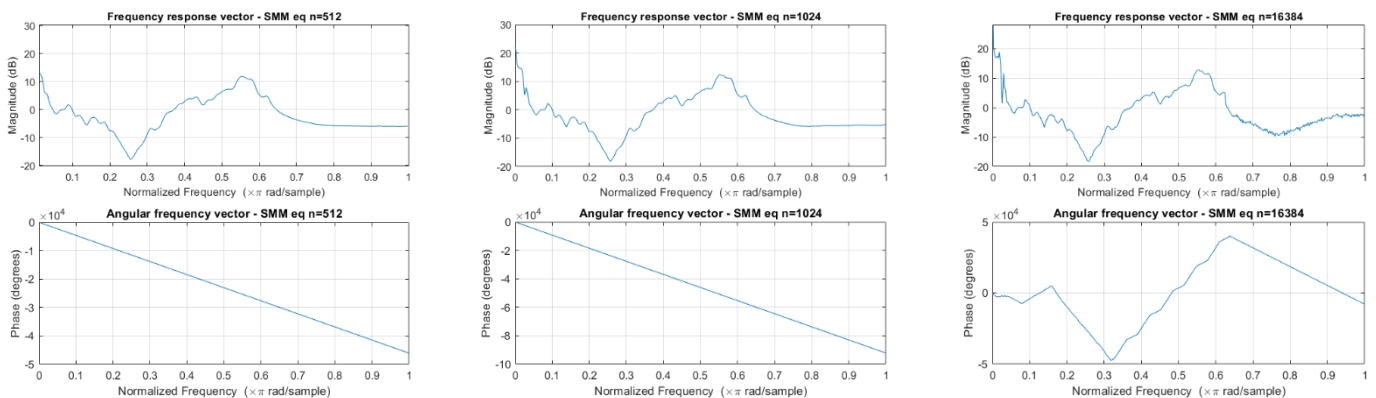


Figure 9. The frequency response vector and angular frequency vector of the equalization curves.

The delay induced by the “filter” function consists of milliseconds of no-audio track placed at the beginning of the recording, shifting the start of the audio without increasing the time duration of the in-field file and thus losing the last recorded milliseconds. Given the linearity of the phase responses (Figure 9), the group delay and phase delay are identical [34]. The delay correction cuts those first milliseconds inserted by the filter, causing a reduction in the length of the recording; this reduction depends on the delay which depends on the order value: it ranges from 0.0053 s using a value of 512 to 0.17 s using a value of 16’384.

Validation of Equalization Process and Practical Example

The validation process (Figure 10) consists of evaluating the effects on the soundscape ecology analysis introduced by the proposed equalization procedure. Focusing on the three soundscape recorder models, it aims at identifying the best filter order to be used.

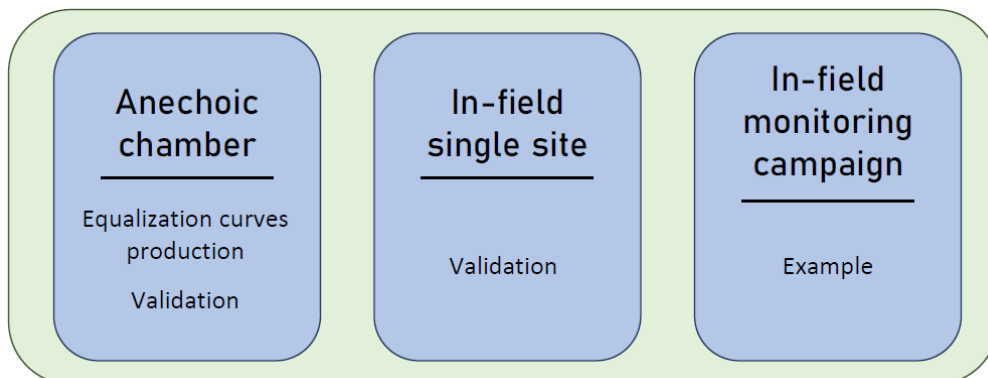


Figure 10. A scheme of the process explained in the following sub-sections.

This validation process was carried out as follows:

- On white noise measures (anechoic chamber measurements);
- In an in-field experiment placing the devices at a single measurement point (urban park).

A practical example was used to better understand the effects of the procedure on ecoacoustic indices’ time trends derived from a monitoring campaign carried out in a Regional Park using two different brands of devices (SMM and SET also used in the previous phases of the validation process).

These three environments were considered due to their different characteristics:

- The anechoic chamber provides an ideal environment for recording identical signals across all devices, facilitating the calculation of equalization curves and enabling a precise comparison of a singular recording for each device.
- The monitoring in the urban park permits the evaluation of the effects of the equalization process in a real case scenario on nine 1 min recordings taken simultaneously at a single measurement site. This site is rich in traffic noise (i.e., cars, buses, motorcycles), birds' vocalizations, cicadas' vocalizations, human voices and airplane overflights; thus, the signals recorded are extremely diverse with events spanning the entire spectrum.
- The example of the Regional Park is proposed as a classic monitoring scheme example [15,16,35]. Its soundscape was assessed by placing nine devices on a regular grid (each point distant 200 m from the others), and the ecoacoustic indices were calculated by analyzing a 24 h time trend both before and after the equalization process. This real-world scenario serves as an excellent example for testing the efficacy of the proposed protocol.

Ecoacoustic Indices

The analysis of recordings in soundscape ecology is carried out using, among other methods, the ecoacoustic indices [12,13,14]. The indices calculated to validate the equalization procedure are the following:

- ACI (acoustic complexity index): This quantifies the vocalizations of avifauna through the study of sound intensity modulation, which varies rapidly over time in the case of biophony but is very constant for numerous anthropogenic noises [14,36]. The implementation is based on the amplitude difference between adjacent time samples within a frequency band, relative to the total amplitude of that band [14].
- ADI (acoustic diversity index): This provides a measure of the diversity of intensity distribution in the spectrum by dividing it into time intervals and calculating the Shannon index [13,14]. Low values are due to extreme diversity in intensity distribution (i.e., nocturnal insects [14]) while high values to a distribution evenness (i.e., high levels of geophony and anthropophony [14] and bird species richness [13]).

- AEI (Acoustic Evenness Index): This is based on the same logic of ADI but applies the Gini coefficient instead of the Shannon index and consequently measures the inequality of signals in bands [37].
- BI (bio-acoustic index): This measures avian abundance by calculating the area under the mean frequency spectrum in the frequency range occupied by biophonies and characterized by a certain amplitude value (this threshold value, expressed in dB, is greater than the lowest value represented in the spectrum) [38].
- NDSI (normalized difference soundscape index): This assesses the distribution of the soundscape between anthropophony and biophony to estimate the level of anthropogenic disturbance of a habitat [39]. It is calculated by dividing the difference between biophony and anthropophony by their sum; the estimation of biophony and anthropophony is carried out by calculating the power spectral density in the frequency ranges of these soundscape components [39]. Values range in the $[-1, +1]$ interval, where +1 ideally indicates the total dominance of biophonies and -1 the total dominance of anthropophonies [39,40].
- H (Acoustic Entropy): This provides an estimate of the total entropy, or heterogeneity, of the recording. It is calculated by computing the product of Shannon's spectral entropy and temporal entropy [41]. Values range in $[0, +1]$; +1 indicates an even signal (i.e., silent recording or faint bird calls), while 0 indicates a pure tone (i.e., insects' vocalizations) [14].
- DSC (Dynamic Spectral Centroid): This returns the spectral centroid of a recording (expressed in Hz) providing information about the sound events of a recording. It is calculated by dividing the spectrum in time intervals and computing the gravity center of the spectrum [13].
- ZCR (Zero-Crossing Rate): This measures the number of times per second that a signal crosses the instantaneous pressure of 0 and provides a measure of noisiness; high values are associated with noisy recordings and the presence of biophony, while low values are linked to tonal sounds [42,43].

These indices were calculated in the “R” environment (version 2023.03.0) [44] using the packages “seewave” and “soundecology”. For computing the DSC, a dedicated script was written [13]. The scripts of the ADI and AEI from the “soundecology” package were modified to add the minimum frequency values and thus mirroring the other ecoacoustic indices (ACI, BI; NDSI, DSC). The indices were calculated using an FFT value of 1024 which corresponds

to a frequency resolution of $FR = 46.875$ Hz and a time resolution $TR = 1/FR = 0.0213$ s. The time duration was set as the minimum of the three FFT values (59.83 s).

For the white noise and pocket park recordings, the indices parameters were set as the following:

- ACI and DSC: $min_freq = 500$ Hz, $max_freq = 12,000$ Hz.
- ADI and AEI: $min_freq = 500$ Hz, $max_freq = 12,000$ Hz, $freq_step = 10$ Hz, $dB_threshold = -50$ dB.
- BI: $min_freq = 1700$ Hz, $max_freq = 12,000$ Hz.
- NDSI: $min_anthro_freq = 500$ Hz, $max_anthro_freq = 1700$ Hz, $min_bio_freq = 1700$ Hz, $max_bio_freq = 12,000$ Hz.
- H and ZCR: the entire spectrum.

The minimum frequency was set to 500 Hz due to the devices' low sensitivity to low frequencies. In fact, even if the equalization process levels out the audio recordings to the one of a level meter, their original sensitivity to low frequencies does not allow for the optimal recording of sounds, and therefore, it is not possible to fully reproduce the fidelity of a sound level meter. For this reason, the minimum frequency was set at 500 Hz.

For the Regional Park monitoring, the indices' parameters were the same except for the ADI and AEI for which the minimum frequency was set to 0 Hz and the $dB_threshold$ to -50 dB.

Statistical Test

Regarding the simultaneous recordings acquired in the urban park, a statistical test was performed to assess the equivalence in the ecoacoustic indices derived from both the sound level meter and the soundscape devices (distinguishing between pre-processed and post-processed using 1 k, 16 k and 32 k FFT points). Given the simultaneity of the recordings, a pairwise test was chosen. Prior to conducting the pairwise Student's test, Shapiro's test and Bartlett's test were employed to verify the assumptions of normality and homoscedasticity [45]. The indices that did not meet the assumptions were analyzed using the pairwise Wilcoxon test. The null hypothesis H_0 of the Student and Wilcoxon test is that the mean difference is equal to 0; it is refused when p -value < 0.05 .

White Noise (Anechoic Chamber)

The validation was first performed on the white noise recorded in the anechoic chamber. The recordings are not affected by the DC offset, probably due to the lack of humidity in the environment which does not alter the conductivity of the electronic circuit.

Two parameters were computed:

- The root-mean-square error (RMSE) of the amplitude (1)

$$\text{RMSE}_{\text{amp}} = \sqrt{\frac{1}{n_f} \sum_{i=f_{\min}}^{f_{\max}} (\text{Amp}_{\text{slm}}(f_i) - \text{Amp}_{\text{recorder}}(f_i))^2}$$

This equation compares the soundscape recording to the level meter one (which serves as reference). It was performed on the entire spectrum, subtracting the amplitude of the soundscape recorder (recorder) from the one of the level meter (“slm”). It was then normalized by the number of frequency bins and rooted.

- Percentage error on the ecoacoustic indices (ACI, ADI, AEI, BI, NDSI, H, DSC, ZCR) using the sound level meter as reference (2)

$$\% \text{error}_{\text{index}} = \frac{\text{Index}_{\text{slm}} - \text{Index}_{\text{recorder}}}{\text{Index}_{\text{slm}}}$$

Field Recordings at Bicocca Urban Park

This in-field validation was performed on a dedicated recording campaign carried out in June 2023 in a pocket park belonging to the University Campus, placing the devices at a single measurement point (Figure 11).



Figure 11. Devices placed in the urban park at a single measurement point.

To obtain simultaneous recordings, each sensor was hung on a steel bar with the microphones oriented in the same direction. They were set with a sampling rate of 48 kHz (same gains used in the anechoic chamber, [Table 1](#)). The Audiomoths were used with their waterproof case.

Nine simultaneous 1 min recordings were acquired for each device. One of the Audiomoths did not work, and thus, it was not considered in the analysis.

Since the recorders were placed at a certain distance from the level meter, the recordings were examined to grant the registrations' simultaneity. This operation was carried out in Audacity by selecting noticeable sound events and cutting the recordings with an accuracy at the millisecond level.

Validation was performed by calculating the ecoacoustic indices and Equations (1) and (2) and by comparing the indices calculated on the level meter with the ones of each soundscape sensor (using the three order values) through a statistical test. Given the simultaneity of the recordings, the Student pairwise test was carried out; the indices that did not meet the Student test assumptions (verified through Shapiro's test and Bartlett's test) were analyzed using the pairwise Wilcoxon test.

Just like for the 831's white noise recording, the amplitude gain in the sound level meter was adjusted in the post-process phase to +18 dB.

Field Recordings in a Regional Park

Using data acquired in the previous steps of this study, the best number of FFT points to use for each device was detected. These parameters were used for the equalization of a monitoring campaign (24 h) performed in April 2022 at the Ticino Regional Park, Lanca del Moriano (Beregardo, Italy), using the same devices employed in the anechoic chamber (in particular, 7 SMM and 1 SET) placed as in Figure 12. The AMs were not employed since the monitoring campaign was organized only by our research group.

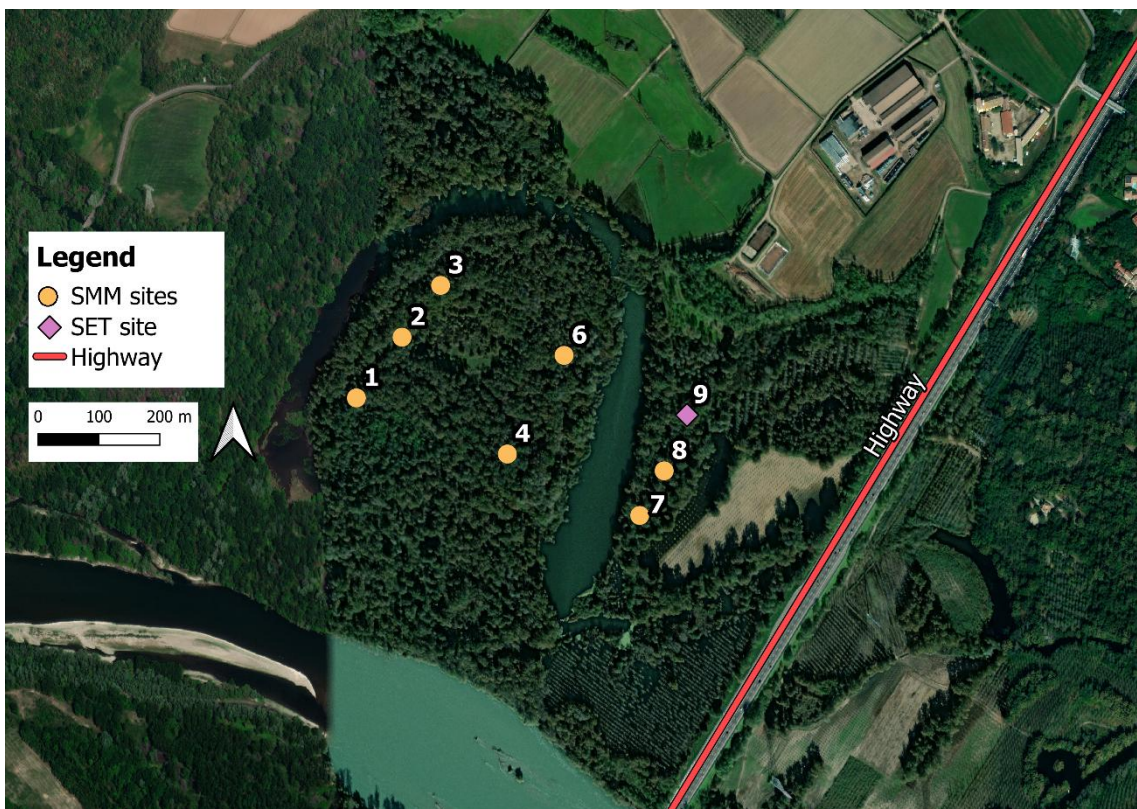


Figure 12. Monitoring scheme at the Ticino Regional Park (Beregardo, PV, Italy). The SMMs are indicated as yellow circles while the SET as a violet triangle. Number 5 is missing due to a malfunction. The main anthropic noise source (highway) is highlighted in red.

2.3 Results

2.3.1 Validation of White Noise Measures

In this section, the mean frequency spectrums of the four devices are compared, before and after the equalization procedure (Figure 13) distinguishing the three cases (512, 1024 and 16,384 order values). In addition to Figure 13, the amplitude RMSE and percentage error on ecoacoustic indices are shown in the form of barplots (Figure 14).

The mean frequency spectrums of the devices before the equalization (Figure 13a) show the evident difference between the level meter and the soundscape recorders. As observable in both Figures 2 and 13, SMMs present a sensitivity peak at 6–7 kHz and a lower response at low frequencies than the level meter. On the other hand, the SETs are characterized by an almost flat response up to 6 kHz which then drops. Finally, the AMs without the waterproof case (AMf) present a nearly flat response up to 5 kHz, while the AMs equipped with the case (AMw) show an extremely oscillating response; differences in the AM frequency response depending on the case were also assessed by [46].

After the equalization (Figure 13b–d), the differences in mean frequency response between devices were reduced in terms of the overall dB difference (see y-axis) and sensitivity oscillation; the amplitude RMSE decreased from a mean value of 10.7 dB in the original recordings to 0.06 dB in the post-processed recordings using the 16,384-order filter (see Table 2). Thus, the best results are noticeable using a 1024- and 16,384-order filter for calculating the equalization curves (i.e., smaller fluctuations of the mean frequency spectrums and less overall amplitude deviation).

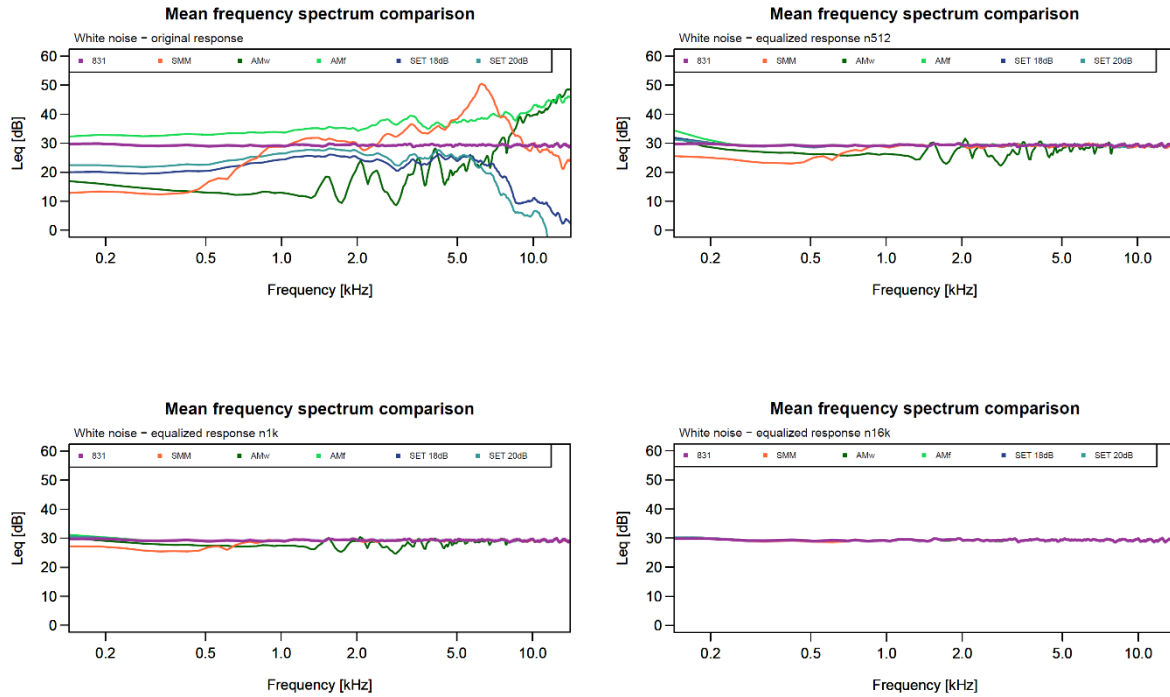


Figure 13. The white noise mean frequency spectrums of the four devices, before and after the equalization procedure. (a) The mean frequency spectrum of the original white noise recordings; (b) the mean frequency spectrum of the equalized white noise recordings using an order of 512; (c) the mean frequency spectrum of the equalized white noise recordings using an order of 1024; (d) the mean frequency spectrum of the equalized white noise recordings using an order of 16,384.

Table 2. The mean amplitude RMSE and total percentage error on the ecoacoustic indices calculated

Device	Noise	Type	Mean RMS amplitude deviation	Total percentage error ¹
AM	White	Original	11.39	3777.26
		Eq n512	2.30	893.51
		Eq n1k	1.40	596.30
		Eq n16k	0.11	52.75
SET 18dB	White	Original	12.65	1567.79
		Eq n512	0.29	104.25
		Eq n1k	0.14	91.57
		Eq n16k	0.02	21.81
SET 20dB	White	Original	10.27	1540.98
		Eq n512	0.23	78.12
		Eq n1k	0.11	70.15
		Eq n16k	0.01	42.86
SMM	White	Original	8.78	1445.55
		Eq n512	0.82	158.96
		Eq n1k	0.49	70.60
		Eq n16k	0.08	777.18

¹ The total percentage error is calculated for each device at each status by summing the errors of the eight indices and averaging over the type of device.

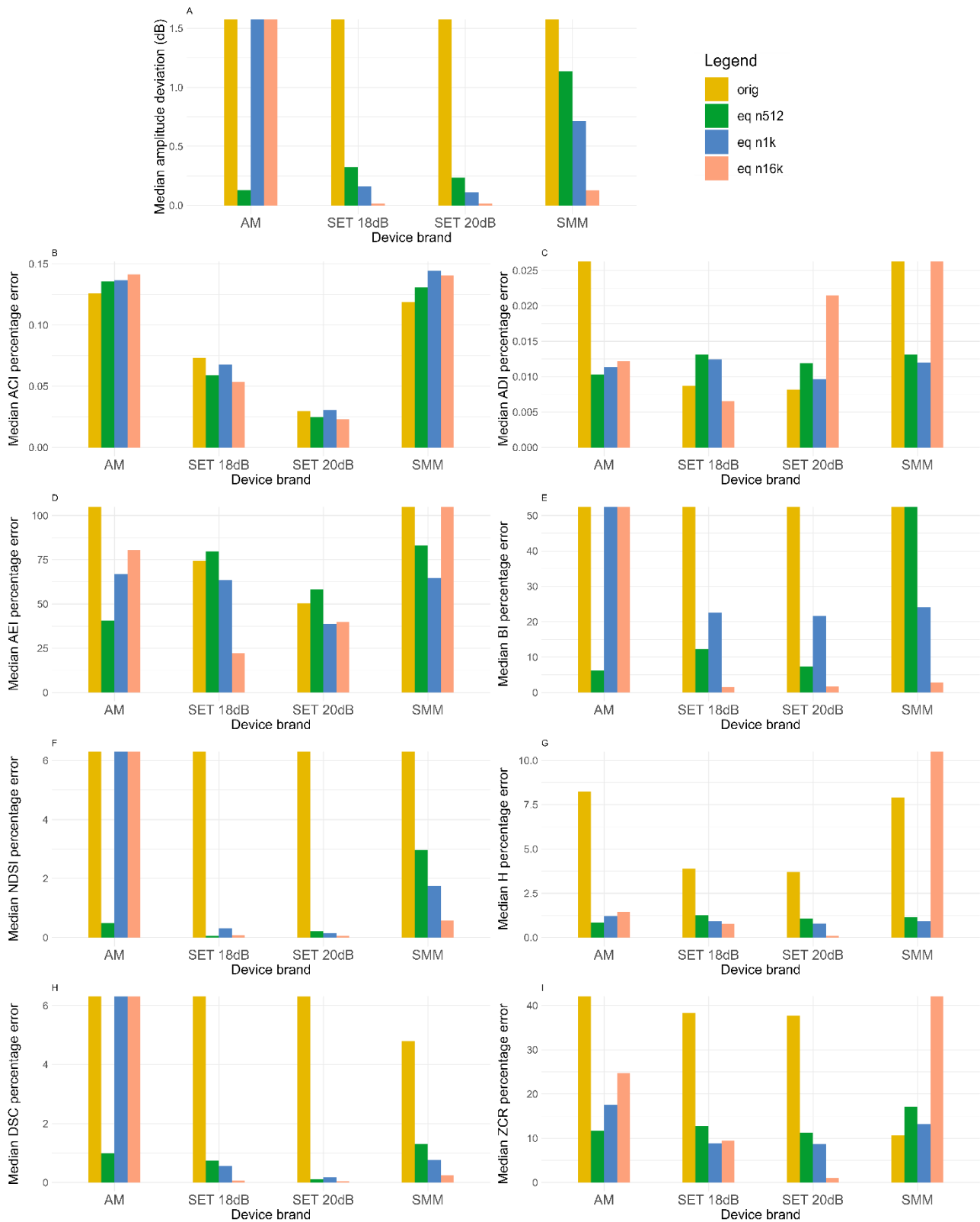


Figure 14. Barplots showing the effect of the equalization process on the amplitude RMSE and the percentage error of the ecoacoustic indices. Each graph represents a parameter (A) median RSME, (B) median ACI percentage error, (C) median ADI percentage error, (D) median AEI percentage error, (E) median BI percentage error, (F) median NDSI percentage error, (G) median H percentage error, (I) median ZCR percentage error. The four devices (x-axis) and the three equalization options (colours) are reported.

Below in Figure 14 are reported the amplitude RMSE and percentage error on the ecoacoustic indices distinguishing the devices and their status (original, post-process using 512, 1 k, 16 k order values). In the case of the AM, only the data about the waterproof-cased one are reported since it was used with this configuration in the field monitoring. Examining Figure 14, the benefits produced are clear by looking at the reduction in the parameters from the original audios (yellow bar) to the equalized audios (green, blue and pink). The best improvements are seen in the AMs (with the case) and SMMs since they are the ones with the most variable frequency response (Figure 13). The amplitude RMSE (A) is reduced for each device. The percentage errors on the ADI, AEI, BI, NDSI, H and DSC are greatly reduced since they analyze the repartition of intensity on the spectrum (which depends on the frequency response). Table 2 shows that the total percentage error of the eight indices is reduced from over 1000% to almost 20%, with some indices (AEI, BI and ZCR) bearing the majority of the error (Figure 11).

Regarding the filter order, the AM equipped with the waterproof case presents less biases when a value of 512 is used, the SETs with the 16,384-order filter and the SMM with values of 512 or 1024 depending on the index (Figure 11, Table 2). These differences may be explained by the different sensitivity curves of devices in comparison with the level meter one.

2.3.2 Validation of In-Field Single Measurement Site (Urban Park)

This section mirrors the previous one, showing the mean frequency spectrums of the four devices, before and after the equalization procedure (Figure 15).

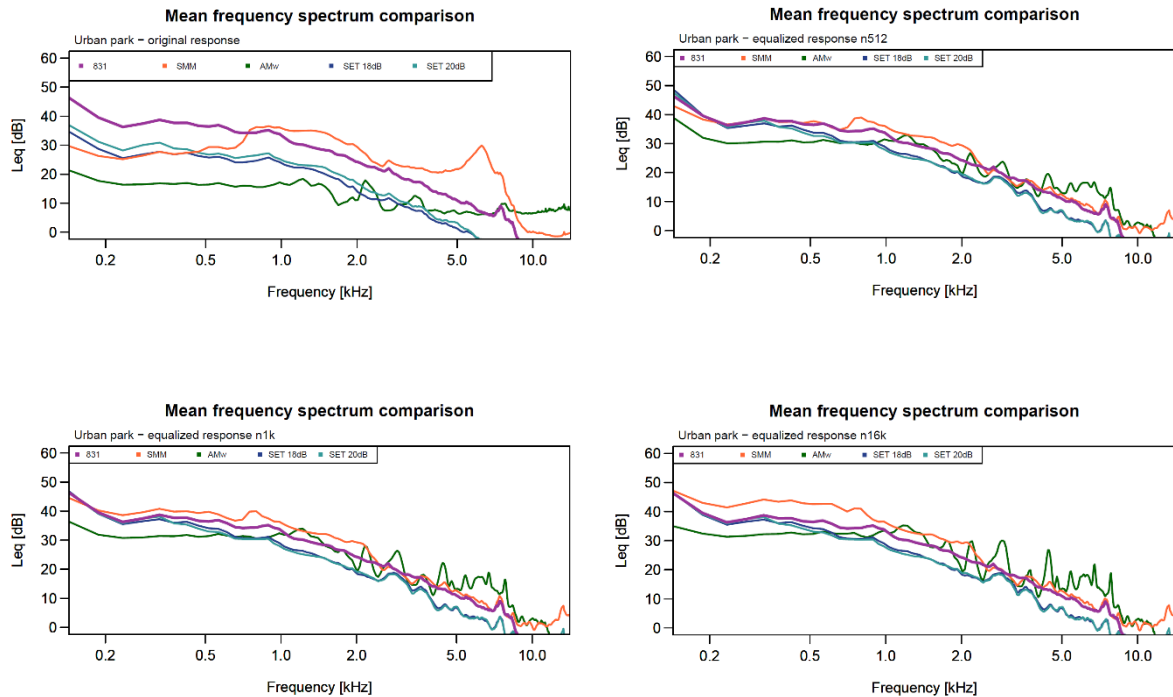


Figure 15. Urban park mean frequency spectrums of the four devices, before and after the equalization procedure. One of the nine recordings is displayed. (a) The mean frequency spectrum of the original in-field recording; (b) the mean frequency spectrum of the equalized in-field recording using an order of 512; (c) the mean frequency spectrum of the equalized in-field recording using an order of 1.024; (d) the mean frequency spectrum of the equalized in-field recording using an order of 16.384.

The original mean spectrums (Figure 15a) show the differences between devices. SMMs and the AM with the waterproof case (AMw) deviate more from the level meter (831) and respectively present a 6–7 kHz peak and an oscillating trend (like in the anechoic chamber). The SETs' trends are more similar to the level meter. After the equalization (Figure 15b–d), the SMMs' trends are very similar to the level meter, especially in the 512 and 1024 cases, while the SETs' trends shift nearer to the reference curve. Finally, the AM is still affected by the oscillatory trend but is indeed nearer to the level meter curve. These benefits can also be seen in Table 3 where the amplitude RMSE decreases from a mean value of 11.6 dB in the original recordings to 4.5 dB in the post-processed recordings using the 512- and 1024-order filter and to 4.8 dB using the 16,384-order filter.

Table 3. The mean amplitude RMSE and total percentage error on the ecoacoustic indices, specified for each device and status, in the urban park monitoring.

Device	Noise	Type	Mean RMS amplitude deviation	Total percentage error ²
AM	Urban park	Original	10.42	3676.39
		Eq n512	4.99	500.41
		Eq n1k	5.30	440.31
		Eq n16k	5.81	729.19
SET 18dB	Urban park	Original	13.89	165.49
		Eq n512	3.94	145.85
		Eq n1k	3.98	170.94
		Eq n16k	4.00	169.44
SET 20 dB	Urban park	Original	12.16	146.55
		Eq n512	4.12	144.50
		Eq n1k	4.14	158.51
		Eq n16k	4.15	173.74
SMM	Urban park	Original	9.95	1876.25
		Eq n512	4.81	454.86
		Eq n1k	4.90	374.68
		Eq n16k	5.07	288.19

Mirroring the white noise validation section, Figure 16 shows the amplitude RMSE and percentage error on ecoacoustic indices calculated on the nine one-minute recordings carried out in the urban park.

The boxplot analysis on the amplitude RMSE and the percentage error on the ecoacoustic indices (Figure 16) reflects the barplot analysis of the white noise recordings (Figure 14). We can assess the following:

- The amplitude deviation is reduced for all devices (graph A);
- The percentage error on the BI, NDSI, DSC and ZCR is greatly diminished, in particular for the AM and SMM; in Table 3, it is possible to notice this decrease in the total percentage error: it is 2000% for AM and 1580% for SMM while only 30% for SET 18 dB and 2% for SET 20 dB;
- The ACI is not affected by the process since it compares adjacent temporal and frequency bins;

² The total percentage error is calculated for each device at each status by summing the errors of the eight indices and averaging over the type of device

- The percentage error on the ADI, AEI and H is reduced in the SMM and AM, while it is increased in the SETs.

This comparison is summarized in Table 3; the total percentage error on the AM and SMM is reduced by 2000% and 1580%, respectively, and in this view, the optimal choice of parameters is using an order of 1024 for AM and 16,384 for SMM, while the error improvement on the SETs is limited from the outset and is not further reduced.

For a complete overview, Figure 17 shows the boxplot of the ecoacoustic indices calculated on the sound level meter and the soundscape recorders. The Student and Wilcoxon pairwise tests were performed on the ecoacoustic indices to better understand the benefits of the equalization procedure.

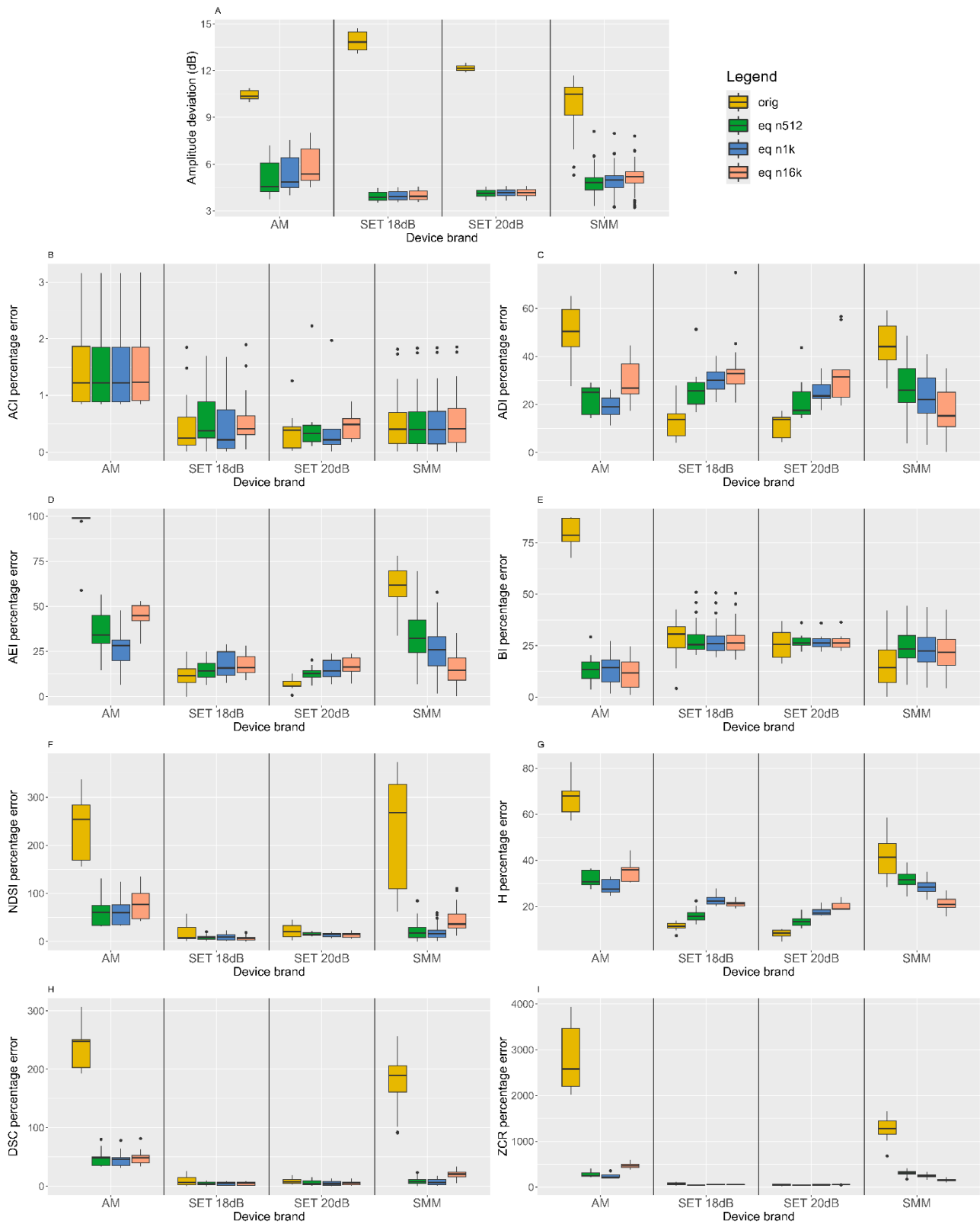


Figure 16. Boxplots of the amplitude RMSE (A) and the percentage errors on ecoacoustic indices (B–I). Each graph represents a parameter and the four measurement settings (original—equalized using orders of 512, 1024 and 16,384) are reported.

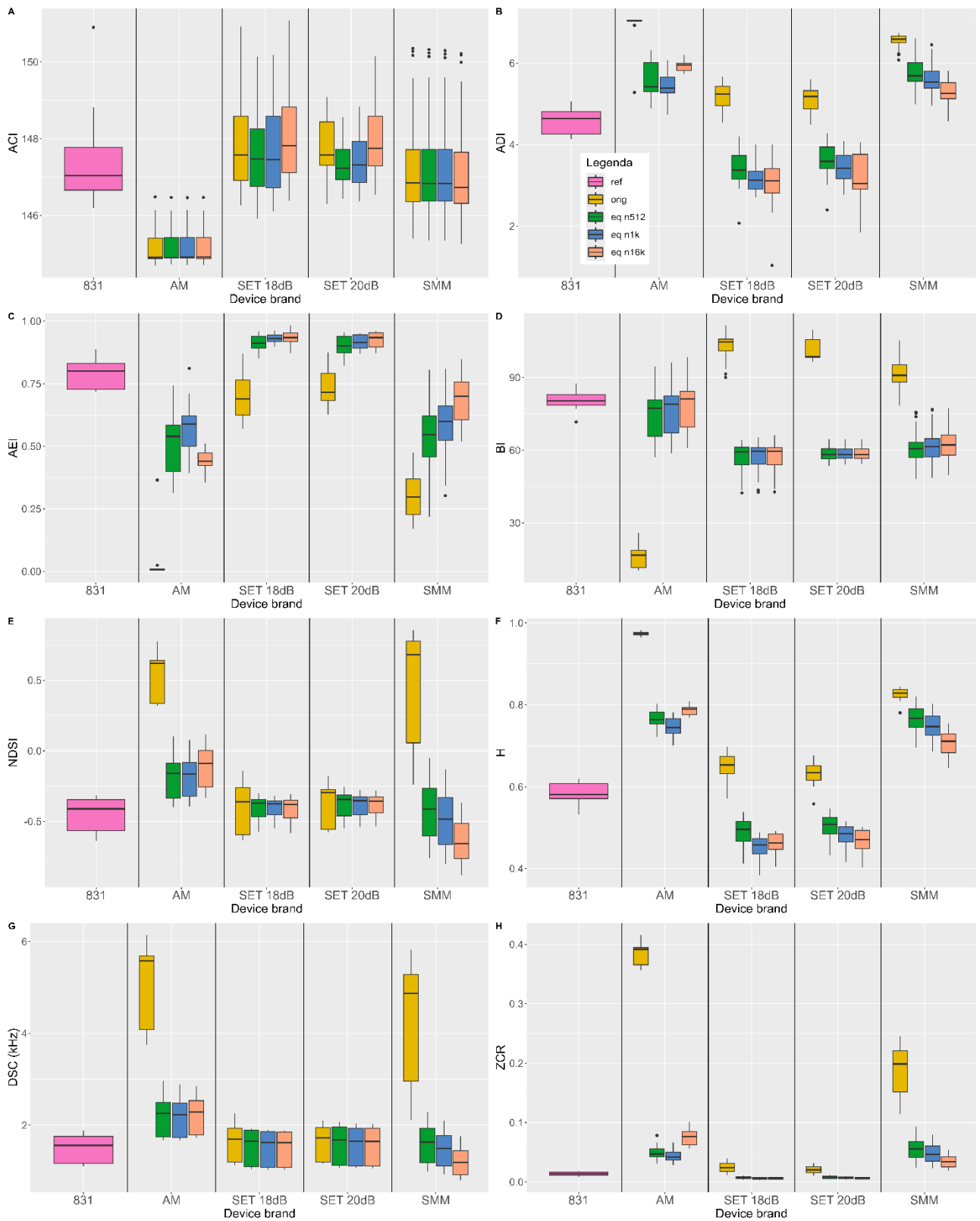


Figure 17. Boxplots showing the ecoacoustic indices. (A–H) Each graph represents an index and the four measurement settings (reference—original—equalized using orders of 512, 1024 and 16,384) are reported.

Examining Figure 17, we can affirm that the indices calculated on the in-field recordings behave as follows:

- ACI: The soundscape devices' values are similar to the level meter ones due to the index calculation method. The AM is an exception probably due to its oscillatory frequency response. Looking at one device at a time, the variation in values between the original recordings and the equalized ones is constant or minor.
- ADI: The equalized values of AM and SMM are more similar to the level meter ones, especially in the 512–1024 case for AM and 16,384 for SMM. On the contrary, the SETs are similar to the reference in the beginning and then deviate. This different behaviour between the soundscape devices may be explained by the linearity of their sensitivity curves and thus of the intensities on the spectrum: the “flatter” the curve, the smaller the deviation of ADI values from the level meter ones.
- AEI: As for the ADI, the AM and SMM values are nearer to the reference when equalized using a filter order of 1024 and 16,384, respectively. On the other hand, the SETs deviate when equalized. The deviation of the SET when equalized may be due to applying the procedure on a device which already presents a “flat” curve; trying to further linearize it generates errors since it is already linear.
- BI: All sensors' original values do not match the reference ones; this can be explained by the frequency response of the soundscape devices that are not linear above 5 kHz. With the equalization, the AM values match the level meters', and the others are nearer to the level meter ones.
- NDSI: Since this index greatly depends on the linearity of the frequency response, AM and SMMs are the ones with the greatest bias. It is possible to notice an improvement for all devices after the equalization, especially for AM and SMMs using an order value of 512.
- H: AM and SMMs benefit from the process but are nowhere near the reference values. The SETs' original values are nearer to the level meter ones than the equalized values due to their already linear sensitivity curve. Moreover, the similar behavior is present in the ADI and AEI which also evaluate the heterogeneity of the recordings.
- DSC: AM and SMMs present the greatest biases due to their frequency response, as for the NDSI; the equalization reduces them, allowing for comparisons. The SETs do not benefit from the process thanks to their more linear frequency response.

- ZCR: Even in this case, AM and SMMs are affected by biases which are reduced with the equalization process. The SETs' original values are very similar to the level meter ones probably due to their more linear sensitivity curve.

It is possible to observe a general trend in the SETs (i.e., ADI, AEI, H, DSC, ZCR) which is probably caused by their already almost "flat" sensitivity curve. When the SETs' recordings are equalized, a deterioration in their similarity to the sound level meter is observed and caused by trying to further linearize their nearly linear frequency response.

To statistically validate the procedure, the ecoacoustic indices calculated on the level meter's urban park recordings were confronted with the ones obtained with the soundscape recorders. In particular, each index series calculated on the nine one-minute-long level meter's recordings were compared to the one calculated on each of the nine one-minute long soundscape recordings before and after the equalization. For this reason, the tests used were the pairwise Student's test (when both series were normally distributed and homoscedastic) or Wilcoxon's test [45]. The tests' null hypothesis H_0 assumes that the mean difference in the distributions is equal to 0; it is refused when $p\text{-value} < 0.05$.

Looking at Table 4, the AM presents indices that confirm H_0 (BI) when equalized. SETs present the same number of indices that confirm H_0 when they are not equalized and equalized using the 512 and 1024 filter order. Finally, the SMMs benefit the most from the equalization when it is performed using an order of 1024 FFT.

Table 4. *p*-values derived from Student's and Wilcoxon's tests performed between the ecoacoustic indices' values of the level meter and the ones of each soundscape sensor. When H_0 is confirmed (p -value > 0.05), the cell is highlighted in green. Here, we report the most interesting results from four devices.

Reference Device (Original)	Soundscape Device	Soundscape Device Status	ACI	ADI	AEI	BI	NDSI	DSC	H	ZCR
831	AM1	Original	3.91×10^{-3}	3.91×10^{-3}	3.91×10^{-3}	1.93×10^{-8}	1.74×10^{-9}	3.91×10^{-3}	3.91×10^{-3}	3.91×10^{-3}
		Eq n512	3.91×10^{-3}	4.14×10^{-6}	1.16×10^{-5}	2.03×10^{-1}	3.21×10^{-5}	1.45×10^{-5}	1.18×10^{-10}	3.91×10^{-3}
		Eq n1k	3.91×10^{-3}	3.39×10^{-6}	3.91×10^{-3}	3.01×10^{-1}	1.50×10^{-5}	9.50×10^{-6}	2.10×10^{-10}	3.91×10^{-3}
		Eq n16k	3.91×10^{-3}	2.59×10^{-6}	3.57×10^{-7}	4.96×10^{-1}	1.39×10^{-6}	2.22×10^{-6}	3.91×10^{-3}	3.91×10^{-3}
831	SET1 ³	Original	8.41×10^{-2}	3.51×10^{-4}	1.97×10^{-3}	2.28×10^{-4}	4.32×10^{-1}	1.95×10^{-2}	2.72×10^{-7}	3.91×10^{-3}
		Eq n512	3.10×10^{-1}	1.30×10^{-5}	3.91×10^{-3}	4.75×10^{-5}	1.83×10^{-2}	9.10×10^{-1}	8.16×10^{-9}	8.90×10^{-7}
		Eq n1k	2.26×10^{-1}	1.52×10^{-7}	3.91×10^{-3}	4.67×10^{-5}	4.73×10^{-2}	5.70×10^{-1}	1.98×10^{-11}	3.91×10^{-3}
		Eq n16k	3.75×10^{-2}	3.91×10^{-3}	4.64×10^{-6}	4.41×10^{-5}	4.31×10^{-2}	4.26×10^{-1}	4.81×10^{-13}	3.91×10^{-3}
831	SET3 ³	Original	6.47×10^{-1}	7.38×10^{-5}	6.26×10^{-4}	2.27×10^{-6}	1.65×10^{-3}	3.76×10^{-3}	1.03×10^{-6}	3.91×10^{-3}
		Eq n512	6.76×10^{-1}	4.78×10^{-5}	3.30×10^{-6}	4.29×10^{-7}	2.26×10^{-5}	6.76×10^{-2}	1.44×10^{-8}	5.06×10^{-7}
		Eq n1k	7.57×10^{-1}	6.04×10^{-7}	1.12×10^{-5}	4.34×10^{-7}	3.88×10^{-4}	1.36×10^{-1}	4.59×10^{-11}	1.35×10^{-6}
		Eq n16k	1.02×10^{-1}	3.91×10^{-3}	3.56×10^{-6}	5.31×10^{-7}	9.60×10^{-4}	1.71×10^{-1}	1.02×10^{-11}	1.72×10^{-6}
831	SMM1393	Original	1.07×10^{-1}	3.91×10^{-3}	3.99×10^{-7}	9.44×10^{-3}	1.95×10^{-2}	3.91×10^{-3}	3.91×10^{-3}	3.91×10^{-3}
		Eq n512	9.68×10^{-2}	7.38×10^{-5}	1.59×10^{-4}	1.38×10^{-5}	3.74×10^{-1}	1.74×10^{-1}	4.91×10^{-11}	3.91×10^{-3}
		Eq n1k	8.98×10^{-2}	1.37×10^{-4}	5.89×10^{-4}	1.87×10^{-5}	4.68×10^{-3}	1.79×10^{-1}	9.57×10^{-11}	3.91×10^{-3}
		Eq n16k	5.58×10^{-2}	1.84×10^{-3}	9.25×10^{-3}	1.78×10^{-5}	7.68×10^{-5}	3.54×10^{-5}	6.53×10^{-10}	3.91×10^{-3}
831	SMM1435	Original	5.65×10^{-2}	1.55×10^{-7}	9.64×10^{-7}	3.91×10^{-3}	3.91×10^{-3}	3.91×10^{-3}	3.91×10^{-3}	3.91×10^{-3}
		Eq n512	7.42×10^{-2}	1.46×10^{-5}	2.96×10^{-5}	1.49×10^{-5}	4.54×10^{-2}	8.23×10^{-3}	3.85×10^{-11}	3.91×10^{-3}
		Eq n1k	7.42×10^{-2}	2.91×10^{-5}	7.41×10^{-5}	2.84×10^{-5}	6.74×10^{-1}	9.39×10^{-1}	7.00×10^{-11}	3.91×10^{-3}
		Eq n16k	5.47×10^{-2}	4.00×10^{-4}	1.15×10^{-3}	4.97×10^{-5}	1.58×10^{-9}	1.69×10^{-7}	2.23×10^{-9}	3.91×10^{-3}

2.3.3 In-Field Monitoring Campaign Example (Ticino Park)

In this section, time trends of the ecoacoustic indices are shown (Figure 18). Given the results of the previous sections, the SMMs were equalized using a filter order of 1024, while the SET was not equalized (the AM was not used in this monitoring campaign).

In Figure 18, the indices' time trends before (left column) and after (right column) the equalization are reported, and it is possible to affirm the following:

- ACI: the time trends remain the same since the index is not affected by the process.
- ADI: in the original time trends graph (C), the presence of the DC offset is noticeable which afflicts all the SMMs except Site 6 (blue curve); after the equalization, the SMMs present a similar trend.

³ SET 1 belongs to the SET 18 dB series; meanwhile, SET3 is the SET 20 dB

- AEI: The DC offset is also visible in these graphs. The effect of the equalization is noticeable since the time trends are more similar in the post-equalization graph (F).
- BI: The SET (Site 9, black) is distant from the SMMs' trends before the process (G) due to its flatter frequency response. After the equalization, the SMMs have a more similar trend to the SET.
- NDSI: The procedure reduces the SMMs' overestimated biophonic contribution to the soundscape and the underestimation of the anthropophonies thanks to the equalization of the frequency response; in fact, values change from being almost constant at +1 for Sites 1–6 (SMMs) to a more oscillatory trend, while the anthroponic disturbance generated by the highway becomes more evident in Sites 7–8–9 (SMM, SMM and SET).
- H: The DC offset is evident for this index just like the ADI and AEI (since it is not possible to define a low-frequency limit in these indices' implementation in R). However, in the post-equalization graph (L), the SMMs' trends are adjusted; given the results in the pocket park, these values may be overestimated.
- DSC: In the pre-equalization graph (M), the bias affecting the SMMs due to their peaked frequency response is extremely evident. After the equalization (N), time trends are corrected since Sites 7–8 (SMMs) are very similar to Site 9 (SET) indicating the influence of the highway (higher intensities at low frequencies); moreover, the general DSC values are reduced from a mean value of 4 kHz to 2.5 kHz, underlining the bias which afflicts this index if not corrected.
- ZCR: The DC offset is evident for this index. After the equalization (P), the values are corrected, and the difference between Sites 7–8–9 (nearer the highway) from the others is noticeable.

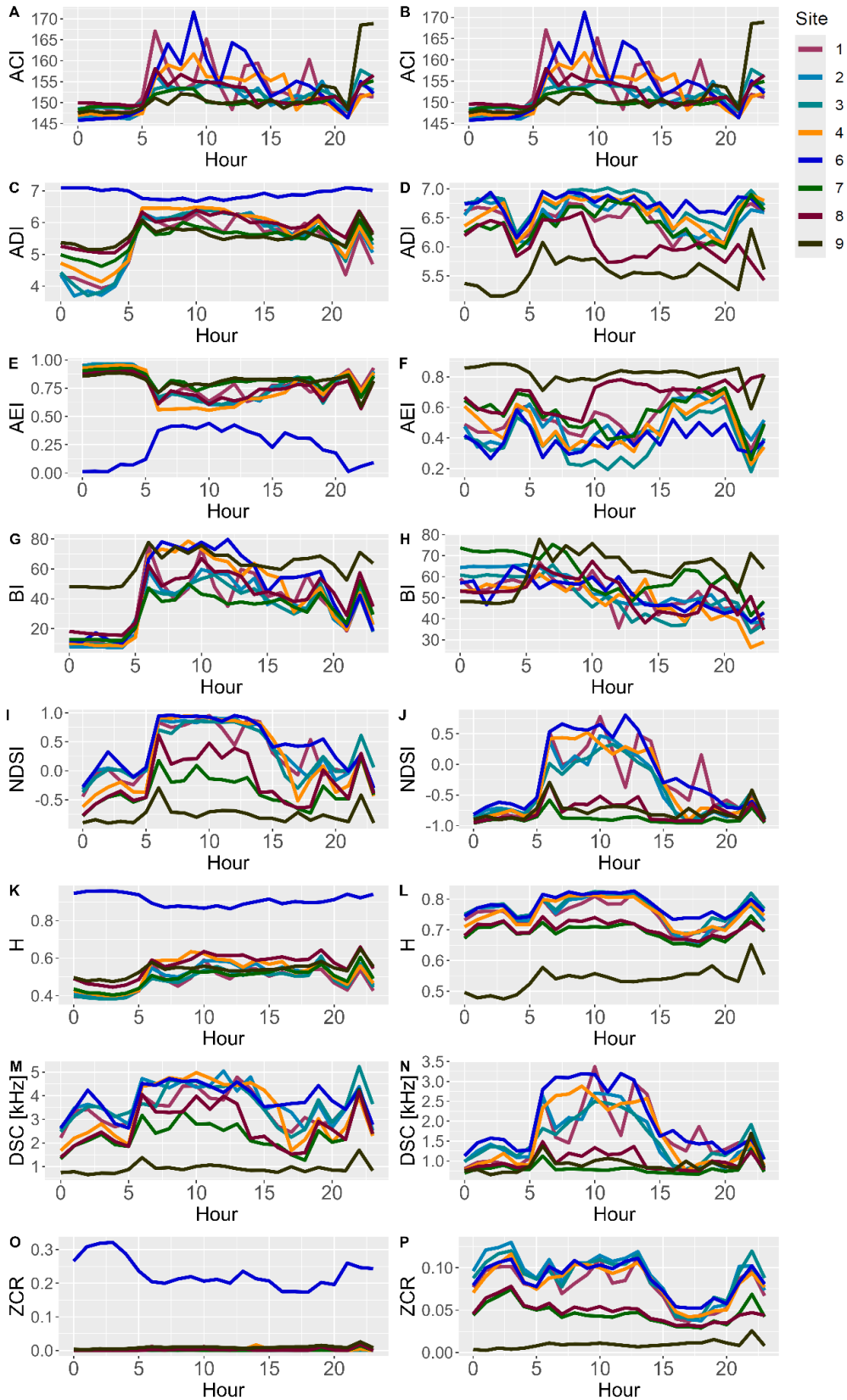


Figure 18. Time trend graphs of the ecoacoustic indices. Each row represents an index, on the left value 1024. Subfigures show: (A,B) time trend of ACI before-after the equalization, (C,D) time trend of ADI before-after the equalization, (E,F) time trend of AEI before-after the equalization, (G,H) time trend of BI before-after the equalization, (I,J) time trend of NDSI before-after the equalization, (K,L) time trend of H before-after the equalization, (M,N) time trend of DSC before-after the equalization, (O,P) time trend of ZCR before-after the equalization

2.4 Discussion

The incongruence of ecoacoustic indices in analysing the soundscape has been stressed by different studies, highlighting different trends [19,22] and limitations in predicting biodiversity parameters [21,47,48].

In particular, Alcocer and colleagues [47] showed the disparity in the number of studies published between 2007 and 2019 that found a correlation between ecoacoustic indices and biological parameters (i.e., avian richness) in favor of a lack of correlation between these two parameters. The absence of correlation was also confirmed by [21] through a meta-analysis involving four datasets from around the world; nevertheless, as the authors acknowledge in their paper, their findings may be explained with a non-harmonized data collection method in terms of the sampling design, bird survey method and recording devices [48].

Our study fits into this context, proposing an equalization protocol to mitigate the biases inherent in soundscape recordings and thus reducing the incongruence of ecoacoustic indices between studies. Nonetheless, the need for an accurate soundscape analysis is not recent, and other studies have covered this issue [24–26].

In [24], a calibration methodology is proposed, and, even if it is a different procedure than equalization, it highlights the need for more accurate soundscape analysis. Unfortunately, the sensitivity curves of the soundscape recorders are not linear; therefore, calibrating different devices will not obtain an equal output in terms of sound pressure levels and ecoacoustic indices' values.

In [25], an equalization is performed on one-third octave bands between 25 Hz and 6.3 kHz using 1 s Leq values acquired with a type 1 sound level meter. This work lays a foundation for comparable recordings, but it is applied to a narrow frequency range (25–6300 Hz) using one-third octave bands, thus not covering the entire diversity of soundscape events (i.e., biophonies, anthropophonies and geophonies), and a single correction factor is used for a wide range of frequencies.

In our study, we performed an equalization procedure by taking as a reference the whole spectrum range using frequency ranges smaller than one-third octave bands thanks to the FFT analysis. Regarding this last point, and considering the validation stages conducted,

we recommend using an order value of 1024 for equalizing the Song Meter Micro and 512 for the Audiomoth, while the Soundscape Explorer Terrestrial does not need to be corrected.

Finally, in [26], a pipeline to obtain similar ecoacoustic indices' values between Audiomoth and Song Meter 4 (SM4) is proposed. The keystone of the process is the identification of comparable frequency ranges between the soundscape instruments (AM and SM4) on which the ecoacoustic indices are calculated. The approach led to a significant reduction of up to 70% in the variability observed in the calculation of ecoacoustic indices.

The selection of continuous comparable ranges suggested in [26] may not always be applicable since some devices may present oscillating sensitivity curves that do not allow for the selection of a continuous range and thus the implementation of ecoacoustic indices. Therefore, an equalization procedure is necessary to adjust the intensities throughout the entire spectrum allowing for the study of soundscapes in their integrity using virtually any recording device available on the market.

2.5 Conclusions

In this paper, we propose and validate an equalization procedure which we suggest implementing when studying soundscapes. In particular, it is extremely important when employing recorders characterized by a nonlinear sensitivity curve because it helps to reduce the biases that affect some ecoacoustic indices. Moreover, it reduces the errors when multiple brands of recorders are employed and when soundscapes from different habitats are compared.

Regarding the application of the procedure, we suggest applying it on devices that present a nonlinear frequency response. In our specific case study, we have proven that the equalization should be calibrated on device brands; moreover, each device should have its own equalization curve since there is a certain variance between devices of the same brand due to manufacturing processes. To calculate the equalization curve, the measurements of the reference signal should be carried out in a controlled environment, free-of-noise sources and with low reflectance (an anechoic chamber is the best choice). The MATLAB script of the procedure is available in the Supplementary Materials Section.

Future steps will involve its examination in different environments and the comparison between areas. Moreover, it will be applied to other soundscape sensors, and a new trial will be carried out using the add-on produced by Wildlife Acoustic to flatten the 6 kHz peak in the Song Meter Micro.

We hope this procedure will be adopted by the scientific community to enhance the understanding of the impacts of anthropic noise and the shaping of soundscapes, to help define guidelines and limits to effectively protect ecosystems and biodiversity

Supplementary Materials: The following supporting information can be downloaded at <https://www.mdpi.com/article/10.3390/s24144642/s1>.

References

1. Erbe, C.; Thomas, J.A. History of Sound Recording and Analysis Equipment. In *Exploring Animal Behavior Through Sound*, 1st ed.; Springer Nature: Cham, Switzerland, 2022; Volume 1, pp. 1–36.
2. Can, A.; Audubert, P.; Aumond, P.; Geisler, E.; Guiu, C.; Lorino, T.; Rossa, E. Framework for Urban Sound Assessment at the City Scale Based on Citizen Action, with the Smartphone Application NoiseCapture as a Lever for Participation. *Noise Mapp.* **2023**, *10*, 20220166. [[CrossRef](#)]
3. Ventura, R.; Mallet, V.; Issarny, V. Assimilation of Mobile Phone Measurements for Noise Mapping of a Neighborhood. *J. Acoust. Soc. Am.* **2018**, *144*, 1279–1292. [[CrossRef](#)]
4. Alsina-Pagès, R.M.; Ginovart-Panisello, G.J.; Freixes, M.; Radicchi, A. A Soundwalk in the Heart of Poblenou Superblock in Barcelona: Preliminary Study of the Acoustic Events. *Noise Mapp.* **2021**, *8*, 207–216. [[CrossRef](#)]
5. Bonet-Solà, D.; Vidaña-Vila, E.; Alsina-Pagès, R.M. Prediction of the Acoustic Comfort of a Dwelling Based on Automatic Sound Event Detection. *Noise Mapp.* **2023**, *10*, 20220177. [[CrossRef](#)]
6. Lee, H.P.; Lim, K.M.; Garg, S. A Case Study of Recording Soundwalk of Miyajima and Itsukushima Shrine Using Smartphone. *Acoust. Aust.* **2018**, *46*, 349–361. [[CrossRef](#)]
7. Aletta, F.; Brambilla, G.; Maffei, L.; Masullo, M. Urban Soundscapes: Characterization of a Pedestrian Tourist Route in Sorrento (Italy). *Urban Sci.* **2017**, *1*, 4. [[CrossRef](#)]
8. Bonet-Solà, D.; Vidaña-Vila, E.; Alsina-Pagès, R.M. Analysis and Acoustic Event Classification of Environmental Data Collected in a Citizen Science Project. *Int. J. Environ. Res. Public Health* **2023**, *20*, 3683. [[CrossRef](#)] [[PubMed](#)]
9. Vidaña-Vila, E.; Navarro, J.; Stowell, D.; Alsina-Pagès, R.M. Multilabel Acoustic Event Classification Using Real-World Urban Data and Physical Redundancy of Sensors. *Sensors* **2021**, *21*, 7470. [[CrossRef](#)]
10. Sugai, L.S.M.; Silva, T.S.F.; Ribeiro, J.W.; Llusia, D. Terrestrial Passive Acoustic Monitoring: Review and Perspectives. *Bioscience* **2019**, *69*, 5–11. [[CrossRef](#)]
11. Erbe, C.; Thomas, J.A. (Eds.) Choosing Equipment for Animal Bioacoustic Research. In *Exploring Animal Behavior through Sound*, 1st ed.; Springer Nature: Cham, Switzerland, 2022; Volume 1, pp. 37–86.
12. Gibb, R.; Browning, E.; Glover-Kapfer, P.; Jones, K.E. Emerging Opportunities and Challenges for Passive Acoustics in Ecological Assessment and Monitoring. *Methods Ecol. Evol.* **2019**, *10*, 169–185. [[CrossRef](#)]
13. Benocci, R.; Brambilla, G.; Bisceglie, A.; Zambon, G. Eco-Acoustic Indices to Evaluate Soundscape Degradation Due to Human Intrusion. *Sustainability* **2020**, *12*, 10455. [[CrossRef](#)]
14. Bradfer-Lawrence, T.; Gardner, N.; Bunnefeld, L.; Bunnefeld, N.; Willis, S.G.; Dent, D.H. Guidelines for the Use of Acoustic Indices in Environmental Research. *Methods Ecol. Evol.* **2019**, *10*, 1796–1807. [[CrossRef](#)]
15. Sugai, L.S.M.; Desjonquères, C.; Silva, T.S.F.; Llusia, D. A Roadmap for Survey Designs in Terrestrial Acoustic Monitoring. *Remote Sens. Ecol. Conserv.* **2020**, *6*, 220–235. [[CrossRef](#)]
16. Benocci, R.; Potenza, A.; Bisceglie, A.; Roman, H.E.; Zambon, G. Mapping of the Acoustic Environment at an Urban Park in the City Area of Milan, Italy, Using Very Low-Cost Sensors. *Sensors* **2022**, *22*, 3528. [[CrossRef](#)]
17. Beason, R.D.; Riesch, R.; Koricheva, J. Investigating the Effects of Tree Species Diversity and Relative Density on Bird Species Richness with Acoustic Indices. *Ecol. Indic.* **2023**, *154*, 110652. [[CrossRef](#)]

18. Retamosa Izaguirre, M.; Barrantes Madrigal, J. Soundscape Structure in Forests Surrounded by Protected and Productive Areas in Central Costa Rica. *Front. Remote Sens.* **2023**, *4*, 1051555. [[CrossRef](#)]
19. Dröge, S.; Martin, D.A.; Andriafanomezantsoa, R.; Burivalova, Z.; Fulgence, T.R.; Osen, K.; Rakotomalala, E.; Schwab, D.; Wurz, A.; Richter, T.; et al. Listening to a Changing Landscape: Acoustic Indices Reflect Bird Species Richness and Plot-Scale Vegetation Structure across Different Land-Use Types in North-Eastern Madagascar. *Ecol. Indic.* **2021**, *120*, 106929. [[CrossRef](#)]
20. Chen, Y.F.; Luo, Y.; Mammides, C.; Cao, K.F.; Zhu, S.; Goodale, E. The Relationship between Acoustic Indices, Elevation, and Vegetation, in a Forest Plot Network of Southern China. *Ecol. Indic.* **2021**, *129*, 107942. [[CrossRef](#)]
21. Sethi, S.S.; Bick, A.; Ewers, R.M.; Klinck, H.; Ramesh, V.; Tuanmu, M.-N.; Coomes, D.A. Limits to the Accurate and Generalizable Use of Soundscapes to Monitor Biodiversity. *Nat. Ecol. Evol.* **2023**, *7*, 1373–1378. [[CrossRef](#)]
22. Bradfer-Lawrence, T.; Bunnefeld, N.; Gardner, N.; Willis, S.G.; Dent, D.H. Rapid Assessment of Avian Species Richness and Abundance Using Acoustic Indices. *Ecol. Indic.* **2020**, *115*, 106400. [[CrossRef](#)]
23. Ulloa, J.S.; Hauptert, S.; Latorre, J.F.; Aubin, T.; Sueur, J. Scikit-Maad: An Open-Source and Modular Toolbox for Quantitative Soundscape Analysis in Python. *Methods Ecol. Evol.* **2021**, *12*, 2334–2340. [[CrossRef](#)]
24. Merchant, N.D.; Fristrup, K.M.; Johnson, M.P.; Tyack, P.L.; Witt, M.J.; Blondel, P.; Parks, S.E. Measuring Acoustic Habitats. *Methods Ecol. Evol.* **2015**, *6*, 257–265. [[CrossRef](#)]
25. Mennitt, D.J.; Fristrup, K.M. Obtaining Calibrated Sound Pressure Levels from Consumer Digital Audio Recorders. *Appl. Acoust.* **2012**, *73*, 1138–1145. [[CrossRef](#)]
26. Luna-Naranjo, D.; Martínez, J.D.; Sánchez-Giraldo, C.; Daza, J.M.; López, J.D. Quantifying and Mitigating Recorder-Induced Variability in Ecological Acoustic Indices. *bioRxiv* **2023**. [[CrossRef](#)]
27. Audacity Team Audacity, Free Audio Editor and Recorder 2021. Available online: <https://www.audacityteam.org/> (accessed on 28 June 2024).
28. Zambon, G.; Potenza, A.; Confalonieri, C.; Bisceglie, A.; Canedoli, C.; Schioppa, E.P.; Benocci, R. Acoustic Monitoring to Evaluate the Effect of Anthropogenic Noise within a Park. In Proceedings of the Internoise 2022—51st International Congress and Exposition on Noise Control Engineering, Glasgow, UK, 21–24 August 2022.
29. Benocci, R.; Potenza, A.; Bisceglie, A.; Confalonieri, C.; Canedoli, C.; Schioppa, E.P.; Zambon, G.; Roman, H.E. Towards an Environmental Sound Map at Parco Nord of Milan, Italy. In Proceedings of the Internoise 2022—51st International Congress and Exposition on Noise Control Engineering, Glasgow, UK, 21–24 August 2022.
30. Cocroft, R.B.; Hamel, J.; Su, Q.; Gibson, J. Vibrational Playback Experiments: Challenges and Solutions. In *Studying Vibrational Communication*; Springer: Berlin/Heidelberg, Germany, 2014; pp. 249–274. [[CrossRef](#)]
31. The MathWorks Inc. MATLAB Version: 9.14.0.2206163 (R2023a); The MathWorks Inc.: Natick, MA, USA, 2022. Available online: <https://www.mathworks.com> (accessed on 28 June 2024).
32. Youngworth, R.N.; Gallagher, B.B.; Stamper, B.L. An Overview of Power Spectral Density (PSD) Calculations. In Proceedings of the Optical Manufacturing and Testing VI, San Diego, CA, USA, 18 August 2005; Volume 5869, pp. 206–216.
33. Arva, M.-C.; Bizon, N.; Stanica, M.; Diaconescu, E. A Review of Different Estimation Methods of DC Offset Voltage For Periodic-Discrete Signals. In Proceedings of the 2019 11th International Conference on Electronics, Computers and Artificial Intelligence (ECAI), Pitesti, Romania, 27–29 June 2019; pp. 1–5.

34. Smith, J.O. (Ed.) Frequency response analysis. In *Introduction to Digital Filters: With Audio Applications*; W3K Publishing: Stanford, CA, USA, 2007; pp. 149–174.
35. Hao, Z.; Wang, C.; Sun, Z.; van den Bosch, C.K.; Zhao, D.; Sun, B.; Xu, X.; Bian, Q.; Bai, Z.; Wei, K.; et al. Soundscape Mapping for Spatial-Temporal Estimate on Bird Activities in Urban Forests. *Urban For. Urban Green.* **2021**, *57*, 126822. [[CrossRef](#)]
36. Pieretti, N.; Farina, A.; Morri, D. A New Methodology to Infer the Singing Activity of an Avian Community: The Acoustic Complexity Index (ACI). *Ecol. Indic.* **2011**, *11*, 868–873. [[CrossRef](#)]
37. Villanueva-Rivera, L.J.; Pijanowski, B.C.; Doucette, J.; Pekin, B. A Primer of Acoustic Analysis for Landscape Ecologists. *Landsc. Ecol.* **2011**, *26*, 1233–1246. [[CrossRef](#)]
38. Boelman, N.T.; Asner, G.P.; Hart, P.J.; Martin, R.E. Multi-trophic invasion resistance in Ha-waii: Bioacoustics, field surveys, and airborne remote sensing. *Ecol. Appl.* **2007**, *8*, 2137–2144. [[CrossRef](#)]
39. Kasten, E.P.; Gage, S.H.; Fox, J.; Joo, W. The Remote Environmental Assessment Laboratory's Acoustic Library: An Archive for Studying Soundscape Ecology. *Ecol. Inf.* **2012**, *12*, 50–67. [[CrossRef](#)]
40. Fairbrass, A.J.; Rennett, P.; Williams, C.; Titheridge, H.; Jones, K.E. Biases of Acoustic Indices Measuring Biodiversity in Urban Areas. *Ecol. Indic.* **2017**, *83*, 169–177. [[CrossRef](#)]
41. Sueur, J.; Pavoine, S.; Hamerlynck, O.; Duvail, S. Rapid acoustic survey for biodiversity appraisal. *PLoS ONE* **2008**, *3*, e4065. [[CrossRef](#)]
42. Quinn, C.A.; Burns, P.; Hakkenberg, C.R.; Salas, L.; Pasch, B.; Goetz, S.J.; Clark, M.L. Soundscape Components Inform Acoustic Index Patterns and Refine Estimates of Bird Species Richness. *Front. Remote Sens.* **2023**, *4*, 1156837. [[CrossRef](#)]
43. Eldridge, A.; Guyot, P.; Moscoso, P.; Johnston, A.; Eyre-Walker, Y.; Peck, M. Sounding out Ecoacoustic Metrics: Avian Species Richness Is Predicted by Acoustic Indices in Temperate but Not Tropical Habitats. *Ecol. Indic.* **2018**, *95*, 939–952. [[CrossRef](#)]
44. Brambilla, G.; Benocci, R.; Potenza, A.; Zambon, G. Stabilization Time of Running Equivalent Level LAeq for Urban Road Traffic Noise. *Appl. Sci.* **2023**, *13*, 207. [[CrossRef](#)]
45. Kim Tae Kyun T Test as a Parametric Statistic. *Korean J. Anesth.* **2015**, *68*, 540–546. [[CrossRef](#)]
46. Osborne, P.E.; Alvares-Sanches, T.; White, P.R. To Bag or Not to Bag? How AudioMoth-Based Passive Acoustic Monitoring Is Impacted by Protective Coverings. *Sensors* **2023**, *23*, 7287. [[CrossRef](#)]
47. Alcocer, I.; Lima, H.; Sugai, L.S.M.; Llusia, D. Acoustic Indices as Proxies for Biodiversity: A Meta-Analysis. *Biol. Rev.* **2022**, *97*, 2209–2236. [[CrossRef](#)]
48. Llusia, D. The Limits of Acoustic Indices. *Nat. Ecol. Evol.* **2024**, *8*, 606–607. [[CrossRef](#)]

Chapter 3.

Preliminary Results On Audio Event Classification Applied To A University Square In Milan (Italy) Before An Urban Regeneration Project

Andrea Potenza, Ester Vidaña-Vila, Andrea Afify, Roberto Benocci, Rosa Maria Alsina-Pagès, Giovanni Zamboni

Forum Acusticum 2025

doi: <https://dx.doi.org/10.61782/fa.2025.0157>

Abstract

Biophonies, anthropophonies and geophonies characterize and shape an environment and contribute to the human appreciation of that place. Thus, sound event classification can be a useful tool to assess its quality and detect changes affecting it.

In this study, different machine learning models for multilabel sound classification are tested to monitor the ante-opera situation of the renewed square “Piazza della Scienza” of the University of Milano-Bicocca (Italy). The one-week monitoring was performed in May 2023 using 7 Song-Meter-Micros. The recordings were equalized to correct the devices’ nonlinear frequency response.

The paper is structured to: (a) test two sets of features in the Piazza’s polluted soundscape by constant ventilation noise and other anthropogenic sources: YAMNet embeddings and classic audio features (such as MFCCs), (b) find the best algorithm between: decision tree, random forest, k-nearest neighbor and support vector classifier and (c) evaluate their performance when filtering the background ventilation noise to increase the datasets size.

Preliminary results are presented with the final aim of optimizing the detection and applying it to describe the Piazza’s soundscape, investigate differences in events spatial distribution, and evaluate the effects of the urban regeneration plan on the soundscape.

3.1 Introduction

Noise pollution is a major environmental health concern in Europe since noise made by traffic, trains and airplanes is the second most important cause of disease, behind air pollution caused by very fine particulate matter [1]. This issue is particularly impactful in urban areas where about 60% of the European population will live by 2050 [1, 2].

In urban centers there are multiple anthropogenic sound sources often overlapping with one another (e.g., engines idling, car horns, technical installations, sirens and alarms, nightlife) [3] and with biophonic sounds (e.g., birds vocalizations, dog barking, cicada sounds) and geophonic ones (e.g. wind, rain, thunder). The noise impact on humans does not depend solely on the overall sound pressure level but also on the typology of noise sources, the individual sensitivity and the social and cultural context [3–5]. This reasoning is also valid for faunal communities which are impacted by noise depending on its typology and on species' aural sensitivity [6, 7]. For these reasons, sound event classification is a topic that gained greater importance in these years and many studies have dealt with it. This technique applied to open environments is useful in many applications, from automatically discriminating against adverse meteorological conditions in large datasets [8,9], to detect specific noises [8] and to collect events for soundscape assessments [10] and bio/ecoacoustic analyses [8, 9, 11, 12]. Linked to urban settlements, many works have been performed on event classification from real in-field recordings, focusing on single events or on overlapping multiple events [10–12]. In this work, sound event classification is applied to a university square in Milan (Italy) which is heavily impacted by constant technical installation noise. The study's final aim is to develop a classifier for different sound events (i.e., road traffic, tram passages, speech, sirens) which will be used to assess the changes in the square's sound environment after an architecture requalification [13] which will improve the public space usage and increase the surface occupied by trees, bushes and lawns instead of cement.

Moreover, the classification will allow a better understanding of the ecoacoustic indices behavior in urban environments and of people's acoustic environment perception already carried out in the square. In this paper, the efficacy of two sets of features on the square recordings was tested: the YAMNet embeddings and more classical features, such as the

Mel-frequency cepstral coefficients (MFCCs), using different machine learning classifiers: Decision tree, Random forest, K-nearest neighbor e Support vector classifier.

3.2 Materials and Methods

3.2.1 Study area

The area under study is the main square of the University of Milano-Bicocca called “Piazza della Scienza”. It is located in the Bicocca neighborhood on the north outskirts of Milan, an area which went through a renovation process in the last fifty years, shifting from an industrial site to a university and third sector district. The Piazza covers a surface area of 8590 sqm and is surrounded by 6-floor buildings and arranged on two levels: a fully cemented ground level and four lowered courtyards, three of them with a lawn cover. In 2024, the Piazza underwent a regeneration process thanks to the MUSA project (Multilayer Urban Sustainability Action) [13]. This project is set into the framework of the National Recovery and Resilience Plan (NRRP) and aims at proposing management strategies to face the environmental, social, and economic sustainability challenges of the metropolitan city of Milan.

The Piazza renovation aims to increase its environmental sustainability in terms of reducing the heat island effect, increasing the water descent into the aquifer, reducing local air pollution, and improving the area’s biodiversity. Moreover, it will allow a better use of the public space and increase students’ quality of life in the Piazza. These results will be achieved through the depaving and greening of the ground level and the renewal of the lowered courts (Figure 19).



Figure 19. Piazza della Scienza before (A) and after (B) the regeneration process of MUSA.

3.2.2 Data collection and annotation

The monitoring campaign used to populate the database was performed in May 2023, from Monday 22nd to Sunday 28th, in 7 sites of the Piazza (Figure 20). To capture the different sound sources present, 2 devices were placed on the ground level floor, 2 in the lowered courtyards and 3 on the first floor of the buildings.

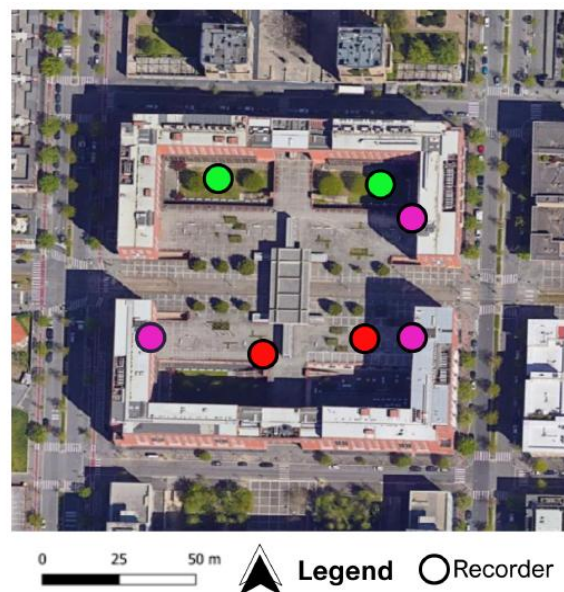


Figure 20. Piazza della Scienza (before the regeneration) and recording sites (pink: first floor, red: ground floor, green: lowered courtyards).

The Song Meter Micros from Wildlife acoustic were used, set with a sampling rate of 48 kHz and an amplitude gain of +12 dB, recording for 1 minute and pausing for 1 minute.

Furthermore, the recordings were equalized to correct the devices' nonlinear frequency response [14,15]. In the Supplementary Materials of [14] it is available the open-source MATLAB script for equalizing the recordings and obtaining linear-comparable audio files with other devices and between ecoacoustic studies. The recording campaign resulted in a total of 75 hours of acoustic data per sensor.

The labelling process was performed on Audacity following previous works of coauthors [16]. Audacity is an audio recording and editing software which allows users to select part of an audio file and associate a text label with it. These labels can be exported in a text file (txt) as a list indicating the labels' name and their starting and ending time (time is expressed in seconds and calculated referencing to the audio beginning as the time zero). In this work, a single label was applied to each sound event independently of its time duration. The total labelled time is 2 hours and 5 minutes. The label taxonomy was adapted from [17] to fit the particular sound events present in the Piazza and discharge those not happening.

In Table 5 are reported the 18 labels kept for this study area and their total time duration in the dataset. To be fed into the classifiers, the txt files from Audacity were converted into one-hot-encoded format.

Table 5. Event labels present in the dataset, their description and total time duration.

Label	Description	Duration (min)
Road	Road traffic	17.55
Brake	Brake noise from vehicles and tram	5.65
Car horn	Car horns	0.24
Vpbor	Vehicles passing by on tram rails	0.89
Tram	Tram passing by, stopping and departing	12.41
Motorbike	Motorbike engine noise and passing by	3.79
Street cleaning	Street cleaning vehicles and operators	1.09
Siren	Ambulance and police sirens	6.10
Signal-Alarm	Signals and alarm noises	4.22
Construction	Noises from construction sites	3.29
Trolley-Cart	Cart and trolley noises on pavementation	5.39
Bird	Birds' vocalizations	5.29
Dog	Dogs' barks	0.34
Insects	Insects sound	4.33
Wind	Wind gusts	1.66
Speech	Speech and human voices, exclamations, laughs	21.57
Ventilation	Technical installation noise	125.00
Complex	Unclassified sounds	3.23

3.2.3 Feature extraction

To detect the sound events in the Piazza two methods have been used to test their efficiency:

- YAMNET's embeddings.
- Features from the python package librosa.

YAMNet's embeddings

YAMNet is a pre-trained neural network model which has been used in many works in literature to perform sound event detection [9, 18] or to obtain features to be used as features for other algorithms [19]. The model relies on the MobileNet V1 architecture which consists of 27 convolutional layers, 1 global average pooling layer, and 1 fully connected layer; it employs ReLU activation functions, batch normalization and Softmax activation to obtain an output feature vector of size 1024 [20, 21]. The model predicts the 521 sound event classes of the AudioSet corpus [22]. Each audio file is first downsampled at 16 kHz and normalized to fit the AudioSet requirements before calculating the features (embeddings) on a time window of 0.96 seconds with a 50% overlap. The embeddings calculation is explained here [23] but, shortly, they are logarithmic Mels calculated in the range 0.125 - 7.5 kHz and fed to the MobileNet V1 model. As the final step, the model calculates the output scores for each of the 521 AudioSet classes. In our study, YAMNet was used as a feature extractor on each labelled audio file and each 0.96 seconds time frame is characterized by 1024 features.

Features from the python package librosa

To compare YAMNet's features performances, another set of features have been calculated. In particular, the python package librosa [24] was used. In this case, downsampling and normalization were not applied. The features were calculated on a 1-second time frame and a 20-millisecond time frame without overlapping; the double timeframes are kept to understand their influence on the classification.

The following spectral features were calculated following previous works [25]:

- Mel-frequency cepstral coefficients (MFCCs), using a number of coefficients of 13.
- Spectral centroid (SC).
- Roll-off frequency, with a rollpercent of 10 and 90.
- Amplitude root-mean-square (RMS).
- Zero-crossing rate (ZCR).
- Static tempo.
- Flatness.
- Spectral bandwidth.

For each feature (except MFCCs and static tempo), 7 statistical descriptors were calculated: minimum, maximum, mean, median, standard deviation, skewness and kurtosis [25]. Thus, each 1-second time frame is characterized by 1272 values (of which 1222 are MFCCs), while each 20-millisecond time frame by 297 values (of which 247 are MFCCs).

3.2.4 Data filtering to increase the datasets

To increase the number of recordings populating the datasets, filtration of the ventilation noise (label “Ventilation”) has been carried out. This operation have been achieved using the “Noise Reduction” function of Audacity. This function elaborates the noise profile of a recording and uses it to reduce that noise in other recordings.

For each site, a midnight recording containing only ventilation noise was selected. Two settings were applied:

- T1 (Noise reduction: 6 dB, Sensitivity: 5, Frequency Smoothing = 4)
- T2 (Noise reduction: 10 dB, Sensitivity: 10, Frequency Smoothing = 8).

Furthermore, due to uneven occurrences of labels (see Table 2 and Figure 3), in the filtered recordings the label with the highest occurrence (“Speech”) and the corresponding features were removed when the event was not overlapped with others.

After these filtering and balancing processes, the datasets are shaped as reported in Table 6 and in Figure 21.

Table 6. Labels occurrences in each dataset.

Label	YAMNet OR	YAMNet filt	Librosa 1s OR	Librosa 1s filt	Librosa 20ms OR	Librosa 20ms filt
-------	-----------	-------------	---------------	-----------------	-----------------	-------------------

Road	2'211	1'115	6'633	3'345	5'435	16'305
Brake	738	2'214	397	1'191	1'866	5'598
Car horn	37	111	26	78	104	312
Vpbor	135	405	105	315	425	1'275
Tram	1'566	4'698	792	2'376	3'844	11'532
Motorbike	488	1'464	260	780	1'241	3'723
Street cleaning	137	411	67	201	334	1'002
Siren	761	2'283	373	1'119	1'842	5'526
Signal-Alarm	536	1'608	285	855	1'384	4'044
Construction	426	1'278	235	705	1'095	3'285
Trolley-Cart	692	2'076	368	1'104	1'760	5'280
Bird	755	2'265	467	1'401	2'074	6'222
Dog	51	153	37	111	158	474
Insects	556	1'668	279	837	1'370	4'110
Wind	240	720	143	429	640	1'920
Speech	2'750	4'864	1'457	2'733	6'931	12'649
Complex	487	1'461	347	1'041	1'430	4'290

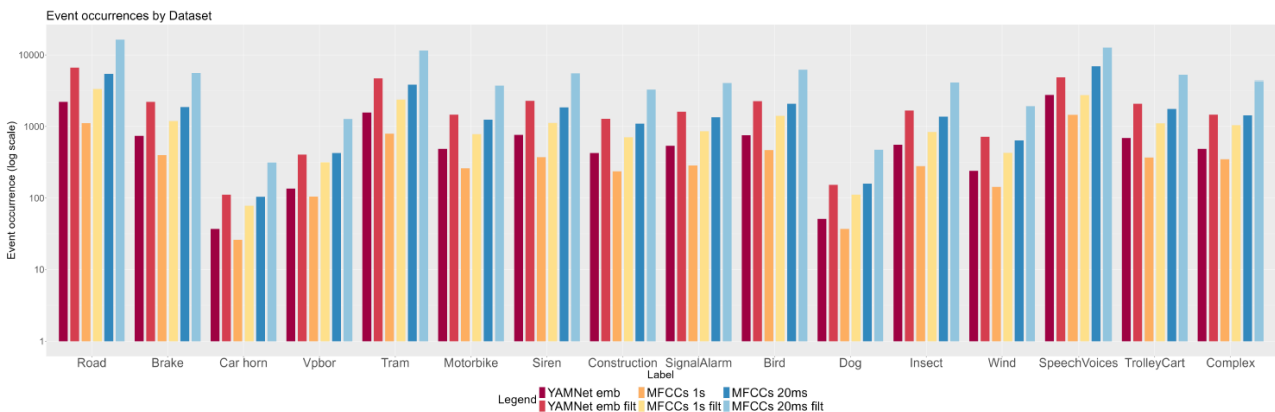


Figure 21. Labels occurrences in each dataset

3.2.5 Detection

For the detection of sound events, different classification models have been implemented in the Python environment. A pipeline has been built to run the following classification models: decision tree (DT), random forest (RF), k-nearest neighbor (KNN), support vector classifier (SVC). These algorithms are executed to perform a multioutput classification to classify overlapping sound events.

Different trials have been performed using three different scalers (standardscaler, minmaxscaler, robustscaler); standardscaler subtracts the mean and scales the data to unit variance, minmaxscaler uses the maximum and minimum values of the dataset to rescale the features in the range [0, 1], and robustscaler is based on the percentiles thus is less affected by outliers [26].

The datasets have been split into training (80%) and testing (20%) using the train test split command from sklearn. The best classifier will be chosen based on three metrics: Precision, Recall and F1-Score.

3.3 Result and Discussion

In Table 7 and Table 8, the best values of Precision, Recall and F1-score are reported for each label and feature typology, indicating the relative dataset, classifier and scaler.

Table 7. Best results using the YAMNet embeddings.

Label	Precision	Recall	F1-score	Dataset	Classifier and scaler
Road	0.64	0.67	0.65	Filter	DT - Std
Brake	0.59	0.62	0.61	Filter	DT - Std
Car horn	1.00	0.45	0.62	Filter	RF - Std
Vpbor	0.56	0.71	0.63	Filter	DT - Std
Tram	0.59	0.65	0.62	Filter	DT - Std
Motorbike	0.53	0.64	0.58	Filter	DT - Std
Street cleaning	0.71	0.77	0.74	Filter	DT - Std
Siren	0.83	0.83	0.83	Filter	DT - Std
Signal-Alarm	0.55	0.61	0.58	Filter	DT - Std
Construction	0.64	0.63	0.63	Filter	DT - Std
Trolley-Cart	0.66	0.67	0.67	Filter	DT - Std
Bird	0.96	0.61	0.74	Filter	RF - Std
Dog	0.45	0.45	0.45	Filter	DT - Std
Insects	0.73	0.72	0.72	Filter	DT - Std
Wind	0.48	0.56	0.52	Filter	DT - Std
Speech	0.91	0.68	0.78	Filter	RF - Std
Complex	0.56	0.56	0.56	Filter	DT - Std

Table 8. Best results using the Librosa features.

Label	Precision	Recall	F1-score	Dataset	Classifier and scaler
Road	0.97	0.61	0.75	20ms Filter	RF - Std
Brake	0.58	0.59	0.58	20ms Filter	DT - Std

Car horn	0.40	0.57	0.47	20ms Filter	RF - Std
Vpbor	0.50	0.60	0.55	20ms Filter	DT - Std
Tram	0.98	0.59	0.74	20ms Filter	RF - Std
Motorbike	0.60	0.64	0.60	20ms Filter	DT - Std
Street cleaning	0.95	0.88	0.91	20ms Filter	SVC - Std
Siren	0.98	0.86	0.92	20ms Filter	RF - Std
Signal-Alarm	0.99	0.56	0.72	20ms Filter	RF - Std
Construction	0.97	0.65	0.78	20ms Filter	SVC - Std
Trolley-Cart	0.99	0.70	0.82	20ms Filter	RF - Std
Bird	0.57	0.64	0.60	20ms Filter	DT - Std
Dog	0.44	0.51	0.47	20ms Filter	DT - Std
Insects	0.93	0.74	0.82	20ms Filter	RF - Std
Wind	0.61	0.61	0.61	20ms Filter	DT - Std
Speech	0.94	0.55	0.70	20ms Filter	RF - Std
Complex	0.54	0.58	0.56	20ms Filter	DT - Std

Looking at the "Dataset" columns of Table 7 and Table 8, we found that the classifiers performed better with the augmented datasets (occurrences increased by filtering the Ventilation background noise). Regarding the librosa features timeframe, the 20-ms windowing allowed a better performance.

Focusing on the typology of Classifier and Scaler, the most frequent one are the Decision Tree (DT), followed by the Random Forest (RF), and the StandardScaler (Std).

In Table 7 (YAMNet embeddings), it is possible to notice that the majority of the F1-scores are above 60% with Street cleaning, Siren, Bird, Insect and Speech being over 70%. On the other hand, in Table 8 (Librosa features) events that have an F1-score higher than 70% are Street cleaning, Siren, Insect, Speech, Road, Tram, SignalAlarm, Construction and TrolleyCart. Dog barking obtained the lowest scores, probably due to its lower occurrence in the dataset (Table 6) and the masking caused by ventilation systems. Siren got the highest score, probably because of its marked distinguished spectrum.

When comparing the F1-score between the datasets, the librosa features received higher scores for the majority of labels. This trend is also visible for Precision and Recall, even if not for the same sound events.

3.4 Conclusions

Sound classification is a rich and growing research field in various acoustic branches nowadays and has been applied to numerous case studies around the world. This paper is focused on classifying the sounds occurring in the Piazza della Scienza in Milan, Italy.

These preliminary results provide important insights which show the better performance of the models using the librosa features instead of the YAMNet embeddings and the usage of a shorter time frame. Future analyses will be implemented on the librosa features dataset. They will consist of different steps like the implementation of confusion matrices and the application of a cross validation. Moreover, the GridSearch algorithm will be applied for tuning the models' hyperparameters. Furthermore, other algorithms will be tested (i.e., CNN-models) and the effects of the time window size on the performances will be studied. Finally, transfer learning will be taken into account to increase the dataset size, alongside the addition of audios recorded outside the Piazza to bypass the ventilation background noise.

References

- [1] B. Lex, Burden of disease from environmental noise. Quantification of healthy life years lost in Europe. City: World Health Organization, 2011.
- [2] U. N. D. of Economic and S. Affairs, World Urbanization Prospects: The 2018 Revision. City: United Nations, 2019.
- [3] M. Raimbault and D. Dubois, "Urban soundscapes: Experiences and knowledge," *Cities*, vol. 22, no. 5, pp. 339–350, 2005.
- [4] S. Dreger, S. A. Schöule, L. K. Hilz, and G. Bolte, "Social inequalities in environmental noise exposure: a review of evidence in the who european region," *International journal of environmental research and public health*, vol. 16, no. 6, p. 1011, 2019.
- [5] N. Singh and S. C. Davar, "Noise pollution-sources, effects and control," *Journal of Human ecology*, vol. 16, no. 3, pp. 181–187, 2004.
- [6] R. J. Dooling and A. N. Popper, "The effects of highway noise on birds. report to the california. Department of transportation, division of environmental analysis, sacramento, california," 2007.
- [7] D. Waddington, M. Wood, B. Davies, and R. Young, "Habitats: Managing the ecological impacts of noise on wildlife habitats for sustainable development," in *INTER-NOISE and NOISE-CON Congress and Conference Proceedings*, vol. 265, pp. 5247–5251, Institute of Noise Control Engineering, 2023.
- [8] A. Brown, S. Garg, and J. Montgomery, "Automatic rain and cicada chorus filtering of bird acoustic data," *Applied Soft Computing*, vol. 81, p. 105501, 2019.
- [9] F. Terranova, L. Betti, V. Ferrario, O. Friard, K. Ludynia, G. S. Petersen, N. Mathevon, D. Reby, and L. Favaro, "Windy events detection in big bioacoustics datasets using a pre-trained convolutional neural network," *Science of the Total Environment*, vol. 949, p. 174868, 2024.
- [10] D. Bonet-Solà, E. Vidana-Vila, and R. M. Alsina-Pagès, "Prediction of the acoustic comfort of a dwelling based on automatic sound event detection," *Noise Mapping*, vol. 10, no. 1, p. 20220177, 2023.
- [11] B. Swaminathan, M. Jagadeesh, and S. Vairavasundaram, "Multi-label classification for acoustic bird species detection using transfer learning approach," *Ecological Informatics*, vol. 80, p. 102471, 2024.

[12] Devos, Paul, "Birdsong of common birds in an urban soundscape as evaluated with recurrent neural networks," in Forum Acusticum 2023 : 10th Convention of the European Acoustics Association, Proceedings, p. 2, 2023.

[13] MUSA, "Multilayered urban sustainability action," 2023. Available at: <https://musascarl.it/>, Accessed on: 31-03-2025.

[14] A. Potenza, V. Zaffaroni-Caorsi, R. Benocci, G. Guagliumi, J. M. Fouani, A. Bisceglie, and G. Zambon, "Biases in ecoacoustics analysis: A protocol to equalize audio recorders," Sensors (Basel, Switzerland), vol. 24, no. 14, p. 4642, 2024.

Chapter 4.

Ecoacoustic monitoring of a regenerated university square and two urban parks: a multidisciplinary approach using ecoacoustic indices, sound events classification and BirdNET

Andrea Potenza, Giorgia Guagliumi, Andrea Afify, Roberto Benocci, Riccardo Tentori, Ilaria Grecchi, Valentina Zaffaroni-Caorsi, Ester Vidaña-Vila, Rosa Maria Alsina-Pagès, Valerio Orioli, Luciano Bani, Giovanni Zambon

Abstract

Ecoacoustics studies the sonoscape to assess ecological process, areas' biodiversity and changes in faunal population and influence of anthropogenic disturbances like human presence and noise pollution.

Of all ecoacoustics studies, urban settlements are scarcely studied, probably due to their homogeneous structure, heavy impacts generated by human activities and complex sonoscapes composed of multiple overlapping sound sources. In these contexts, urban regeneration processes are blooming aiming at restoring degraded areas, creating new green areas to contrast heat island effect and improve people's life quality and wellbeing.

In this study the effects of an urban regeneration intervention on a university public square in Milan (Italy) are investigated. To understand if the changed regenerated sonoscape is similar to the one of urban parks, two monitoring have been carried out in a peri-urban Regional Park (Parco Nord) and in a small pocket park, both near the Bicocca University.

The ante and post-operam sonoscapes recorded using Song Meter Micros while Song Meter Micro and Audiomoth have been used to monitor the green areas. Due to the different devices, the equalization procedure has been applied.

The Piazza has been studied using ecoacoustic indices (ACI, ADI, AEI, H, DSC, ZCR, NP), a custom-made machine learning model to classify sound events, BirdNET and a linear mixed-effects model. The two green areas were investigated by means of ecoacoustic indices (ACI, ADI, AEI, H, ZCR) and BirdNET.

Ecoacoustic indices setting parameters values were calculated according to the areas' sonoscape (i.e., dB threshold) while ADI, AEI H and ZCR have been modified to include the maximum and minimum frequency thresholds. These indices detected a sonoscape change, in terms of higher variance of indices' values, which has been confirmed by the computation of the cosine dissimilarity index.

In the Piazza, boxplot analysis, PCA and dissimilarity index computed on the ecoacoustic indices assessed changes in its sonoscape. The machine learning classifier confirmed it in terms of a different presence and time occupancy of the 17 sound classes considered,

especially for speech, birds vocalizations and cart passages. Alongside, BirdNET proved it as improved avian richness after the renovation as well as vocalizations rates distribution changes throughout the day. Finally, the linear mixed-effects model was employed to address the effect of species richness, birds' presence and five sound classes' presence on ACI. The model confirmed the change in ACI values after the intervention and the existence of a relationship between ACI and avian richness, birds' vocalizations and human speech.

When comparing the Piazza with Vivarium and Parco Nord, the PCA, dissimilarity index and non-parametric multidimensional scaling detected a clear acoustic separation between the ante-operam Piazza and the two urban green areas. After the regeneration, the square showed a higher acoustic variability and a partial convergence towards the characteristics of the soundscape of the parks, especially at the ground floor and courtyards measurement sites where pavement removal and greening occurred. BirdNET results highlighted an increment of avian richness in the square and an even temporal distribution of vocalization rates which is similar to the parks investigated.

These findings confirm the efficacy of ecoacoustics as a multifaceted tool (indices and sound event classification) to assess the effectiveness of urban regeneration projects in terms of soundscape changes. This has been particularly evident in this case where no direct action has been undertaken on noise sources present in the square yet a positive effect on the soundscape has been produced.

4.1 Introduction

Noise pollution is the second most common human health issue in Europe, after air pollution [1]. Exposure to environmental noise has been linked to a wide range of adverse outcomes, including physiological stress, sleep disturbance, cardiovascular disease, and cognitive impairment [reference in comments]. This issue is particularly impactful in urban areas where about 60% of the European population will live by 2050 [2]. In addition to affecting human health, noise pollution also impacts terrestrial and marine habitats, disturbing fauna and potentially reducing species abundance and diversity [3].

In urban environments, soundscapes play an important role in shaping both human well-being and biodiversity [4]. Several studies have shown that exposure to natural sounds, and birdsong in particular, can reduce stress, improve mood, enhance well-being, and support cognitive performance [5]. Moreover, improved emotional states have been observed in environments characterized by greenery and natural elements [6-8]. Thus, urban green areas are fundamental components of cities, especially densely populated ones, as they can serve as acoustic refuges by mitigating anthropogenic noise, promoting biophonic activity, and reintroducing vegetation into otherwise concrete-dominated landscapes [9]. At the same time, urbanization alters natural environments, causing habitat loss, fragmentation of native vegetation, and increased biotic homogenization [10, 11]. Although urban green spaces such as parks, gardens, and courtyards can support biodiversity, their ecological role depends strongly on their design, including habitat heterogeneity and the presence of water features such as wetlands or small ponds [12]. In addition, in small patches, ecosystem dynamics may be strongly influenced by external pressures from the surrounding urban matrix, including pollution and human disturbance [13].

Over the last two decades, ecoacoustic monitoring of green-area soundscapes has expanded worldwide. Based on passive acoustic monitoring (PAM), ecoacoustics provides a framework to quantify biotic and abiotic sounds and to analyse their ecological dynamics across spatial and temporal scales [14]. This approach is increasingly used for long-term environmental monitoring, including the assessment of anthropogenic impacts and the effects of management or restoration interventions [15]. Ecoacoustic studies generally rely on two complementary approaches: ecoacoustic indices and sound event detection/classification algorithms.

Ecoacoustic indices summarize soundscape structure through acoustic features and frequency-related sound-energy distributions [16-19], allowing large datasets to be synthesized and compared across areas. They have proved useful in highlighting differences among landscapes and in capturing signatures of human activity [9-11]. However, their interpretation in situ remains challenging, and comparability across studies is still limited [20-22].

Sound event detection and classification algorithms, by contrast, aim to identify specific animal, anthropogenic, or technological sounds and can therefore provide more direct ecological interpretation [23-26]. Yet they also present important limitations, including model tuning, detection reliability, and difficulties in estimating the number of sound sources [27-30]. Recent efforts to improve the interpretability of ecoacoustic indices, including reference databases and dedicated guidance resources, indicate that this remains an open methodological issue [31, 32].

Despite the growing number of ecoacoustic studies conducted in forests, mountains, marine environments, and subterranean systems [31], urban environments remain underrepresented. According to the most recent review, they account for only 4% of the terrestrial dataset, corresponding to 405 measurement sites and 21 recorded hours [31]. This underrepresentation likely reflects the methodological complexity of urban soundscapes, where overlapping sound sources, strong anthropogenic pressure, and context-dependent biases can complicate both the interpretation of ecoacoustic indices and the detection of biophonic components [26, 33]. Moreover, although ecoacoustics is increasingly used to monitor environmental change, its application to restoration and regeneration interventions in urban settings remains limited.

Urban regeneration projects have been implemented worldwide to address urban decay, strengthen social cohesion, improve environmental quality, and stimulate local economies [34-36]. Among the strategies adopted, soil de-sealing has gained attention as a way to redesign sealed urban surfaces while promoting water infiltration, reducing flood risk and urban heat island effects, and supporting biodiversity [37]. This practice consists of removing impermeable surface coverings and replacing or restructuring underlying materials to restore permeability or establish a new land use. Although applied in many urban interventions worldwide [37, 38], it is still poorly represented in the scientific literature, particularly from an ecoacoustic perspective. This gap is relevant also in light of European

Union targets calling for zero net loss of urban green space by 2030 and a net increase in urban green space coverage by 2050.

Milan represents a particularly relevant context for investigating these issues, as several urban regeneration strategies have been implemented there over time [39-41]. Within this framework, the MUSA (Multilayered Urban Sustainability Action) project supported the regeneration of Piazza della Scienza at the University of Milan-Bicocca, with the aim of reducing the heat island effect, mitigating local air pollution, and improving biodiversity and quality of life in the area. The intervention involved pavement removal and replacement, the introduction of new green elements, and broader improvements in the design of the public square. Because the project was accompanied by multidisciplinary environmental monitoring, it also offered an opportunity to evaluate whether ecoacoustic methods can detect soundscape changes associated with urban regeneration.

In this study, we investigated the regeneration of Piazza della Scienza using three complementary approaches: I. ecoacoustic indices; II. a custom-made classification model for urban sound events; and III. BirdNET for avian species assessment. In addition, we compared the soundscape of Piazza della Scienza with those of two urban green areas in Milan using ecoacoustic indices and BirdNET, in order to assess whether the regenerated square shifted towards acoustic characteristics more similar to those of established green spaces. Because of major differences in soundscape composition, the same custom classification model could not be reliably applied to the reference green areas.

Overall, this study aims to expand current knowledge of urban soundscapes, test the potential of ecoacoustics for evaluating urban regeneration processes, and contribute empirical evidence to a still limited body of literature on restoration-related acoustic change in urban environments.

4.2 Materials and Methods

4.2.1 Study areas

Three study areas were compared in this study: Piazza della Scienza, the main square of the University of Milano-Bicocca; Vivarium-Bicocca, a pocket park corresponding to a former university vivarium; and Parco Nord, a regional peri-urban park located on the northern outskirts of Milan. All three areas are located in northern Milan, and the maximum distance between monitoring points was 5.5 km (Fig. 1). Piazza della Scienza represented the intervention site, whereas Vivarium-Bicocca and Parco Nord were used as reference green areas for comparison. Their close spatial proximity reduced broad-scale climatic and geographical variability among sites.

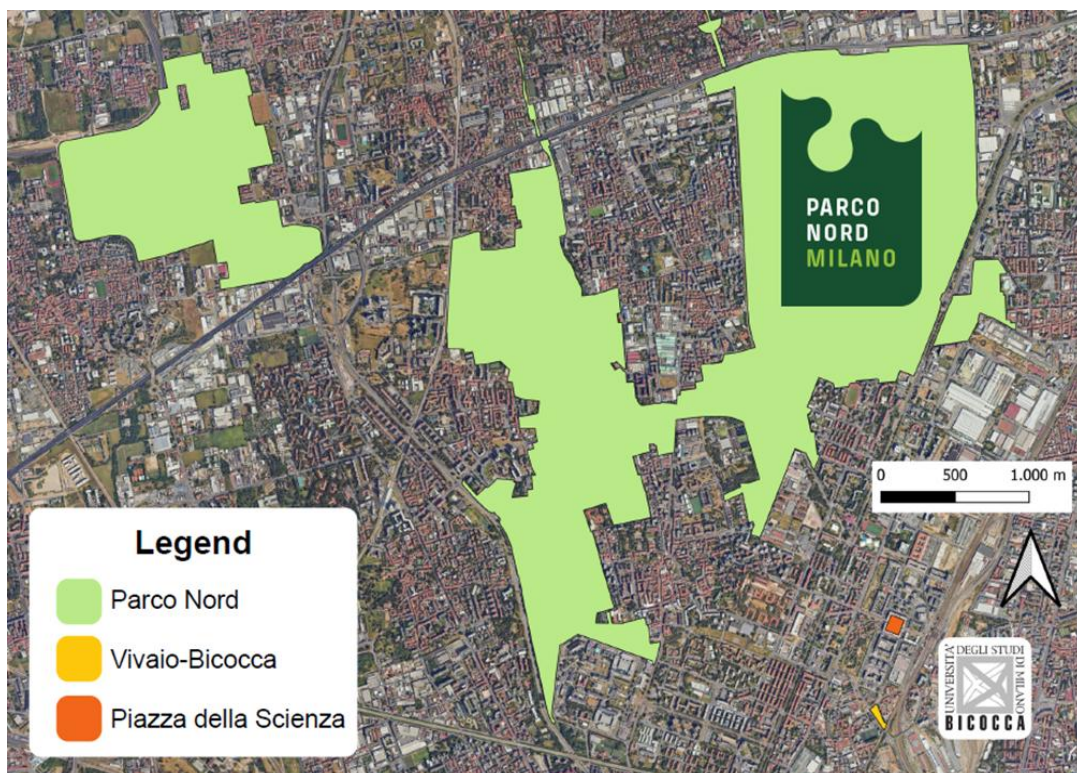


Figure 1. Map showing the three study areas.

Piazza della Scienza

The study area is the main square of the University of Milano-Bicocca, called “Piazza della Scienza”. It is set in the Bicocca neighborhood in the northern outskirts of Milan, an area

that has been renewed over the past fifty years, repurposed from an industrial site into a university and tertiary sector district.

The Piazza covers a surface area of 8'590 sqm. It is surrounded by 6-floor buildings and is arranged on two levels: a ground level and 4 lowered courtyards, 3 of them characterized by a lawn cover and three trees of the genus Tilia. The ground level is a pedestrian zone, intersected by a tram line running through its center. Dual and single carriageway roads surround the buildings.

The ante-opera Piazza (Figure 2) is characterized by a fully cemented ground floor with very minute lawn patches (both flat and on a slope) used as test areas for a preliminary study on the heat island effect. Only twelve magnolia trees are planted in the square, arranged to reflect the site's architectural symmetry.

In 2023, the Piazza underwent an urban regeneration process (Figure 2) thanks to the MUSA project (Multilayer Urban Sustainability Action). The renovation aims to increase the Piazza's environmental sustainability, reducing the heat island effect, the water run-off and the local air pollution, and improving the area's biodiversity. Moreover, it will allow better use of the public space and increase students' quality of life in the Piazza.



Figure 2. Piazza della Scienza before (left) and after (right) the MUSA regeneration project.

The ground floor was redesigned to reduce impermeable surfaces and increase greenery: 2'000 sqm were de-sealed and planted with trees, shrubs and herbaceous plants, while the remaining surface has been substituted with more heat-repellent materials such as white granite slabs and gray Luserna cobblestone (Figure 2). The vegetated areas were designed to include a minimum soil depth of 60 cm to support plant growth. Flowering plants were selected for attracting pollinators, while the phenological spectrum and the adaptation of plants to the local climate context were taken into account to ensure continuous and sequential flowering throughout the year. Autochthonous species were primarily preferred, while non-invasive allochthonous species were considered only for their ability to thrive under low irrigation or drought conditions. The species richness established in the flowerbeds allows the formation of robust plant associations and provides a wide variety of ecological niches capable of hosting many animal species (i.e., insects and birds). Finally, to restore the square social role of aggregation, the new green areas have been surrounded by seats, allowing students and people to gather and experience the place.

Two of the lower courtyards underused green spaces have been closed to the public for future renovation (will be equipped with tables and chairs). The concrete court has not been renovated because it is not suitable for plant growth, being in the shade all day, and is already equipped with chairs and tables for studying.

Vivarium-Bicocca

Vivarium-Bicocca (Fig. 1) is a pocket park acquired by the University of Milano-Bicocca in 2020 and opened to students and the public in 2022. It has a total green cover of 7,000 sqm and includes approximately 100 trees belonging to 17 species, as well as a small pond and beehives. It is located at the edge of the Bicocca University campus and is bordered by roads on two sides and by a railway line. One of the adjacent roads is a flyover, and one side of the park is bordered by an elevated vegetated slope that partly screens road noise. The remaining side borders a manufacturing area.

Parco Nord

Parco Nord (Fig. 1) is a regional park located on the northern outskirts of Milan. It extends across the northern metropolitan edge of the city, covering 800 hectares (8 km²), and represents one of the largest green areas in Milan. It was established in the early 1970s as an urban and environmental regeneration project, mainly through the recovery of disused industrial land and extensive tree planting. Today, the park includes wooded patches, lawns, cultivated areas, small lakes, and the nearby Bresso Airport. It represents an important biodiversity hotspot within the Milan metropolitan area, functions as an ecological corridor for various species, and also provides spaces for leisure, recreation, and education.

4.2.2 Passive acoustic recorders and monitoring

Two different brands of passive audio recorders have been used to monitor the three areas. The Song Meter Micro v1 made by Wildlife Acoustic have been employed to monitor the Piazza della Scienza and the Vivarium-Bicocca. The Audiomoth recorders made by the Open Acoustic Devices have been deployed at Parco Nord.

The Song Meter Micro v1 (Wildlife Acoustics, Inc., Maynard, MA, USA) has a maximum sampling rate of 96 kHz and a sensitivity of the whole transmission chain of 2 dBV \pm 4 dBV relative to 1 Pa at 1 kHz Full-Scale, measured using a gain of +18 dB. It generates output files in non-compressed, 16-bit wave format. The sensitivity curve is not linear alongside the spectrum [63] and thus an equalization procedure has been applied to avoid biases in the ecoacoustic indices calculation and sound event detection.

The Audiomoth 1.2.0 (Open Acoustic Devices, Oxford, UK) is a programmable, low-cost recorder equipped with an analog MEMS (Micro Electrical-Mechanical System) microphone with a maximum sampling rate of 384 kHz. The sensitivity of the microphone is -38 dBV \pm 6 dBV relative to 1 Pa at 1 kHz, and its frequency response is almost flat without the waterproof case but is distorted by the waterproof case resulting in amplitude oscillations across the spectrum. Its output files are .wav, 16-bit and not compressed.

Monitor campaigns

To monitor the ante-opera and post-opera sonoscapes of the square two campaigns were carried out. The ante-opera monitoring was conducted in May 2023, over the course of one week, from Monday 22nd to Sunday 28th. The post-opera assessment phase took place in May 2025, extending over one week, from Monday 19th to Monday 26th. The datasets were cleaned of sporadic rainfall events to ensure the correct evaluation of the sonoscape.

The monitoring campaign consisted of 7 sites: 2 at the ground level, 2 in the lowered courtyards, and 3 at the first floor of the buildings (Figure 3). This arrangement was planned to capture sound from distinct areas (ground floors, lower courts) and prevent duplication of recordings, considering the square's limited size. Moreover, since the monitoring focused on urban renewal, data was not collected in the concrete courtyard (next to Site 5 in Figure 3), since it was not scheduled for any specific intervention.

Song Meter Micros v1 (SMM hereafter) were set with a sampling rate of 48 kHz and an amplitude gain of +12 dB, recording for 1 minute and pausing for 1 minute to collect the sound variability of the area. The amplitude gain was chosen after a trial on the field to avoid overloads.

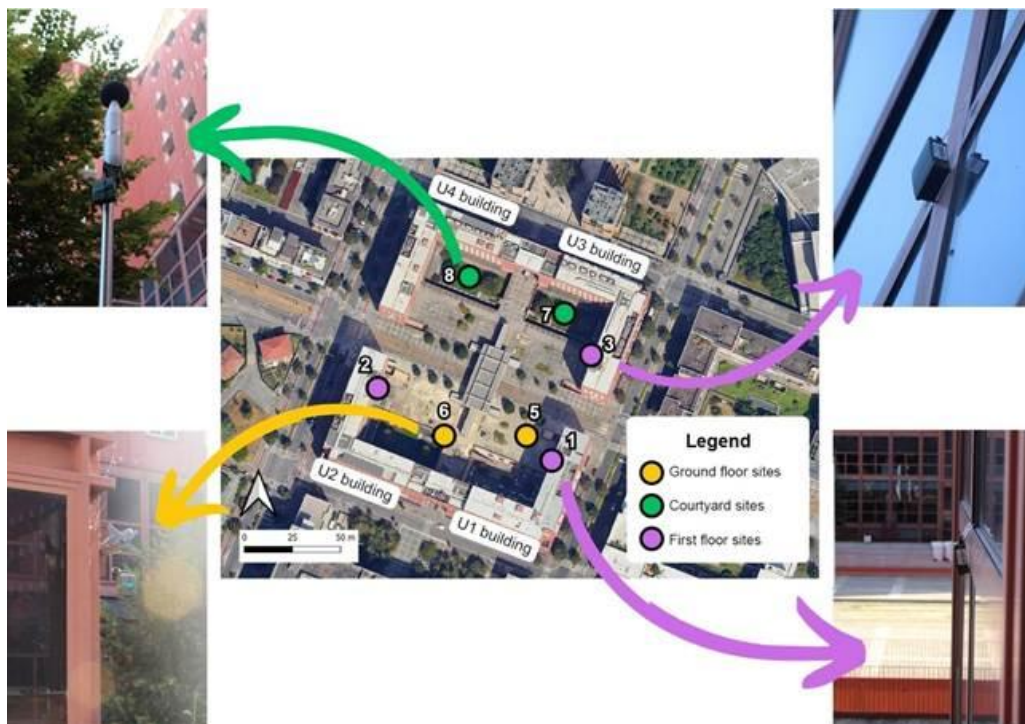


Figure 3. Monitoring sites and relative photos.

The Vivarium-Bicocca has been monitored using a single Song Meter Micro given the small and homogeneous area (Figure 4). It was set to record at 96 kHz with a gain of +18 dB for 1 minute after 5 minutes of pause all day long. The campaign has been performed in 2022 for two weeks, from May 31st to June 14th.



Figure 4. Monitoring site of Vivarium-Bicocca.

In Parco Nord, 9 Audiomoths were positioned in selected sites based on habitat characteristics (Figure 5). Audiomoths have been equipped with the original waterproof case by Open Acoustic Devices and set to record at 96 kHz with a medium gain for 1 minute after 1 minute of pause in four time slots during the day, namely 3:00-5:00, 6:00-11:00, 14:00-16:00, and 19:30-22:30. The Parco Nord campaign was carried out in May 2025 for two weeks, from the 8th to the 19th.

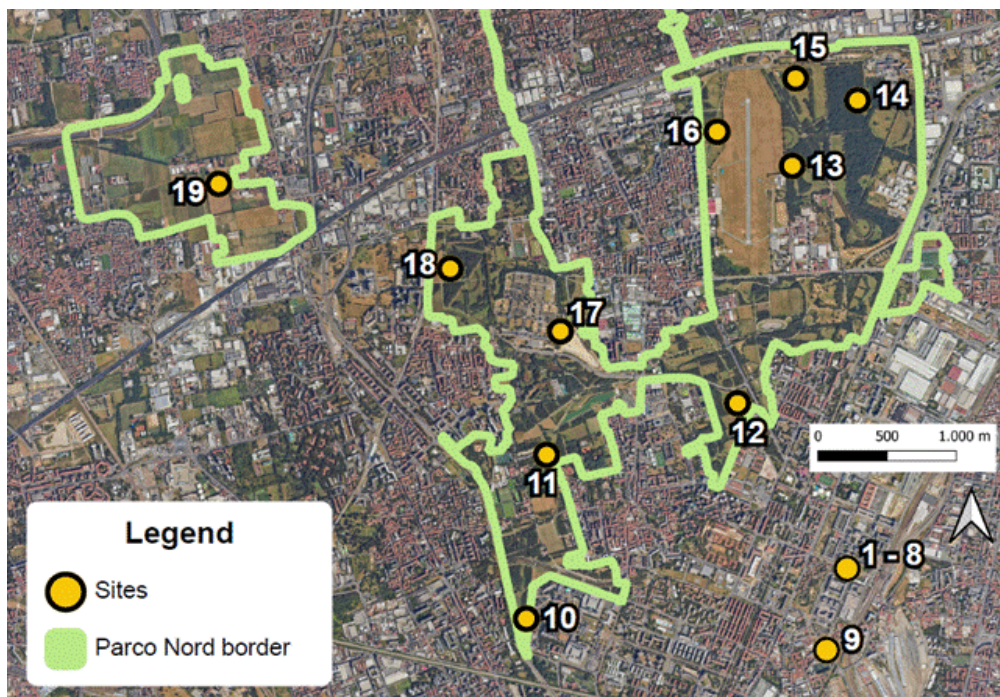


Figure 5. Monitoring sites showing the three areas and relative monitoring sites. Parco Nord sites are numbered from 10 to 19.

Equalization of acquired recordings

Given the different devices used and their non-linear frequency responses [18-20], an equalization process has been carried out [18] for both Song Meter Micro and Audiomoth to uniform the frequency response and gain amplification. In the Supplementary Materials of [63] the open-source MATLAB script is available for equalizing the recordings and obtaining linear-comparable audio files with other devices and between ecoacoustic studies. The same script allows the removal of the DC-Offset, ensuring the correct analysis of audio files.

Due to a different frequency response of the Audiomoths used at the Parco Nord from the ones used in [18], they were equalized in open field at Piazza del Calendario (near Piazza della Scienza) after having checked no external sound sources were present (such as traffic, people, technical installations and cicadas), as visible in Figure 6. Moreover, the sampling frequencies were uniformized by downsampling the Parco Nord and Vivarium recordings at 48 kHz before equalizing.



Figure 6. Recording of white noise with Audiomoth, Hydromoth and SET at Piazza del Calendario (Milan).

Permanent monitoring in Piazza della Scienza

The recorders used in all areas are not permanent because they are limited in battery duration and storage capacity without the possibility of connecting to a continuous power supply and transmitting the recorded data. Thus, as foreseen within the MUSA project, a permanent autonomous acoustic monitoring system has been acquired and installed in the

Piazza della Scienza. The goal is to better assess the changes in square sonoscape throughout the years taking into account vegetation growth and people accustomization to the new square.

The permanent system consists of 4 monitoring stations ACT-400 (AESSE Ambiente - ACOEM) which are sound level meters of Class 1 also able to record the sonoscapes in non-compressed WAV format. They are resistant to adverse weather, allowing for their deployment in long-term monitoring campaigns. The year-long continuous monitoring is ensured by powering through electric 220 V cables and data transmission to servers by means of an ethernet cable connection. The sensors will be installed on the ground floor (2) and in the lowered courtyards (2). The first station has successfully completed its initial configuration and testing phase (Figure 7) and will enable continuous, real-time monitoring of the Piazza's acoustic environment beyond the project duration.



Figure 7. ACT-400 monitoring station located in Piazza della Scienza.

4.2.3 Ecoacoustic indices

The computation of ecoacoustic indices has been carried out using RStudio and the packages 'tuneR', 'seewave', and 'soundecology'.

Since it is well assessed in literature that a single index can't describe the multiple characteristics of sonoscapes [42], 7 ecoacoustic indices were considered for assessing the urban sonoscape of the square. The commonly used indices BI and NDSI were excluded because of the biases introduced by the technophonies present in the urban environment [33], which doesn't allow a frequency separation between anthropogenic and biophonic sounds.

The indices used in this study are: the Acoustic Complexity Index (ACI) [43], the Acoustic Diversity Index (ADI) [17], the Acoustic Evenness Index (AEI) [44], the Acoustic Entropy (H) [45], the Dynamic Spectral Centroid (DSC) [17], the Zero Crossing Rate (ZCR) [46, 47] and the Number of Peaks (NP) [48].

A single value for each index was calculated on the whole 1 min long recording. The analysis was performed using the Fast Fourier Transform (FFT), with a window of 1024 points. This results in a spectral resolution of 46.87 Hz and a time resolution of 0.02 s, which is optimal for accurately describing the acoustic events present. The maximum frequency was set at 12 kHz and the minimum frequency at 500 Hz.

To get harmony between the indices calculation methods in R and the Python package `scikit-maad` [49] and avoid biases, the scripts of ADI and AEI have been modified, adding the minimum frequency parameter as already explained here [50, 51]. On H and ZCR, we couldn't access their internal script thus couldn't add a maximum and minimum frequency; for this reason, before their calculation the audios were downsampled at 24'000 Hz while using an FFT value of 512 points to maintain the same spectral and time resolution. These adjustments allow consistency between the indices' values and avoid biases because otherwise ADI, AEI, H, and ZCR would be calculated on the whole spectrum (0-24'000 Hz). Finally, on ADI and AEI, the `dB_threshold` value was calculated using the methodology explained in [50, 51]. For the Piazza a mean value of -74 dB was calculated on the ante-opera recordings and used for the two campaigns since no modifications were performed on the ventilation installations and traffic fluxes were consistent thus the background noise was consistent. For the Vivarium it was set at -73 dB. At the Parco Nord, a mean value of -63 dB was used. The parameter `freq_step` was set using the default value of 10.

Given the extensive time-sampling and days, a for cycle with `tryCatch()` command has been used to save time in the calculation process avoiding the cycle stop if a computation error

occurred. Skipped audio filenames were saved and the audio were checked and eventually fed again to RStudio to ensure the consistency of the dataset.

4.2.4 Sound events detection

Given the main goal of understanding the soundscape and its changes in the Piazza, sound classification has been implemented. This study has been carried out to both speed up and refine a process that, in earlier work, was conducted by manually listening to recordings and annotating sound events [52, 53]. Indeed, the manual listening of audio recordings resulted to be time-consuming thus only one day of recording were analyzed and it didn't account for all sound sources but only to birds' vocalization (abundance, temporal activity, richness, relative intensity), other animal sounds (presence), traffic (presence, relative intensity and typology), and other sound sources (presence) [53]. Thus, a multilabel classification has been performed to speed up the manual listening process of the Piazza recordings, accounting for more sound events and to predict more than one label in the same time sample, since in urban settings sounds often overlap one another [25].

The elaborations were performed in Python on Google Colab and on the PyCharm environment.

Model implementation

A preliminary study on the square's ante-opera recordings has been conducted [Art Forum 2025], testing two sets of features (YAMNet embeddings and MFCCs + librosa features) and different classifiers and scalars. In that study, the best features resulted to be the MFCCs + librosa, calculated on a 0.2-second timeframe, while the best model appeared to be the Random Forest classifier combined with the MultiOutputClassifier (thus, one tree was trained for each label). The hyperparameter values were set to default mode and the `class_weight` was set to "balanced". To prevent data leakage between the training and test dataset, the splits were based on recording order rather than on random sampling.

The audio dataset created for [54] is also used in this study. The labeling process was carried out using Audacity, following the previous work of coauthors. Eighteen different

sound events were labeled and organized in a one-hot encoding format, where each column characterizes a sound class, and rows assume the value 0 when the event is not present and 1 when it is present. Each row represents the timeframe analyzed, which lasts 0.2 seconds (the same one used in [54]). To improve the results of [54], a more time-detailed annotation method was implemented: instead of assigning a single continuous label over multiple discrete occurrences of a sound, each event was labeled individually to avoid including intervening silent segments. This was particularly important, for example, for labels like “Cart” where repetitive fast impulses were produced by the cartwheels impacting the paved ground. Finally, to ensure a balance in classes, the audios where the most frequent labels were present (Speech and Insect labels) were filtered out from the dataset to obtain a more even frequency distribution. This could potentially reduce representativeness but since the input manually labelled recordings were randomly selected, the exclusion of recordings that contain solely these two sound classes is not considered problematic; moreover, keeping the class balance helps the model perform better avoiding it focusing on predominant classes and underperforming on less representative ones. Finally, the Ventilation class (always present due to the ventilation systems on the rooftops of the University) was removed. This decision has been taken to prioritize the simplification of the classification process over broadening the model’s applicability, as such models rarely generalize beyond their training area.

Given the results of [54], the MFCCs + librosa features calculated on 0.2-second timeframes and the Random Forest model with the Standard Scaler were used in this paper. The MultiOutputClassifier function was used to solve the multilabel problem by training a Random Forest classifier on each label. The class_weight parameter was set to “balanced”, increasing the weight if classes are unbalanced. Hyperparameters were set to default values thus the Forest is composed of 100 trees, each tree doesn’t have a set depth (nodes expands until all leaves are pure or contain less than min_samples_split samples which its equal to 2 samples), the minimum number of samples required to be at a leaf node (min_samples_leaf) is equal to 1 and the splitting criterion used is the Gini coefficient. The optimization of hyperparameters is excluded from the main scopes of this study and the reported performances should be interpreted as baseline.

Cross validation was carried out using 10 folds to assure that the model performances do not depend on a specific partition of the dataset. MultilabelStratifiedKFold has been used to ensure the distribution of all labels remains proportional in each fold. The values on the 10

folds for precision, recall and F1-score and mean values per sound event are reported in the Results section. Finally, the model was trained on the whole dataset.

Recording campaigns classification

The MFCCs + librosa features were calculated for each recording of the ante and post-opera campaigns and the classifier was applied to them.

The one-hot-encoded outputs were condensed into two pieces of information: presence and total duration of each sound class. The total duration is calculated as the sum of the total predicted positive frames for each class multiplied by the timeframe length (0.2 seconds).

4.2.5 BirdNET assessment

Birds are one of the most vocalizing taxonomic groups, especially in urban contexts. They can be used as indicators of a healthy environment because avian population changes can signify impacts such as pollution, habitat destruction, or climate change [55].

The custom classifier explained beforehand allowed the classification of birds' vocalizations regardless of their species. To get avian biodiversity metrics, such as richness and vocalization rate per species, the birdNET software has been used. BirdNET is a convolutional neural network that allows the classification of more than 6000 species worldwide [56]. It is widely used worldwide for assessing birds' species and other animals through vocalizations. The model analyzes audio in 3-s segments, predicting for every class (i.e., species) on which it has been trained [27]. BirdNET assigns at each classification made on the clip of 3-s a confidence score which ranges from 0 to 1. Scores closer to 1 mean greater confidence that the sound belongs to the target species [57].

Two approaches were used to assess avian population in the three areas:

Fed to BirdNET a predetermined list of species ("custom species list" in the BirdNET GUI) potentially present in the area during their monitoring.

Use of BirdNET “species by location” function setting the areas central coordinates and then comparing the results with a customized species list.

The use of a species list aims at reducing species misidentification due to similar vocalization or migration phases. Although BirdNET allows selecting species by location through coordinates and week of recording, we thought using a custom list would be a more robust strategy. The same species list has been used for the three areas given the short distance between areas and the possibility of flyovers by different species. The list was produced by an expert ornithologist (coauthor V.O.).

The first approach has been used for Piazza della Scienza and Vivarium-Bicocca. BirdNET performance has been tested since it can be influenced by factors such as background noise and overlapping vocalizations and acoustic signals [28] and that the Piazza’s sonoscape is characterized by constant ventilation noise and overlapping anthropogenic sounds (e.g., engines idling, tram pass-by, car horns, sirens and alarms, people chatting) and other vocalizations (e.g., dog barking, cicada sounds). In particular, combinations between minimum confidence values (0.5, 0.6, 0.7), sensitivity (1, 1.5) and overlap (0, 1, 1.5, 2) have been considered. Minimum confidence values were not set higher than 0.7 due to the background noise and other sounds, since they are known to affect the model's performance. Precision, recall and F1-score of each combination have been calculated using the Piazza labelled dataset as ground truth for bird vocalization presence and mislabeling with other sounds. Specifically, BirdNET output has been transformed into a one-hot-encoded list with a 3 seconds pace as well as the one-hot-encoded Piazza labelled dataset; then, the correspondence between birds’ presence (1) and absence (0) have been computed and Precision, recall and F1-score calculated.

Once the best combination was identified, BirdNET was applied to the recordings of Sites 5-8 (ground floor and courtyards) of the ante- and post-opera campaign.

The second method introduced in the bullet point list was applied to the Parco Nord recordings. Since it presents quieter areas, the BirdNET parameters values tested were the following: minimum confidence (0.5, 0.75, 0.9), sensitivity (0.75, 1, 1.25) and time overlap (0, 0.5, 1, 2). The dataset used to test BirdNET performance was composed of the recordings of one day from six sites (36 hours total) to get an even representation of its diverse sonoscapes. To decide the best combination of variables’ values, the mean richness

of detected species and the mean number of detected species actually present in the ornithologist-made list were calculated. A comparison between the two was carried out to get the most in-list species and the fewer out-of-list species. These parameters were calculated for each single variable (confidence, sensitivity and overlap) and for the combination of two variables at a time (confidence-sensitivity, confidence-overlap, sensitivity-overlap) and for the combination of all three variables.

Having identified the best combination of parameters, BirdNET was applied to the Parco Nord recordings.

4.2.6 Data analysis

Rainfall periods were collected from the nearest ARPA (Environmental and Technical Services for Regional Protection) meteorological station, and those recordings were excluded from the dataset after an aural check. Moreover, recordings with extreme outlier values were removed.

Ecoacoustic dataset

A preliminary analysis on the relationship between indices values and sound sources have been carried out by aurally listening to the Piazza's recordings. It puts the relationship into context but it does not take into account all the sound sources assessed using machine learning since defining the boundaries for each class is complex given the variability of the sounds and the surrounding conditions.

For each ecoacoustic index, the distribution shape parameters (skewness and excess kurtosis) and the percentage of outliers (IQR criterion) were calculated to assess their deviation from normality. These preliminary analyses guided the choice of the most appropriate correlation method, favoring nonparametric approaches in the presence of highly skewed or heavily tailed distributions.

Piazza dedicated analysis on the two scenarios

The Piazza was more accurately investigated to assess differences between the two scenarios. For this reason, the Piazza dataset has been split into ante- and post-operam periods and in dawn-day-night periods. The dawn period spans from 1 hour before dawn (5:44) to 1 hour after dawn. Thus, the day period starts at 6:44 and ends at 22:00, according to Italian acoustic regulations.

To characterize the sonoscape of the two scenarios, a boxplot analysis has been carried out. Boxplots show data distributions highlighting the median value (middle line in the boxplot), the first and third quartile (box limits), the maximum and minimum values (whiskers) and the outliers (points). The analysis is carried out by grouping the values by sites and comparing side-by-side the ante and post opera values divided by dawn, day and night.

Furthermore, the ecoacoustic indices database has been analyzed using principal component analysis (PCA). The analysis was carried out to highlight the variables that better explain the dataset variance, and reduce the dimensionality of the dataset and the contribution due to variable redundancy and casual information [58]. PCA was performed on all indices, after standardization by z-score, using the correlation matrix to attenuate scale effects and heterogeneous variance among variables. The selection of relevant components was based on inspection of the eigenvalues and the scree plot. To simultaneously visualize the structure of the variables and samples, a PC1-PC2 biplot was constructed; in it, observations were classified into six groups resulting from the combination of phase ("ANTE", "POST") and time slot ("dawn", "day", "night") and are represented by 95% concentration ellipses and group centroids. The ecoacoustic indices loading vectors were reported as arrows originating from the origin, scaled with respect to the range of the components.

To better characterize the internal structure of the sites and assess the possible presence of acoustic homogeneous groups, a clustering analysis was conducted separately for the ante- and post-operam phases, using the seven ecoacoustic indices standardized via z-scores. Four clustering algorithms commonly used in the ecological and multivariate fields (hierarchical [59], k-means [60] pam [61], diana [61]) and a range of possible cluster numbers between $k = 2$ and $k = 6$ were tested. For each method-k combination, the average

silhouette was calculated, used as an objective criterion to identify the optimal solution: a higher value indicates more compact and well-separated groupings. For each phase, the configuration with the maximum silhouette was selected, so as to obtain the best compromise between internal homogeneity and separation between clusters.

Comparison between the three areas

To assess differences between the three areas, the ecoacoustic indices datasets have been analyzed using the principal component analysis (PCA) to get information about indices contribution to the dataset variance in the three study areas (as done in [30]) and sites distribution on the PC1-PC2 biplot. PCA was performed after standardization. To simultaneously visualize the structure of the variables and samples, a PC1-PC2 biplot was constructed with 95% concentration ellipses and group centroids. The ecoacoustic indices loading vectors were reported as arrows originating from the origin, scaled with respect to the range of the components.

Subsequently, the three areas datasets (of which the Piazza contains two datasets due to the regeneration project) were merged into one, standardized and the PCA have been carried out to highlight differences between the areas' observations through the PCA biplot; 95% concentration ellipses of the areas and sites centroids were used.

Sonoscapes dissimilarity between sites and areas

Finally, to quantify sites' dissimilarity and thus sonoscapes' quality differences, the dissimilarity index between sites and areas/scenarios has been calculated following the methodology of [62].

To calculate the dissimilarity, indices distributions of all sites in the form of histograms were calculated setting the same number of bins per index and calculating the maximum and minimum values of the indices' distributions across all sites' observations. Then, on each index distribution the dissimilarity between each site was calculated, employing the following equation:

$$D_{i,j} = 1 - \frac{\sum_m H_i(m) H_j(m)}{\sqrt{\sum_m H_i(m)^2} \sqrt{\sum_m H_j(m)^2}}$$

where i and j are two sites and the denominator is the normalizing factor that ensures that $D_{i,j} = 0$.

In the dissimilarity formula, the terms H_{ix} refers to the index distribution where $x=m*b$ with b being the bin size used to build the histograms and m the m th component of the histogram itself. $D_{i,j}$ ranges from 0 to 1, with values near 1 indicating an elevated dissimilarity and near 0 a lower dissimilarity or even equality.

To get a single value of sonoscape dissimilarity between sites i and j , an arithmetic mean was calculated on the indices' dissimilarities. Heatmaps have been used to show the dissimilarity between sites.

Lastly, non-metric MultiDimensional Scaling (NMDS) has been carried out on the dissimilarity matrix to graphically represent the spatial similarities between sites as done in [33]. NMDS is non-parametric and handles non-linear relationships and non-normal distributions [33]. Moreover, it has the advantages of preserving the rank-order of among-samples dissimilarities in the rank order of variables and is resistant to outliers. The stress parameter has been calculated to demonstrate the analysis strength.

The dissimilarity was also calculated between areas by computing (1) on the whole areas' indices distributions (without dividing by site). Heatmaps show the indices and areas dissimilarities.

Sound event classification dataset

The model ran on the MFCCs+librosa features calculated for each campaign recording, output a csv file for each recording in one-hot-encoded format with values 0-1 for each sound label for each 0.2 s timeframe. These csv files were summarized by summing all columns' values, obtaining an overall time-duration of each sound label; they were merged in a single dataframe covering the two monitoring campaigns.

This dataset has been analyzed by computing the daily duration of events per site. A pie chart showing this parameter per site per scenario has been plotted using ggplot2 in RStudio. Each pie chart shows the daily mean duration of events scaled to 100%; slices

gaps are present when no sound event (as variable) was classified. Moreover, a ggplot2 barplot showing the 5 most lasting events per site per scenario have been produced.

Differences between sites are derived from these representation graphs and compared to the cluster analysis and dissimilarity heatmap.

BirdNET dataset

The BirdNET results dataset has been investigated for erroneous species identification in a highly anthropized environment such as the square. Aural checks of these species' detections have been performed by an expert ornithologist and were removed from the dataset.

The BirdNET dataset has been analysed by producing a barplot showing species richness per site in the two scenarios and green areas, and another barplot presenting the daily mean number of vocalization per site in the two scenarios and green areas. Moreover, the daily time trend mediated on sites of the 5 most identified species per scenario and area have been produced.

Piazza analysis through regression models on ACI, Sound events ID and BirdNET ID

To assess changes in acoustic complexity associated with the urban regeneration intervention and understand the effects of avian richness and sound events, we analysed the Acoustic Complexity Index (ACI) using linear mixed-effects models.

The index chosen for this study is the ACI because it is one of the most diffuse and employed indices in ecoacoustics. Other reasons are linked to the Piazza's sonoscape so the reader is referred to the Results section for further information.

The response variable (ACI) has been computed for each audio recording, while the main explanatory variable was intervention phase (Ante vs Post), representing ante- and post-intervention conditions. Avian species richness was included as a fixed effect to account for the biological component of the soundscape. In addition, a subset of sound events categories derived from the machine-learning classification was included as fixed effects.

Among all detected sound classes, five categories were selected a priori based on their consistency across the study area and phases. Specifically, only sound sources that were present in all sites and occurred with a relatively high number of events in both the ante- and post-intervention phases were retained. This selection criterion ensured that included sound sources were representative of the overall soundscape dynamics and avoided model instability due to rare or site-specific events. The selected categories comprised bird vocalizations (Bird), human speech (Speech_Voices), tram passages (Tram), motorbike noise (Motorbike), and cart/trolley passages (Cart_Trolley). All sound source variables were coded as binary predictors (0 = absence, 1 = presence) at the level of individual recordings.

To account for repeated measurements within the same spatial context and to control for site-specific baseline differences in acoustic structure, recording site was included as a random intercept. This approach allowed the estimation of fixed effects while accounting for non-independence among recordings from the same site, without explicitly modelling site-level differences.

Based on a priori hypotheses related to the effects of urban regeneration on soundscape functioning, interaction terms between intervention phase and selected key predictors were included to test whether the mechanisms structuring acoustic complexity differed between phases. Specifically, interactions between phase and avian species richness, bird presence, and human speech were included, allowing the strength and direction of these relationships to vary between the ante- and post-intervention conditions. Other sound sources (Tram, Motorbike, and Cart_Trolley sounds) were included as main effects only, as they were treated as control variables rather than focal drivers of phase-specific changes.

The global model therefore included fixed effects for phase, species richness, the selected sound source categories and the specified interaction terms. Site was included as a random intercept. Models were fitted using maximum likelihood estimation to allow information-theoretic model comparison.

Model selection was performed using an information-theoretic approach based on Akaike's Information Criterion corrected for small sample size (AICc). All possible submodels nested within the global model were generated and ranked according to AICc. Model support was evaluated using AICc values and Akaike weights. When a single model showed clear support ($AICc < 2$), this model was retained for inference; when multiple models fell within

this threshold, model averaging was applied to obtain parameter estimates weighted by model support.

Model assumptions were evaluated through visual inspection of residual diagnostics. These included plots of residuals versus fitted values to assess linearity and homoscedasticity, normal Q-Q plots to evaluate deviations from normality, histograms of residuals to examine overall error distribution, and comparisons of residual distributions between ante- and post-intervention phases to detect potential phase-specific biases. No major violations of model assumptions were detected. Minor deviations from normality were observed in the upper tail of the residual distribution, which were considered acceptable given the large sample size and the distributional properties of acoustic indices.

4.3 Results

4.3.1 Ecoacoustic analysis

Piazza della Scienza

The results of the aural study carried out to highlight the association between the indices values and the sound sources is shown in Table 1.

Table 1. Ecoacoustic indices values and corresponding sounds in the Piazza.

Index	Values	Sound source
ACI	$ACI < 143$	Alarms and ambulance sirens
	$143 \leq ACI \leq 145$	Silence, ventilation systems
	$ACI > 145$	Bird vocalization, speech, tram, cart passage on pavement
ADI	$ADI < 7$	Ambulance, tram, ventilation systems
	$ADI > 7$	Construction noises, cart passage on pavement, bird vocalization
AEI	$0 \leq ACI \leq 0,25$	Bird vocalization, speech, tram, cart passage on pavement, ventilation systems
	$0,25 \leq ACI \leq 0,55$	Silence, ventilation systems
H	$H < 0,6$	Silence, ventilation systems
	$0,6 \leq H \leq 0,8$	Bird vocalization, speech, tram, construction noises, street cleaning
DSC	$DSC < 0,7$	Silence, ventilation systems
	$0,7 \leq DSC \leq 0,85$	Bird vocalization, tram
	$0,85 \leq DSC \leq 1$	Speech
	$DSC > 1$	Engine ignition, cart passage on pavement
ZCR	$ZCR < 0,015$	Silence, ventilation systems
	$ZCR > 0,015$	Tram, ambulance, speech

Distribution analysis highlighted strong deviations from normality for the various ecoacoustic indices.

Piazza ante-operam ACI presented a mean value of 145.74 with a standard deviation of 3.32, a strong right skewness of 3.40 and an excess kurtosis of 15.36. ADI_{min} presented a mean value of 7.01 (SD = 0.08 kHz) with a left skewness of -5.55 and an elevated excess of kurtosis of 39.03. AEI_{min} had a mean value of 0.10 (SD = 0.09), a skewness of 2.67 and 6.34 of excess kurtosis. DSC presented a mean value of 0.85 kHz (SD = 0.10) and 3.31 of skewness and an elevated excess of kurtosis of 43.28. H_{new} mean value was 0.69 (SD = 0.02) showing an almost symmetric distribution (skewness = -0.23) and a near-zero excess kurtosis (0.13). Finally, ZCR_{new} mean value equal 0.04 (SD = 0.01) and a skewness of 0.84 and an excess kurtosis equal -0.80. The outlier rates of all indices were inferior to 0.10%.

Piazza post-operam ACI presents a mean value equal to 145.89 (SD = 4.47) with a skewness of 5.88 and an elevated excess kurtosis equal to 58.71. ADImin mean value sets at 6.98 (SD = 0.14) with a left skewness equal to -4.69 and a great excess kurtosis of 26.83. AEI showed a mean value of 0.12 with a high standard deviation (SD = 0.12) with a right skewness equal to 2.39 and an excess kurtosis of 3.84. DSC presented a mean value of 0.88 kHz (SD = 0.15 kHz) with a right skewness (3.69) and an elevated excess kurtosis equal to 59.28. Hnew mean value attested at 0.70 (SD = 0.02) with a nearly symmetric distribution (-0.84) and skewness equal to 0.99. Finally, ZCRnew presents a mean value of 0.04 (SD = 0.01) with a skewness of 4.88 and a zero-excess kurtosis.

The Spearman correlation matrix highlighted some stable relationships between the ecoacoustic indices. The highest correlation was between ADI and AEI, characterized by a strongly negative coefficient ($\rho = -0.98$, $p < 0.001$). A second group of significant correlations concerns Hnew, ZCRnew, and DSC, which show moderate-high positive associations ($0.43 \leq \rho \leq 0.72$, $p < 0.001$). The other indices present low-intensity correlations: ACI always shows values lower than 0.25 in absolute value, while NP is weakly associated with all variables ($|\rho| \leq 0.31$).

Boxplot analysis (Figure 4) showed differences between Piazza's scenarios (ante vs post):

- ACI post-operam boxplots show increase in boxes' dimensions during dawn in all sites while day and night boxes are more peculiar. Post-opera day box of site 1 shows an increase in box dimensions with a decrease in median value, while sites 3 and 7 show an increase in box dimensions with a stable median value; the other sites (2, 5, 6, 8) show a decrease in box dimensions and lower median values. The post-opera night boxes of sites 1, 2, 6, 7 show a decrease in box sizes while sites 3, 5, 8 present wider boxes.
- ADI post opera boxplots during dawn, day and night periods presents a wider and lower box in all sites except for site 8 which present an opposite trend with ante-opera values being lower (whole box and median value).
- AEI post-opera dawn and night boxplot of sites 1, 2, 3, 5 increases in values while decreases for sites 6, 7 and 8. Day boxplot increases in all sites except 7 and 8 while site 6's is stable.
- H post opera dawn boxplots are lower in sites 1, 3 and 5, wider but stable in median values in sites 2 and 6 and higher in sites 7 and 8. During daytime, post opera boxplot

of site 1 is wider but lower while sites 2, 3 and 6 present lower boxplots; sites 7 and 8 present higher boxplots. Finally, nighttime boxplots are lower in all sites except for sites 7 and 8 where they show higher values.

- DSC post opera dawn, day and night boxplots of site 1 are wider but the median values are stable while site 5 are narrowed. Dawn, day and night boxplots of sites 2 and 3 are narrowed and lower in general values. Site 6 presents higher DSC values during dawn and lower values during the day and night. Finally, sites 7 and 8 present higher DSC post-operam boxplots in all three time periods.
- ZCR boxplot shows a distinct separation between sites 3 and 5 from the others. Nonetheless, focusing on the single sites, ZCR dawn boxplot decreases in post-opera for sites 1 and 6 while increases in other sites. Day and nighttime boxplots increase in sites 2, 5, 7 and 8 while remain stable in site 3; site 1 has a wider range of values with a lower median one and site 6 has a narrowed range of values and a stable median value.
- NP boxplots show site 6 as distinct from the others. Focusing on each site, the number of peaks remains equal in every time period for site 1, during dawn and day in site 8 and during daytime in site 7. During dawn they decrease in sites 2, 3, 5 and 6 while increase in site 7. During daytime values decrease in sites 3, 5 and 6 while boxplot is narrow but stable in site 2. Finally, during nighttime values decrease in all sites except for site 7.

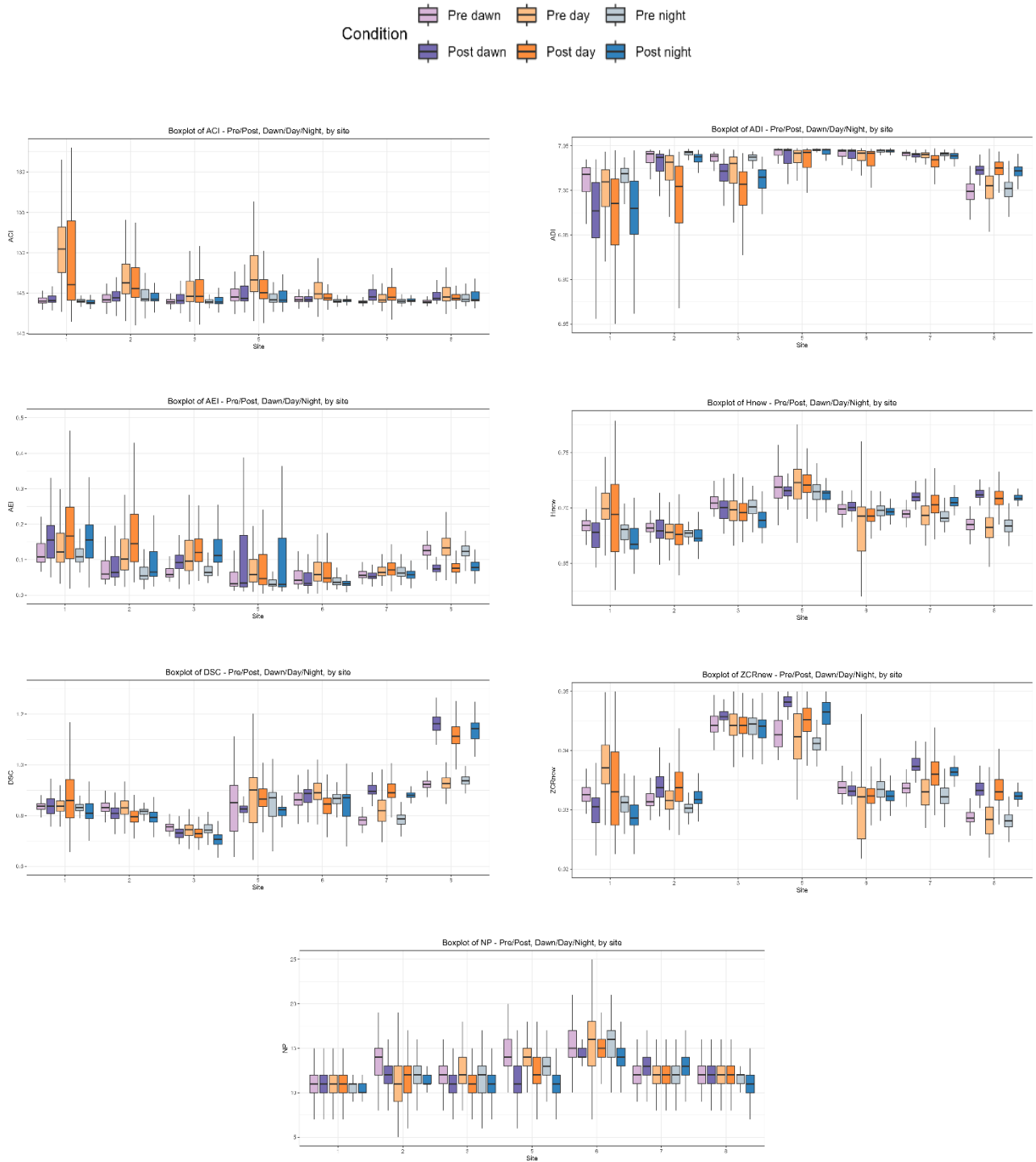


Figure 4. Boxplot analysis to compare the ante-opera (light colors) with the post-opera (darker colors) time periods.

PCA carried out on the whole dataset (ANTE + POST) identified five principal components, of which the first two were found to be the most informative and were used for the graphical representation (Figure 5). In Figure 6, the first component (PC1) is strongly characterized by the Hnew (loading = 0.82), AEI (-0.82), and ADI (0.77) indices, which represent the

predominant contributors to the component's variance (26.9%, 26.8%, and 23.8%, respectively). The remaining variables show much lower loadings on PC1 (loading ≤ 0.44). The second component (PC2) is mainly determined by ACI (loading = 0.74; contribution = 31.2%) and ZCRnew (loading = 0.62; contribution = 21.9%), while ADI (-0.55; contribution = 16.9%) and AEI (0.50; 14.3%) provide secondary contributions. The subsequent components reflect single-variable structures: PC3 is dominated by DSC (loading = 0.78; contribution = 58.1%), PC4 by NP (loading = 0.86; contribution = 85.7%), and PC5 by ACI (contribution = 62.9%).

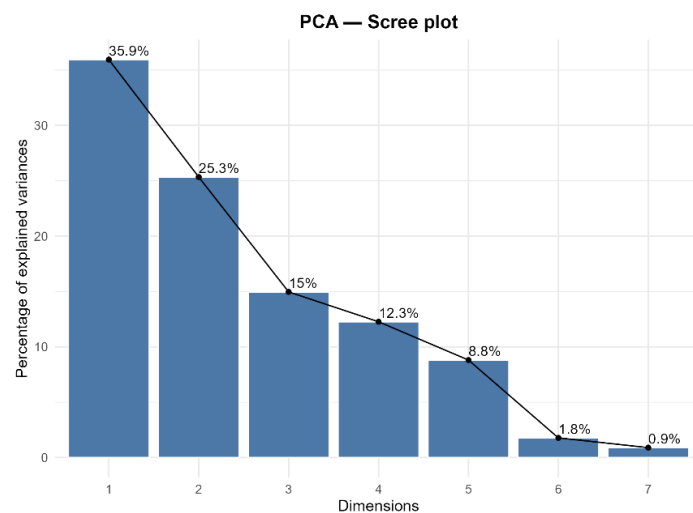


Figure 5. PCA scree plot.

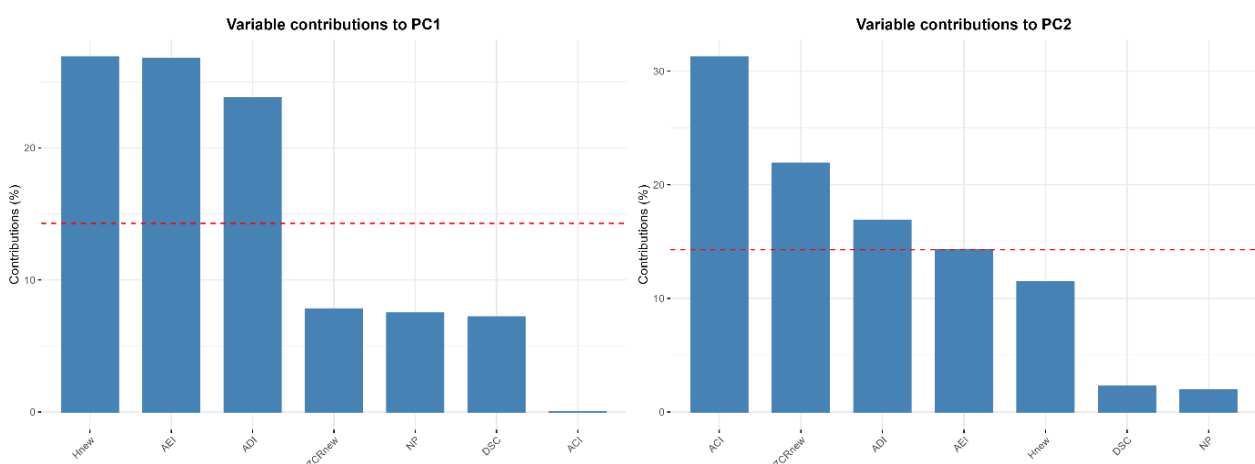


Figure 6. Indices contributions to PC1 (left) and PC2 (right).

In the PC1-PC2 biplot (Figure 7), the six ANTE/POST × dawn/day/night groups are distributed differently both in terms of orientation and extension of the 95% concentration ellipses. The ellipses related to the ANTE period show an orientation mainly associated with the positive direction of PC1, while those of the POST period show a visible shift towards the positive direction of PC2. Furthermore, the size of the ellipses differs systematically between the two periods: the ANTE groups are characterized by more compact ellipses, while the POST groups show ellipses of greater amplitude, indicating a more extensive overall variability along the PC1-PC2 plane. The centroids of the six groups are clearly separated according to both phase and time slot, and are reported in the figure with the synthetic labels a^\wedge , a' , a'' , p^\wedge , p' , p'' .

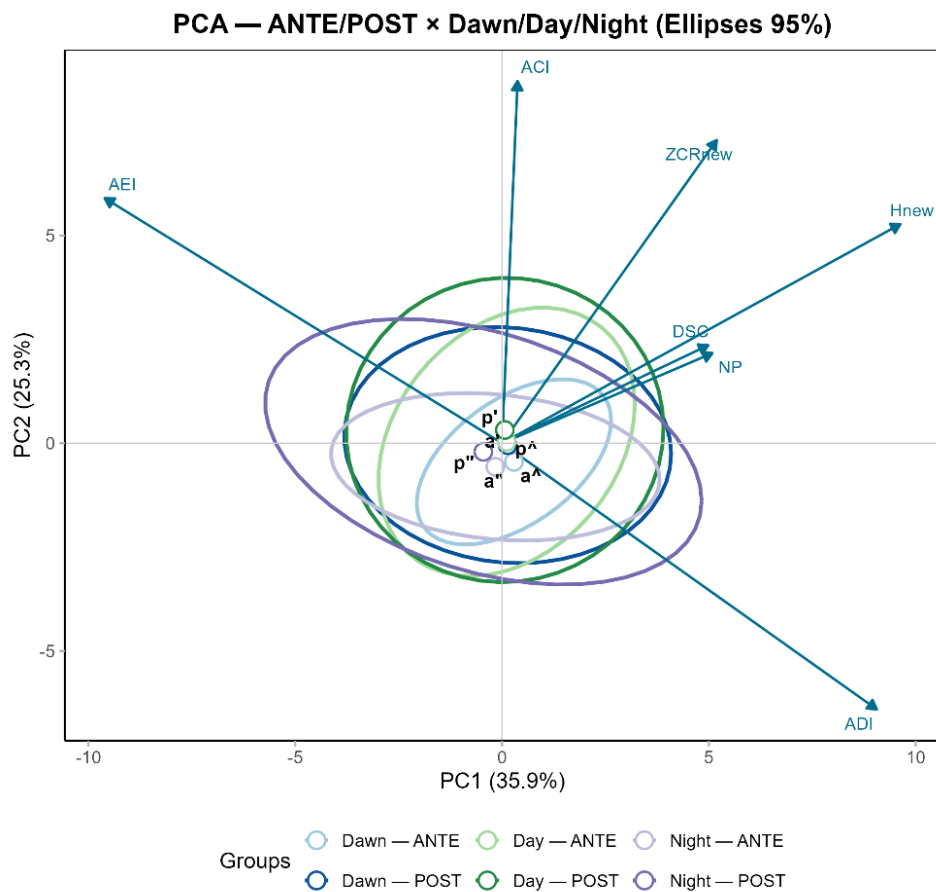


Figure 7. PC1-PC2 biplot showing the ellipses and centroids for each group.

About the cluster analysis (graphical representation in Figure 8), in the pre-intervention period, the silhouette values obtained for the different methods (k combinations) ranged from 0.04 to 0.21. The maximum value was observed for $k = 2$ with hierarchical clustering

(silhouette = 0.207), which represents the best configuration for the ante opera. With this solution, the sites were divided into two groups: Cluster 1 includes sites 1, 2, and 8, while Cluster 2 includes sites 3, 5, 6, and 7. In the post-intervention period, the silhouette values showed a wider range (0.08-0.31). The optimal solution was obtained for $k = 2$ using k-means, with a silhouette value of 0.31. In this configuration, Cluster 1 includes sites 1, 2, and 3 while Cluster 2 includes sites 5, 6, 7, and 8.

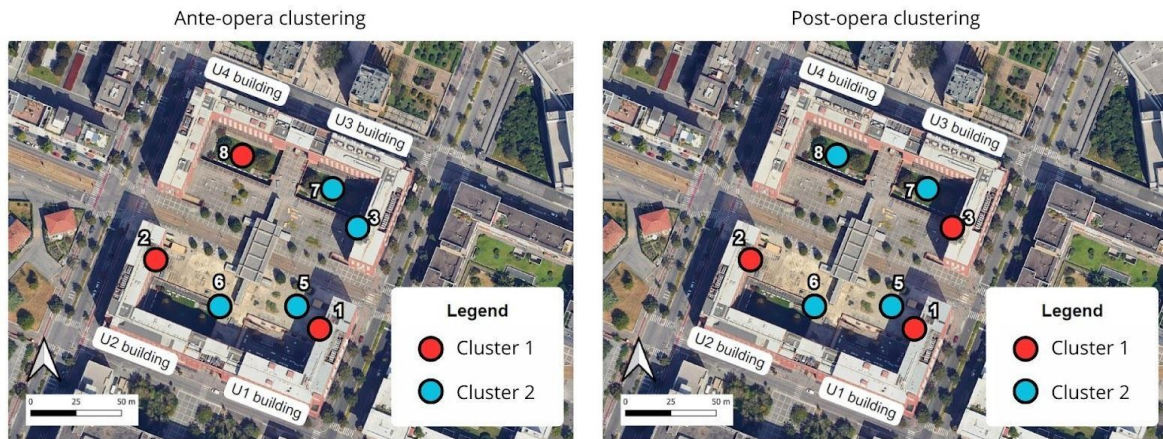


Figure 8. Graphical representation of cluster analysis results for the ante-operam scenario (left) and post-operam scenario (right).

Comparison between the three areas

Descriptive analysis of Vivarium and Parco Nord

The Vivarium ecoacoustic dataset is composed of 3,218 acoustic recordings. ACI showed a mean value of 147.95 (SD = 5.17), with a strongly right-skewed distribution (skew = 3.42) and elevated excess kurtosis (16.24). The outliers proportion was assessed for 7.2% of the data. The ADI_{min} exhibited a high mean (7.01, SD = 0.12) and an extremely non-normal distribution, characterised by strong negative skewness (skew = -6.41) and an excess kurtosis (47.04). The outlier rate was equivalent to 15.7% of the dataset. For AEI_{min}, the mean value was 0.079 (SD = 0.11), with a markedly right-skewed distribution (skew = 3.19) and high excess kurtosis (8.82). Outliers accounted for 10.8% of observations. The DSC index showed a mean of 0.99 (SD = 0.32) and was characterised by strong right skewness (skew = 4.43) and very high excess kurtosis (28.37), with an outlier rate of 11.0%. Hnew presented a mean value of 0.78 (SD = 0.04) and showed an approximately symmetric

distribution (skew = -0.22) with near-zero excess kurtosis (-0.21). The proportion of outliers was relatively low (3.5%). Finally, ZCRnew had a mean of 0.076 (SD = 0.030) and displayed a right-skewed distribution (skew = 2.58) with elevated excess kurtosis (6.72). Outliers represented 6.7% of the data.

Parco Nord ecoacoustic dataset is composed of 30'395 occurrences. The Acoustic Complexity Index (ACI) showed a mean value of 150.78 (SD = 7.84) and a median of 148.20, with values ranging from 108.65 to 258.16. The distribution was strongly right-skewed (skew = 2.38) and highly leptokurtic (excess kurtosis = 7.81), with an outlier rate of approximately 5.1%. The minimum Acoustic Diversity Index (ADlmin) had a mean of 5.99 (SD = 0.71) and a median of 6.08, with values between 3.60 and 7.05. Its distribution showed mild negative skewness (skew = -0.44) and pronounced negative excess kurtosis (-3.50), while the proportion of outliers was negligible (0.1%). For AEImin, the mean value was 0.733 (SD = 0.210) and the median was 0.786, with a wide range (0.006-0.985). The distribution was markedly left-skewed (skew = -1.56), with slightly negative excess kurtosis (-0.87) and an outlier rate of 7.5%. The DSC index presented a mean of 1.21 (SD = 0.90) and a median of 0.79, with values ranging from 0.54 to 7.06. The distribution was strongly right-skewed (skew = 1.96), with near-zero excess kurtosis (0.02) and a relatively high outlier rate (16.4%). The diversity index Hnew showed a mean of 0.591 (SD = 0.097) and a median of 0.575, with values between 0.323 and 0.936. The distribution exhibited moderate positive skewness (skew = 0.92) and negative excess kurtosis (-2.31), with an outlier rate of 8.6%. Finally, ZCRnew displayed a mean of 0.026 (SD = 0.032) and a median of 0.017, with values ranging from 0.005 to 0.317. This index showed extreme positive skewness (skew = 5.01) and very high excess kurtosis (27.19), with 10.9% of observations classified as outliers.

For all indices, the Parco Nord large sample size ($n = 30'395$) precluded the use of the Shapiro-Wilk test. Distributional assessment based on skewness, excess kurtosis, and outlier rates indicated substantial deviations from normality for all indices.

PCA on single areas

In this section, PCA results of single areas are shown, distinguishing between the Piazza ante and post opera scenario.

Figure 9 shows eigenvectors' plots. It is noticeable that for Parco Nord (A), 80% of the dataset variance is explained by the first two dimensions, representing 60,5% and 20,7% respectively. The Vivarium 80% variance (B) is explained by the first three dimensions, accounting for 50,8%, 28,1% and 14% respectively. Finally, Piazza's ante-operam (C) three dimensions account for the 80% threshold with 39,1%, 29,4% and 18,6% respectively; the post-operam (D) shows similar values with 39,7%, 28,4% and 18% respectively.

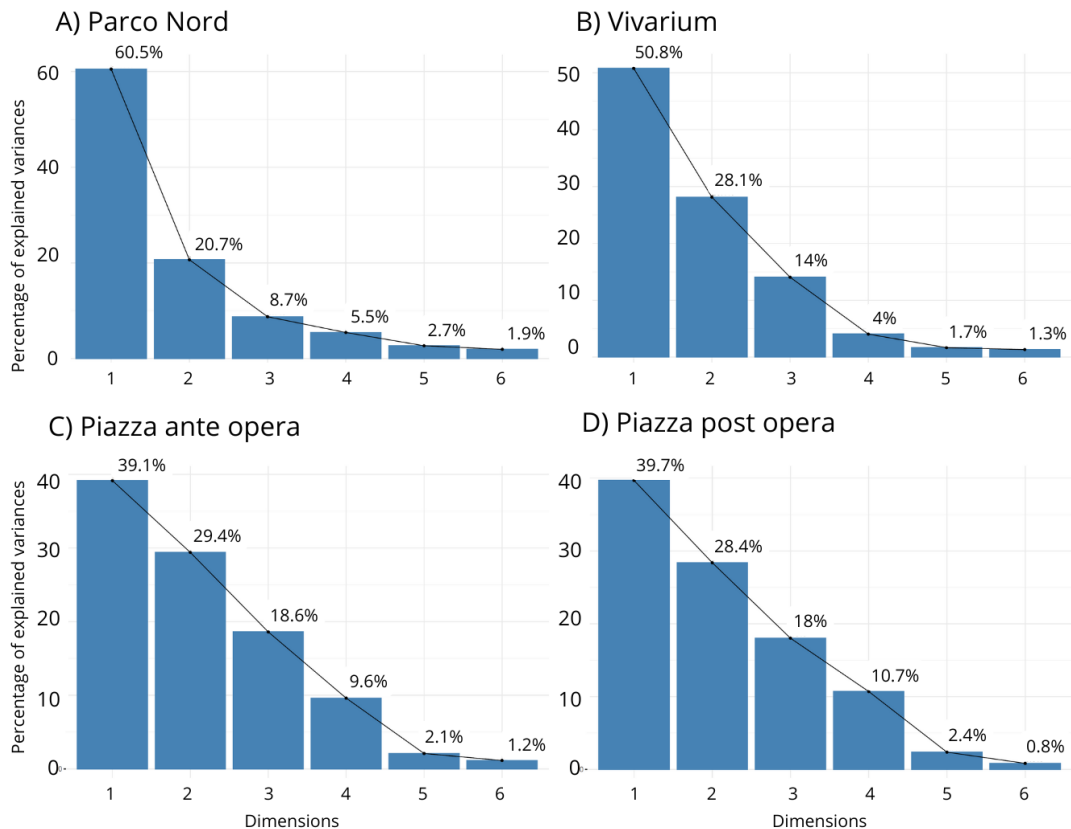
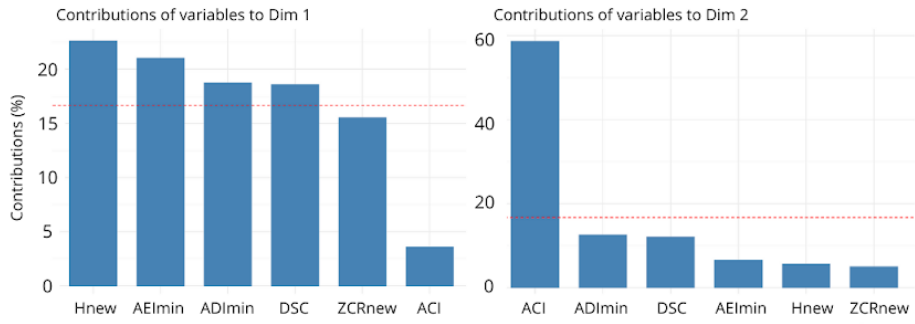


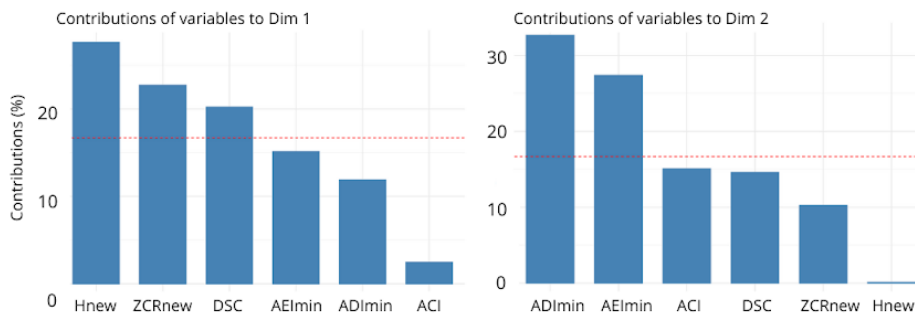
Figure 9. Eigenvectors plots results from PCA computed on single areas.

Figure 10 shows the contribution of each index to the first two dimensions of the dataset. The first dimension (PC1) of Parco Nord is explained by Hnew, AEImin and ADImin while the second dimension (PC2) by ACI mainly. The Vivarium PC1 is driven by Hnew (like Parco Nord) followed by ZCRnew and DSC, while the PC2 by ADImin and AEImin. On the other hand, both scenarios of Piazza PC1 are explained by AEImin, ADImin and Hnew with similar percentages, as well as PC2 where ZCRnew and ACI are flipped in the scenarios.

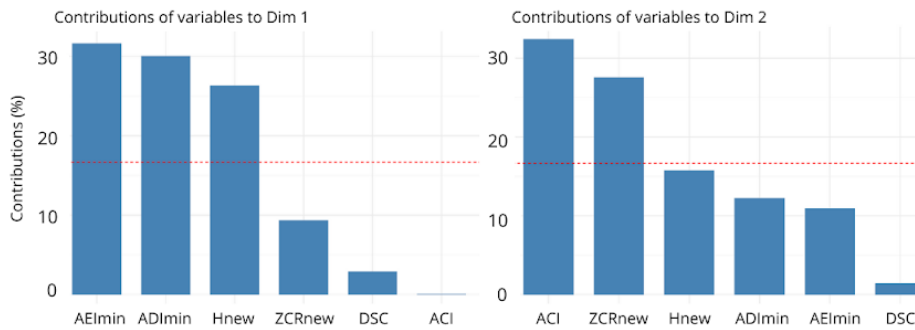
A) Parco Nord



B) Vivarium



C) Piazza ante opera



D) Piazza post opera

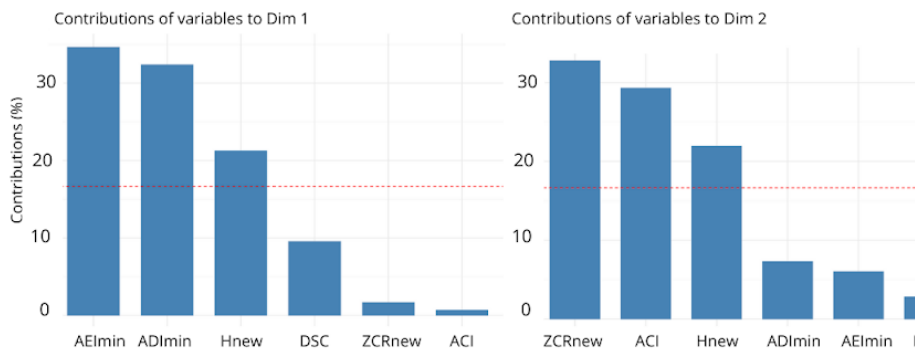


Figure 10. Contribution of indices to dimension 1 and 2 of the datasets.

PCA on all areas merged

The areas' observations were plotted on a PC1-PC2 biplot by means of 95% concentration ellipses (Figure 8). Parco Nord presents the highest variation in observation values, probably due to the wider and diverse surface covered by the ecoacoustic recorders. Similarly, the Vivarium ellipse mimics the Parco Nord ellipses orientation and presents a greater variance than the square, probably due to the higher diversity of sound sources. Finally, the Piazza ante and post-operam ellipses are smaller than the parks' and oriented in a different direction even if the post-operam one is more stretched indicating a possible higher diversity in the observation and thus sonoscape compared to the ante-operam scenario. Considering the arrows, the parks ellipses depend more on DSC and ZCRnew (coherent with Figure 9) while the Piazza's are influenced by ADImin and AEImin, with a greater role of DSC in the post-opera scenario, confirmed by Figure 9.

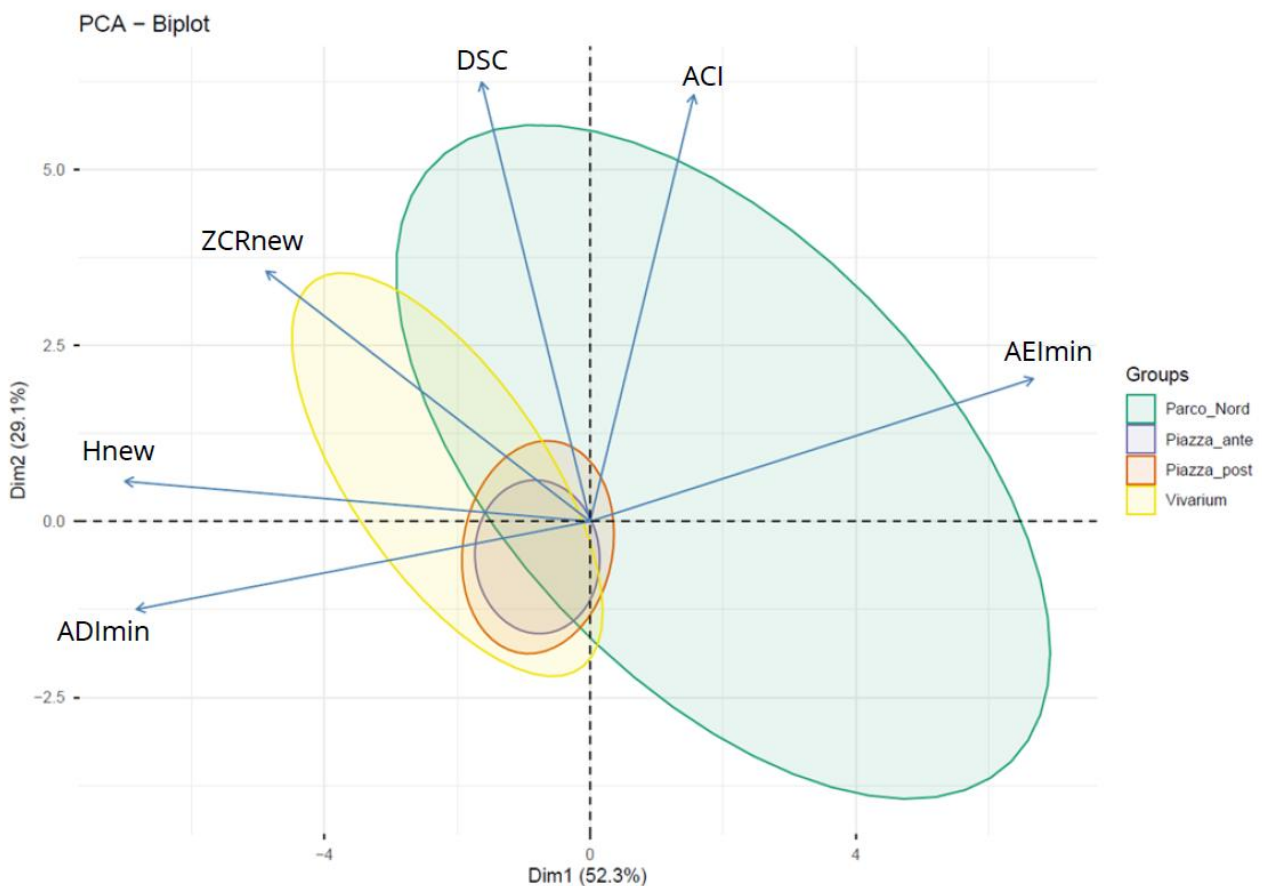


Figure 11. PCA biplot showing the areas' ellipses. The arrows indicate the indices contributions.

In Figure 12, the sites' centroids of the three areas are represented on the PC1-PC2 biplot. It is possible to notice that the areas' centroids are distinguished in two main groups and two outcasts. In particular, Piazza's sites are close to one another due to the sites' spatial vicinity in the square even if there is a noticeable difference between scenarios. The second group is composed of the Parco Nord sites which are separated from the Piazzas' ones and present a higher variance. Finally, the Vivarium site and the Site 16 of Parco Nord are separated from all the others underlying a diverse role of indices in PC1-PC2.

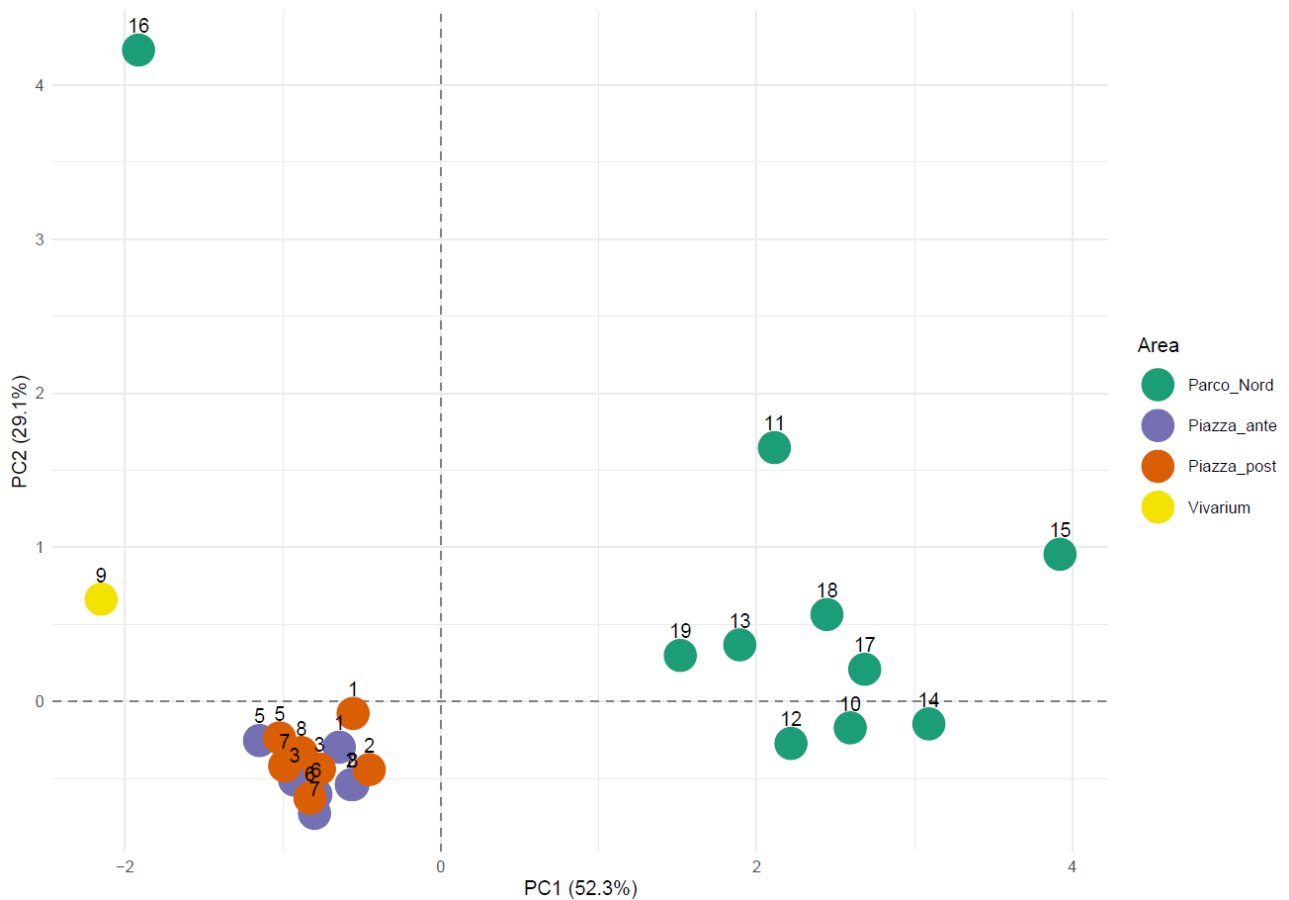


Figure 12. PCA biplot showing the sites' centroides colored by area.

Dissimilarity index analysis

The heatmap in Figure 13 highlights the dissimilarities between sites. Three main colour groups are visible in the figure: a high-dissimilarity block in the left-up corner and two low dissimilarity blocks in the bottom and right corners. The diagonal shows no dissimilarity referring to the same site (Di,i).

Using the y-axis as starting point, it is possible to notice that the high-dissimilarity block is produced by comparison between the Parco Nord sites, Vivarium site and some Piazza post-operam sites (5-6-7-8) with Piazza ante-operam sites and some Piazza post-operam sites (1-2-3).

In this heatmap section, the columns of Piazza pre-intervention S7 present the highest dissimilarity while Piazza pre-intervention S8 presents the lowest values inside this block. The low corner regards the comparison between the Piazza's sites; site 1 ante-operam is lowly dissimilar to sites 1-2-3 post-operam while it increases progressively to sites 6-5-7-8 post-operam. Sites 2-3 ante-operam presents a higher dissimilarity with their post-operam counterparts and less with the post-operam ground floor (5-6) and courtyards (7-8). Site 5 ante-operam values are always quite high while site 6 presents a low dissimilarity to site 5 post-operam. Finally, courtyards (7-8) ante-operam show low dissimilarity especially with respect to sites 5 and 6 post-operam.

Finally, the upper right corner of the heatmap, shows the relation between post-operam sites 5-6-7-8, Vivarium and Parco Nord sites; the dissimilarity here is oscillatory but it is visible a low dissimilarity between the post-opera Piazza sites and the Parco's ones, especially with sites 11-12-13-14-15-16.

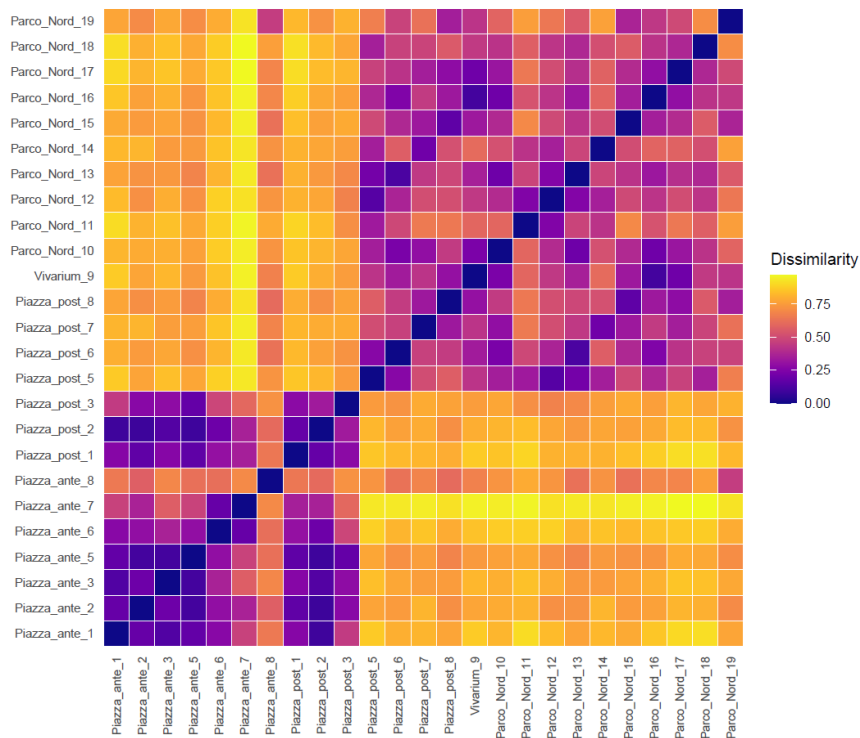


Figure 13. Heatmap representing the dissimilarity between the sites.

The dissimilarity matrix between sites has been also represented by means of the NMDS analysis (Figure 14). It is possible to notice two groups in the plot, the left one composed by all Piazza's ante-opera sites and some post-opera ones, and the right one populated by Parco Nord sites, Vivarium one and some Piazza's post-operam sites. This distinction is extremely interesting because it highlights the greater similarity between the green areas sites with the Piazza post-operam, suggesting the positive effect of the regeneration project on the square's soundscape. In particular, the post-operam sites close to the Parco Nord sites (5-6-7-8) are those located on the ground floor and lowered courtyards where the depaving and greening took place, while the Piazza's sites located at the first floor (1-2-3) remained more similar to the ante-operam scenario probably due to the dominance of ventilation noise at that height and of less sound contribution from the ground floor.

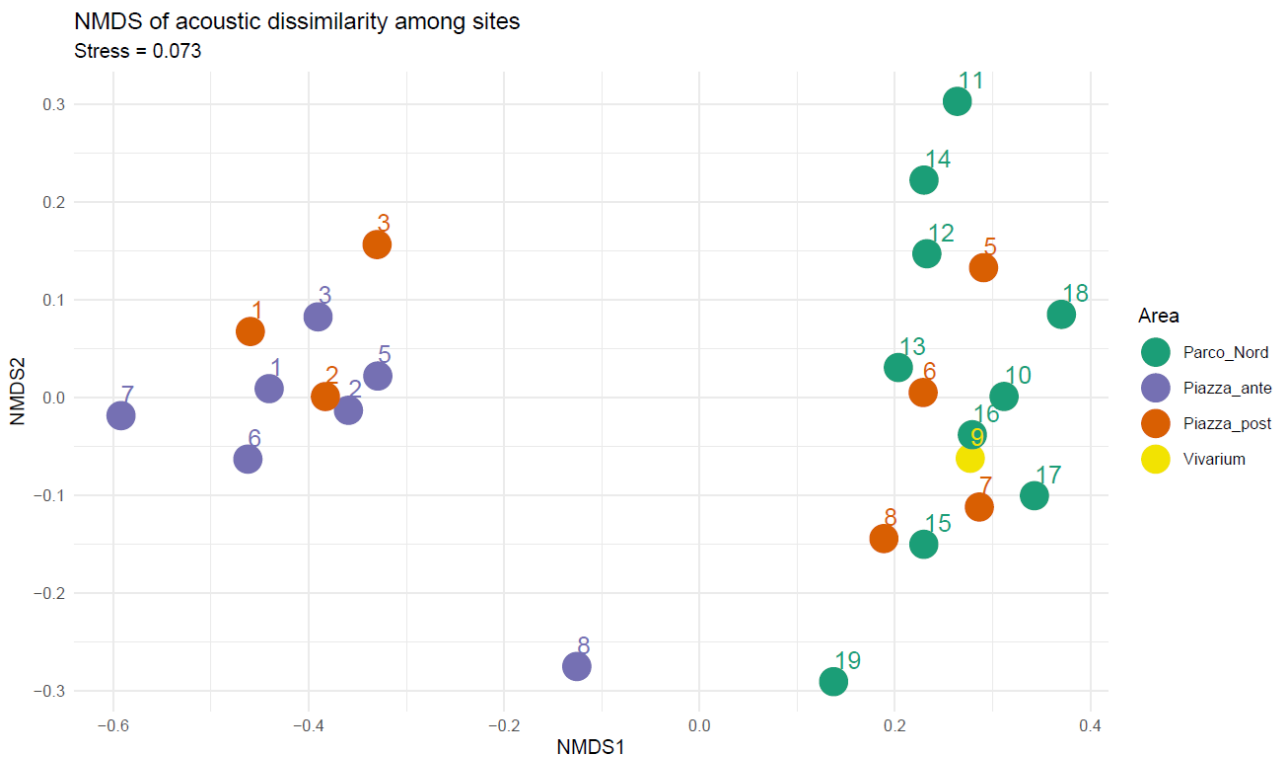


Figure 14. NMDS plot representing the dissimilarities between sites as distances: greater the distance greater the dissimilarity. Colors represent the different areas.

Finally, in Figure 15 is shown the dissimilarity index between areas in the form of heatmap. Taking as starting point the x-axis, the Piazza ante-opera is dissimilar to all other areas while

the post-opera scenario is more similar to Parco Nord, then Vivarium and finally is dissimilar compared to the ante-operam scenario. Finally, Parco Nord is equally dissimilar compared to Vivarium and Piazza post-operam.

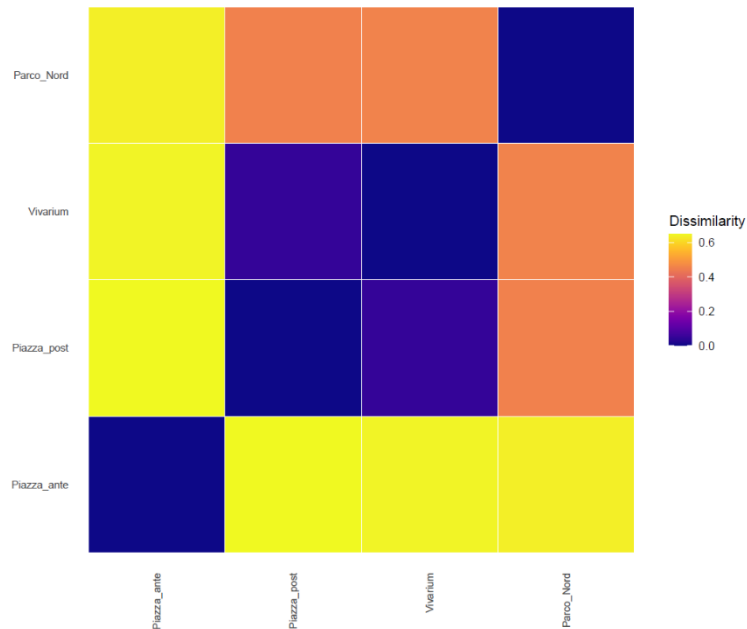


Figure 15. Heatmap showing the dissimilarities between areas.

4.3.2 Sound event classification

Model implementation

Sound events' occurrences in the dataset are reported in Figure 16.

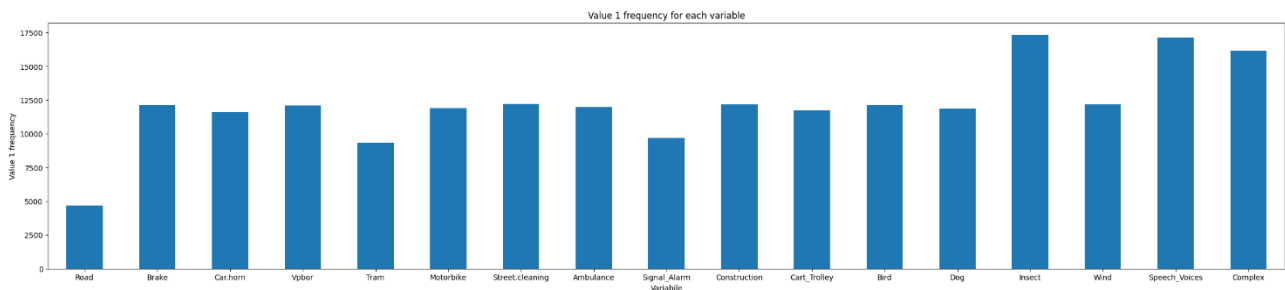


Figure 16. Sound sources events' occurrences in the dataset.

The results for the cross-validation training on the 10 folds are reported in Table 2. The values for the three parameters are consistent in all folds indicating the subdivision of the dataset doesn't influence the model's performance.

Table 2. Precision, Recall and F1-score of each dataset fold.

Fold	Precision	Recall	F1-score
1	0.938	0.663	0.772
2	0.939	0.658	0.767
3	0.939	0.660	0.770
4	0.934	0.656	0.766
5	0.938	0.663	0.772
6	0.935	0.663	0.770
7	0.939	0.658	0.768
8	0.938	0.661	0.770
9	0.934	0.665	0.771
10	0.940	0.658	0.768
Overall	0.937	0.660	0.770

In Table 3 are reported the mean precision, recall and F1-score values for each sound event on the 10 folds.

Table 3. Mean Precision, Recall and F1-score on the 10 folds for each sound event label.

Label	Mean precision	Mean recall	Mean F1-score
Road	0.97	0.71	0.82
Brake	0.56	0.41	0.47
Car.horn	0.88	0.50	0.64
Vpbor	0.98	0.65	0.78
Tram	0.99	0.55	0.71
Motorbike	0.99	0.56	0.72
Street.cleaning	1.00	0.99	0.99
Ambulance	1.00	0.75	0.85
Signal_Alarm	0.89	0.60	0.72
Construction	1.00	0.84	0.92
Cart_Trolley	0.99	0.82	0.90
Bird	1.00	0.58	0.73
Dog	0.88	0.69	0.77
Insect	0.92	0.67	0.77
Wind	0.98	0.73	0.84
Speech	0.97	0.65	0.78
Complex	0.96	0.52	0.68

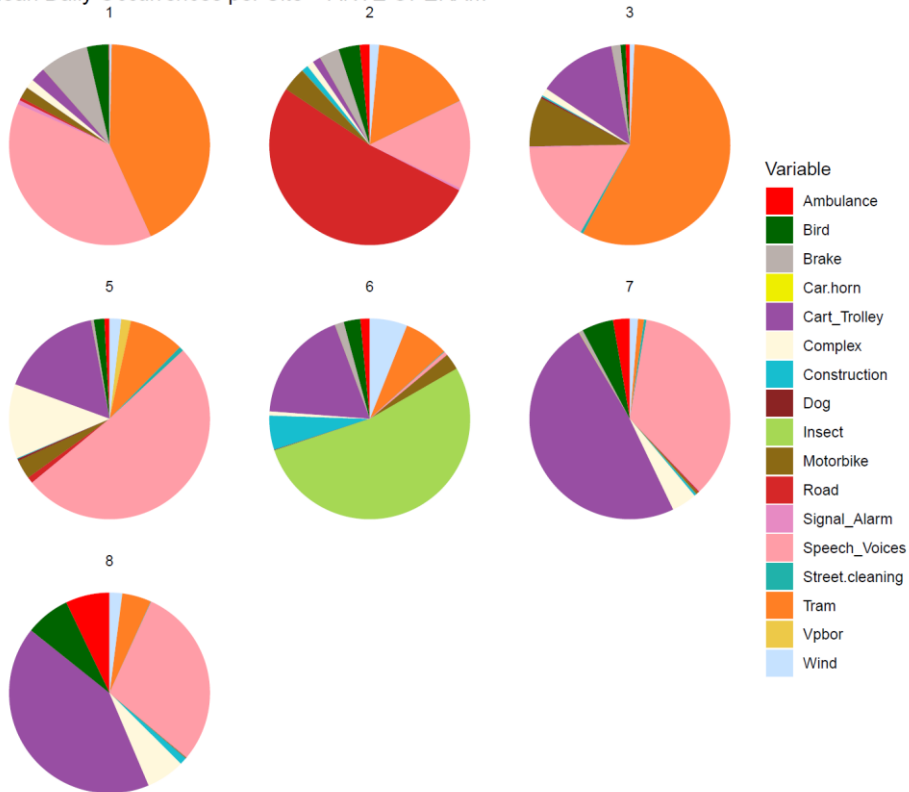
Compared to [54] results, on the 17 sound events investigated, Precision values increased for 13 of them and decreased for 2 only while Recall increased for 10 events and decreased for 7 of them. In particular, recall values increased for Brake, Car.horn, Vpbor, Tram, Motorbike, Street.cleaning, Ambulance, Construction, Bird, Dog, Wind, Speech and Complex. Recall values increased for Road, Vpbor, Street.cleaning, Alarm_Signal, Construction, Cart_Trolley, Dog, Wind, Speech and Complex.

Recording campaigns classification

The ante-operam classification results are explained in Figure 17. Sites 1 and 3 present a consistent slice corresponding to tram passages which decrease in sites 2-5-6 and are absent in sites 7-8 because the lower courts shield them from that particular source. Road is present in site 2, probably due to the device orientation. Speech is present in all sites especially in sites 5 (used as an open study area) and 1 (above site 5), 7 and 8. Cart passages were detected by all devices, probably because the routes skim the border between the ground floor and the courtyards. Birds were detected in all sites, especially in 7-8, while insects dominate site 6. Motorbike passages or ignitions and ambulance sirens are also present in all sites. Finally, wind is present in site 6 because it is set next to the walk passages from and to the square between buildings U1-U2 where wind currents are created (Figure 3).

The post-operam pie chart is shown in Figure 17. Tram passages are still present in sites 1-2-3-5. Speech is still one of the most frequent events in almost all sites. Also Cart passages still occur. Insects are still present in site 6 even if only partially. Wind occurs also in sites 6-2-3-7. Bird vocalizations occupy a large slice of the pies of sites 1-2-6-7. Complex sounds and Motorbike passages or ignitions are still present.

Mean Daily Occurrences per Site – ANTE OPERAM



Mean Daily Occurrences per Site – POST OPERAM

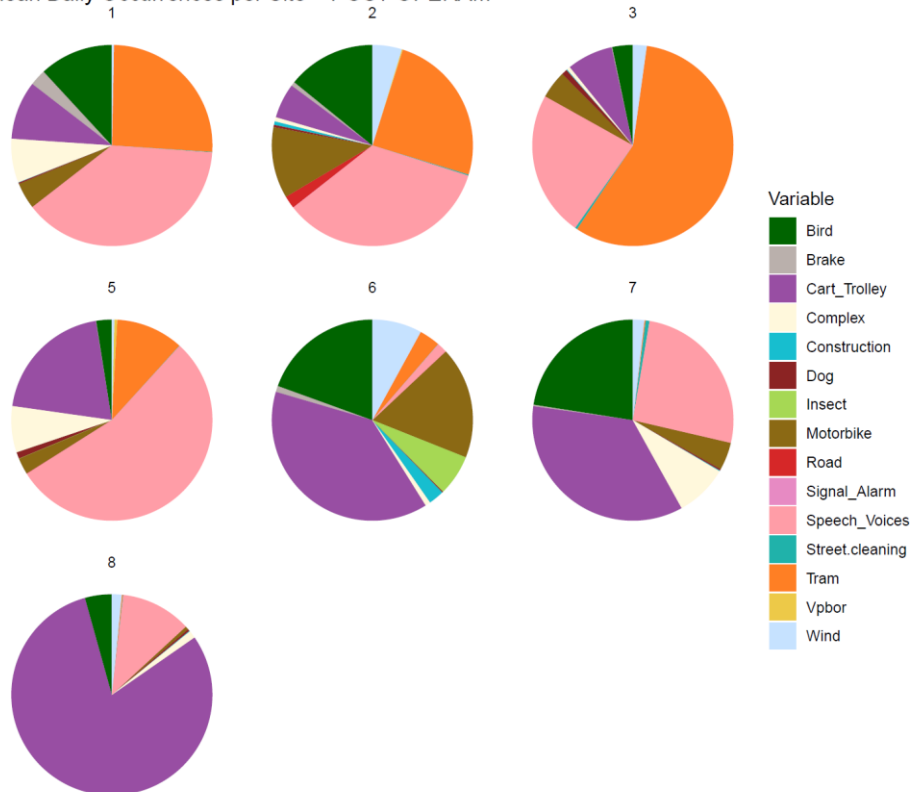


Figure 17. Pie charts on sound event classification in ante-operam (above) and post-operam (below).

Finally, barplots showing the 5 most lasting sound sources per site per scenario mean on are displayed in Figure 18. The measuring unit is expressed in minutes by converting the occurrences using the timeframe length allowing comparison between scenarios. Comparing the scenarios, the duration of the events classified is lower in the post-operam. Tram events in sites 1-2-3-5 are consistent in the two scenarios. The same works per Speech (except in site 7 post-opera where it surpasses the Cart event) and Cart passages. Bird vocalizations are more present (last longer) in the post-operam campaign. Motorbike noise and complex noises are present in both scenarios.

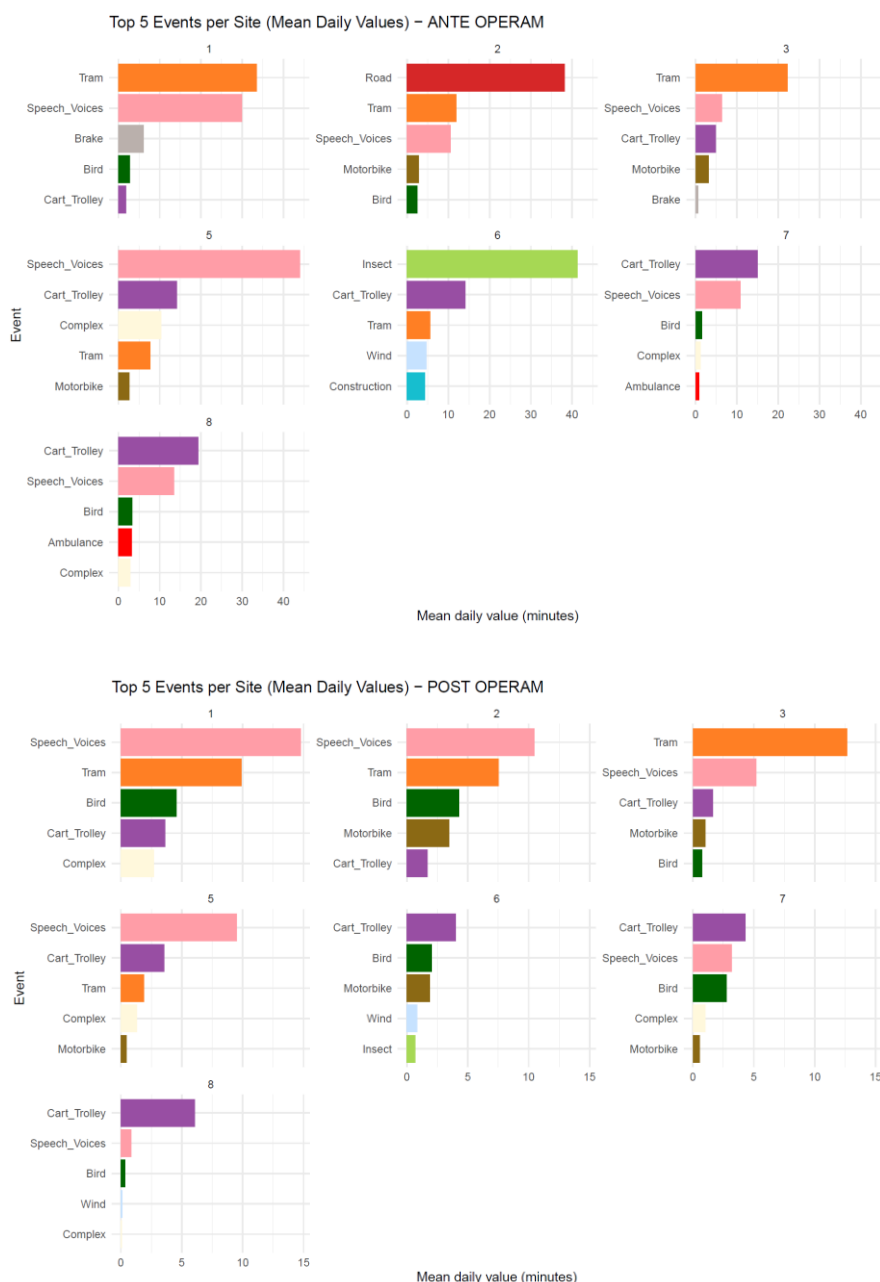


Figure 18. Top5 most frequent sound events in ante-operam (above) and post-operam (below) expressed in minutes.

4.3.3 BirdNET analysis

Parameters choice

For Piazza della Scienza, precision, recall and F1-score were calculated and are shown in Table 4. To maximize the recall while preserving precision, the best parameter combination resulted to be: minimum confidence = 0.5, sensitivity = 1.5 and overlap = 2 s, obtaining precision = 0.97, recall = 0.65 and F1-score = 0.78.

Table 4. Precision, Recall and F1-score of each BirdNET parameter combination for Piazza della Scienza dataset.

Minimum confidence	Sensitivity	Overlap	Precision	Recall	F1-score
0.5	1	1	0.95	0.32	0.48
0.5	1	1.5	0.95	0.42	0.59
0.5	1	2	0.97	0.65	0.78
0.5	1.5	1	0.95	0.32	0.48
0.5	1.5	1.5	0.95	0.42	0.59
0.5	1.5	2	0.97	0.65	0.78
0.6	1	1	1	0.29	0.44
0.6	1	1.5	0.99	0.34	0.51
0.6	1	2	0.99	0.53	0.69
0.6	1.5	1	1	0.23	0.38
0.6	1.5	1.5	1	0.27	0.42
0.6	1.5	2	1	0.44	0.61
0.7	1	1	1	0.23	0.38
0.7	1	1.5	1	0.27	0.42
0.7	1	2	1	0.44	0.61
0.7	1.5	1	1	0.15	0.27
0.7	1.5	1.5	1	0.20	0.33
0.7	1.5	2	1	0.30	0.46

For Parco Nord parameters decision, the following graphs were produced (Figure 19, Figure 20) showing the mean values on number of species detected by BirdNET using the Parco Nord coordinates (N) and of those species how many were present in the ornithologist list (N-in-list). The mean values have been calculated by averaging the number of species on the other two varying parameters for Figure 19 (i.e., when examining Confidence, Confidence values are fixed and the mean is calculated on Sensitivity and Overlap) and on the last parameter for Figure 20.

To balance between total number of species and species actually present in the list, the following parameters' values were chosen: minimum confidence 0.75; sensitivity 1; overlap 0.5 s.

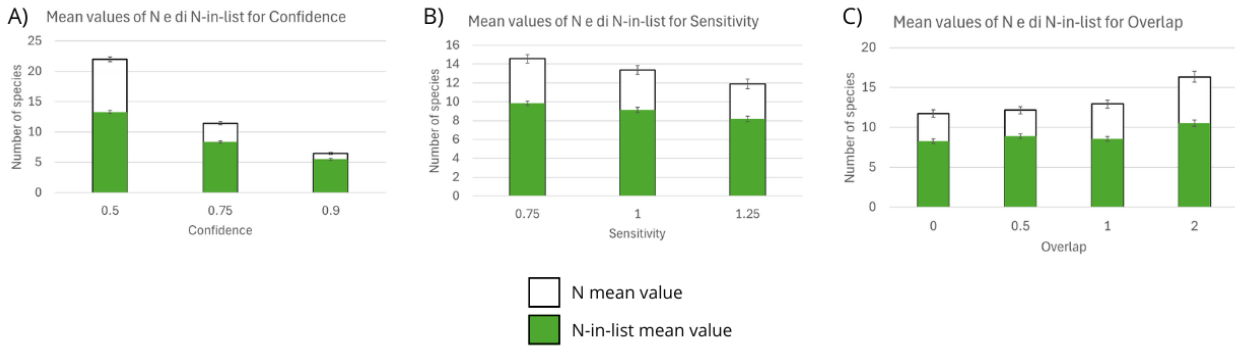


Figure 19. Graphs showing the changes of the mean values of BirdNET species detection (N) and of those the species in the list (N-in-list) by changing one parameter.

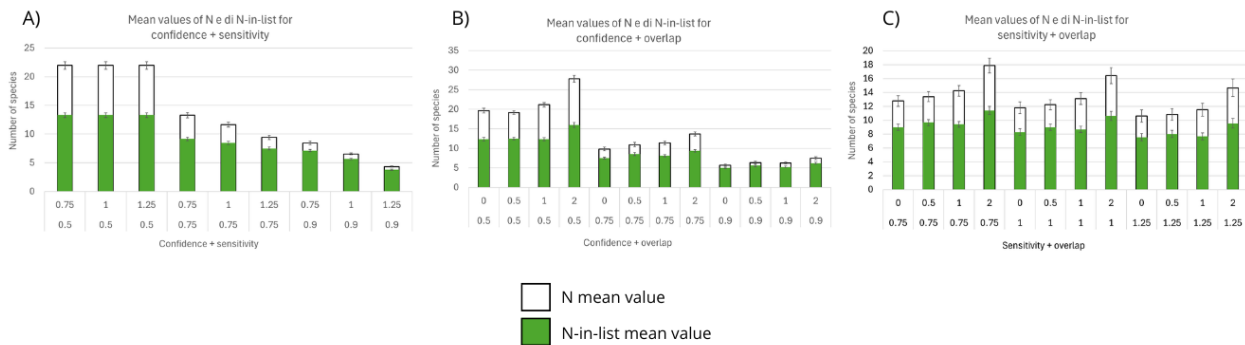


Figure 20. Graphs showing the changes of the mean values of BirdNET species detection (N) and of those the species in the list (N-in-list) when varying two parameters

BirdNET results

Piazza della Scienza ante-operam has a species richness of 10 while the post-operam has 14 species. Vivarium hosts 16 species while Parco Nord 72 species overall.

Species richness by site is shown in Figure 21 and 22.

Figure 21 refers to the Piazza della Scienza ante and post-operam scenario; there is an overall increase in species richness in the post-operam campaign and the highest improvement happens in site 2.

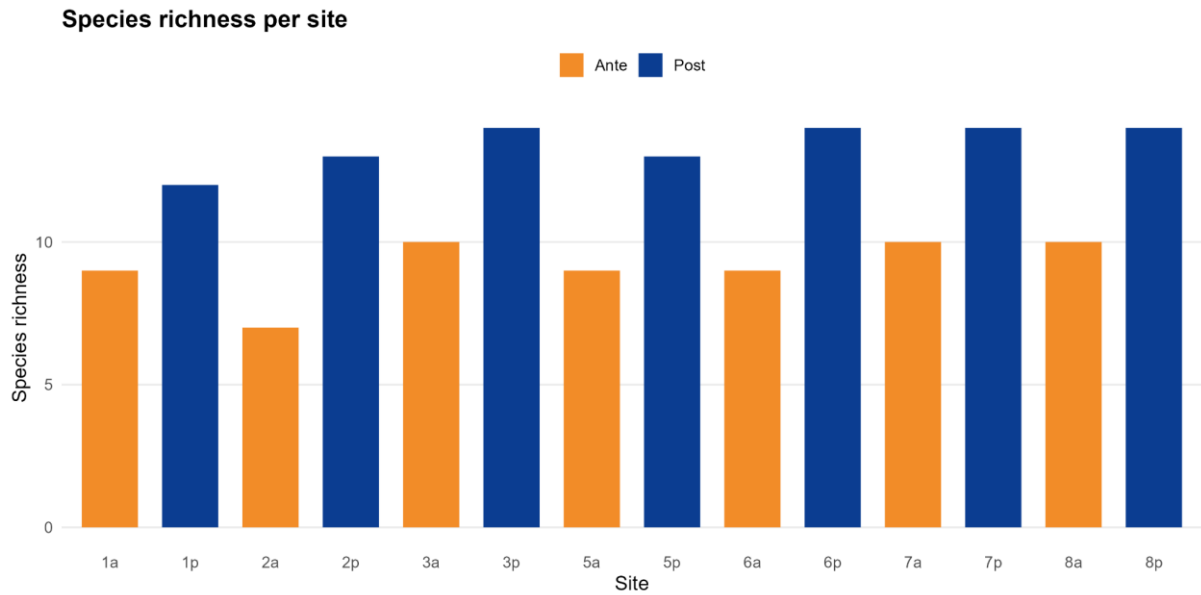


Figure 21. Avian richness per sites of Piazza ante-operam (orange) and post-operam (blue)

Figure 22 shows Parco Nord daily mean species richness. The sites (green) are characterized by similar overall richness with the exception of sites 18 and 13.

Mean daily species richness at Parco Nord

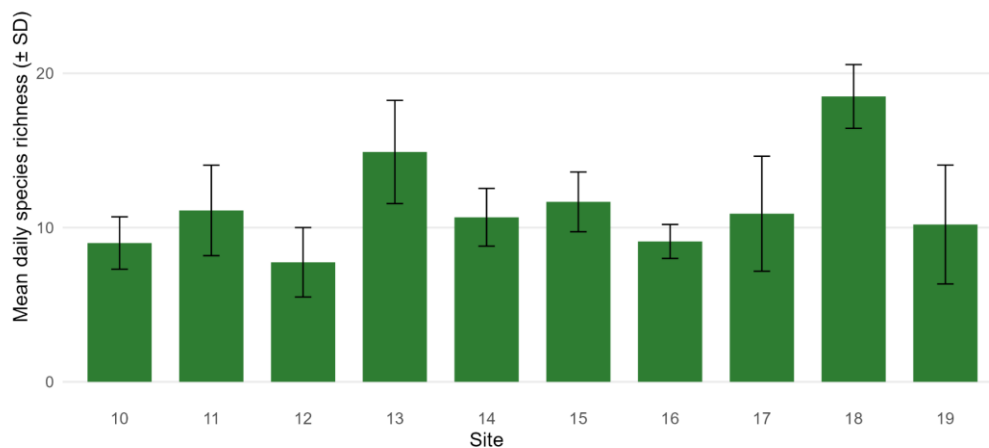


Figure 22. Avian richness per sites of Parco Nord.

For the Piazza (Figure 23), the mean number of daily vocalizations increase in all post-operam sites especially in sites 2-3-7.

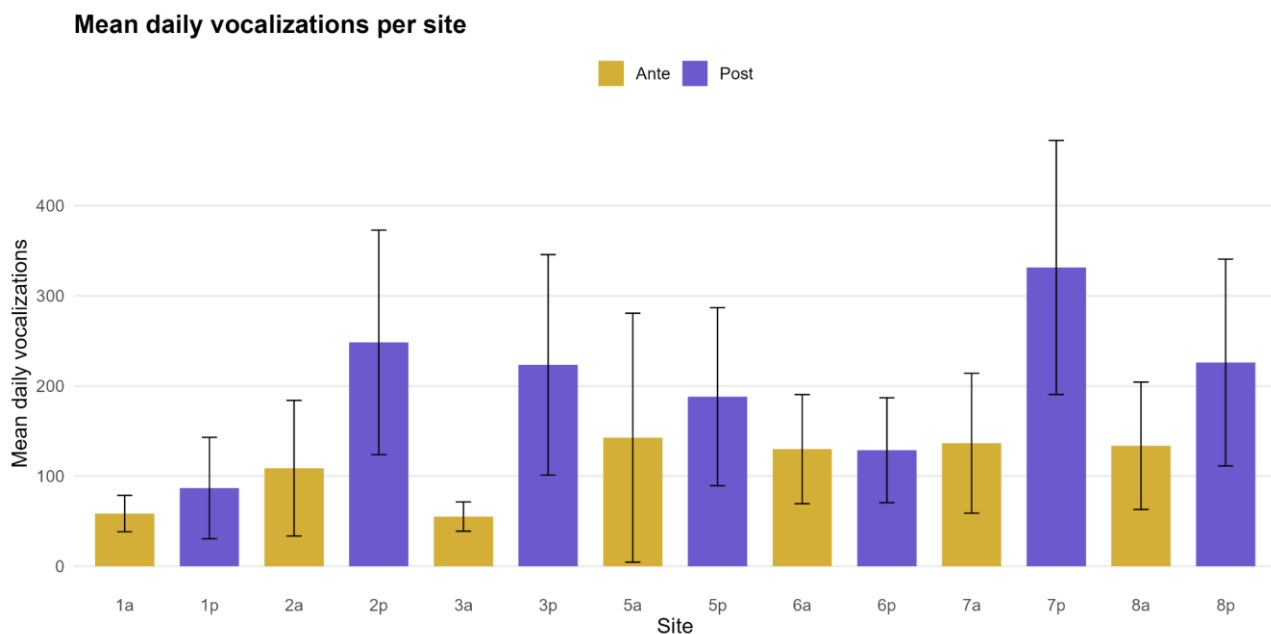


Figure 23. Vocalization rates per sites of Piazza ante-operam (gold) and post-operam (violet)

Finally, top5 vocalizing species time trends in the areas are shown (Figure 24, 25, 26).

In Piazza (Figure 24), 3 species out of 5 remained the most vocalizing ones (*Turdus merula*, *Apus apus*, *Parus major*) and the vocalizations' temporal distribution did not change for *Apus apus*.

Vivarium species are shown in Figure 25 and the major activity happens before slightly after dawn, with *Fringella coelebs* being the only one to vocalize more during daytime than at dawn. In this area *Turdus merula* vocalizes especially before dawn.

Finally, Parco Nord (Figure 20) shows a concentration in vocalization rates at dawn and in morning, with only *Turdus merula* vocalising almost constantly all day.

Some of the top5 vocal species are present in more than one area; *Turdus merula* is present in all areas and *Sylvia atricapilla* are present at Parco Nord and Vivarium.

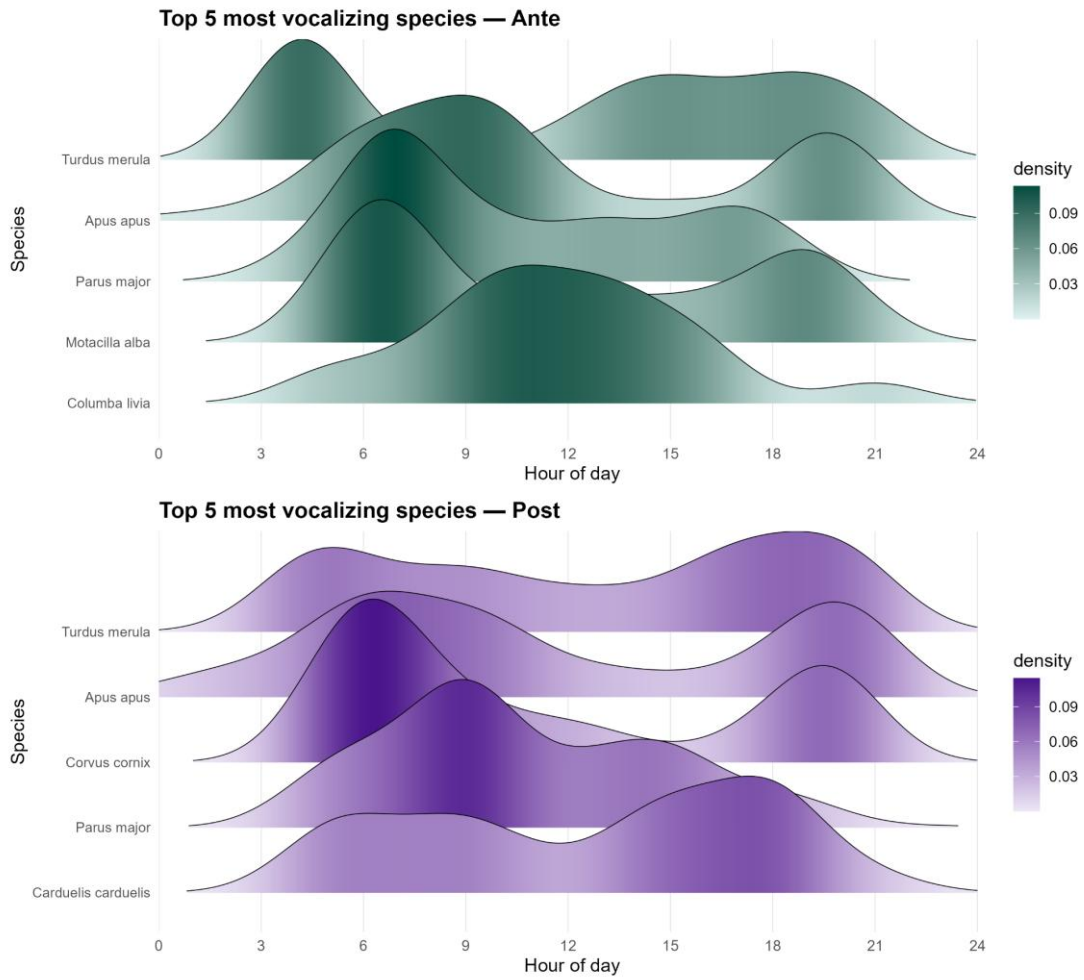


Figure 18. Ridgplot of mean vocalization time trend for the 5 most vocalizing species in Piazza (ante above, post below)

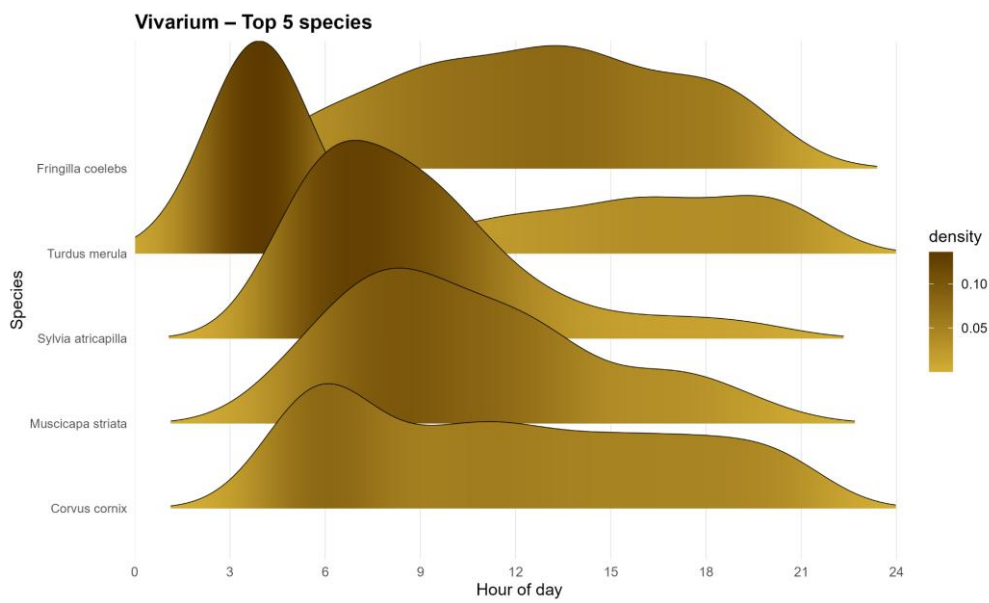


Figure 25. Ridgplot of mean vocalization time trend for the 5 most vocalizing species at Vivarium

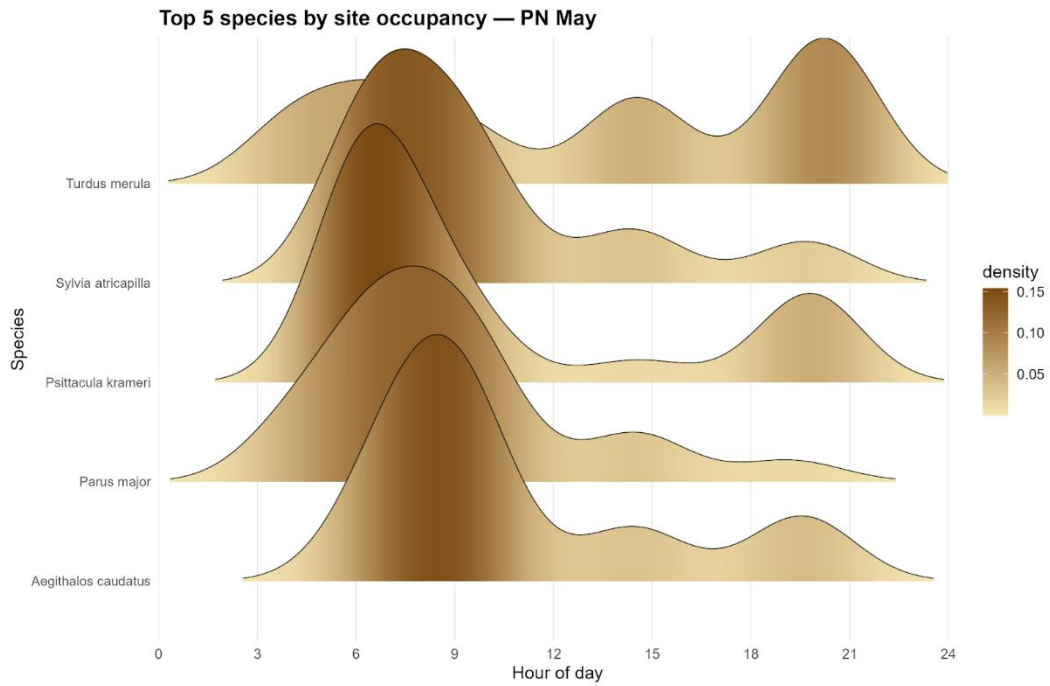


Figure 26. Ridgplot of mean vocalization time trend for the 5 most vocalizing species in all Parco Nord

4.3.4 Regression models on ACI, Sound events and BirdNET

A significant overall increase in acoustic complexity was observed in the post-intervention phase (PhasePost: $\beta = 0.0047$), indicating higher ACI values after the urban regeneration independently of species richness and sound source presence. Model-based predictions illustrate this general upward shift in ACI across conditions in the post-intervention phase (Figure 27, 28, 29).

In the ante-operam, acoustic complexity was positively associated with species richness ($\beta = 0.0026$), with model predictions showing a clear positive relationship between richness and ACI (Figure 16, solid line). Acoustic complexity was also positively associated with the presence of bird vocalizations in the ante-operam phase ($\beta = 0.0028$), as reflected by higher predicted ACI values when birds were present compared to absent conditions (Figure 17). Human voices were positively associated with ACI in the ante phase as well ($\beta = 0.0036$), together with other anthropogenic sources such as motorbikes ($\beta = 0.0023$) and Cart_Trolley sounds ($\beta = 0.0215$).

Significant interaction effects revealed marked differences between phases. The contribution of bird vocalizations to ACI was significantly reduced in the post-intervention phase (Bird × PhasePost: $\beta = -0.0022$), resulting in a weaker contrast between bird presence and absence in post-intervention conditions compared to the ante phase (Figure 28). Similarly, the positive relationship between species richness and ACI was attenuated in the post-operam (Richness × PhasePost: $\beta = -0.0017$), with model predictions indicating a flatter slope in the post-intervention phase relative to the ante phase (Figure 27, dashed line).

In contrast, the contribution of human voices to acoustic complexity increased substantially after the intervention (Speech_Voices × PhasePost: $\beta = 0.0050$). Model predictions show a stronger difference in ACI between recordings with and without human voices in the post-intervention phase compared to the ante phase (Figure 29), indicating a phase-dependent effect of speech presence on acoustic complexity.

Finally, the random effect of site accounted for a limited proportion of total variance (SD = 0.0067), compared to residual variability (SD = 0.0254), indicating that observed patterns were consistent across sites and not driven by site-specific acoustic baselines.

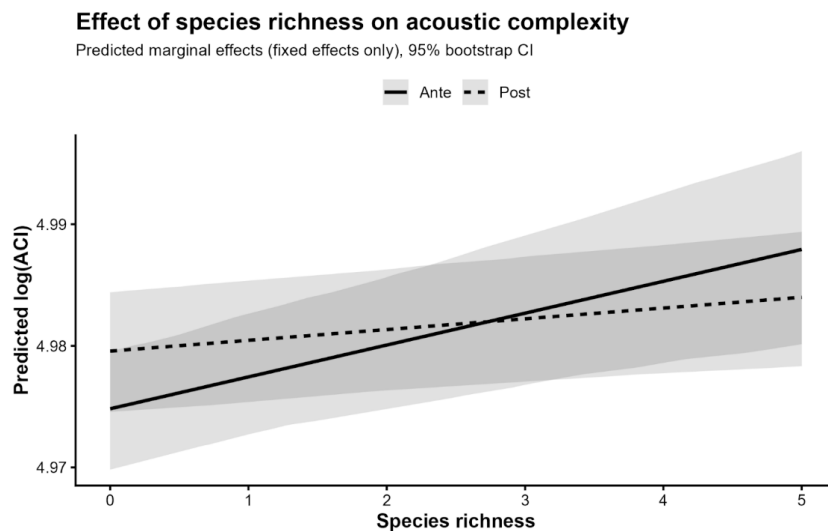


Figure 27. Effect of avian richness on ACI, ante and post-operam scenario.

Effect of bird presence on acoustic complexity

Predicted at richness = 0 (fixed effects only), 95% bootstrap CI

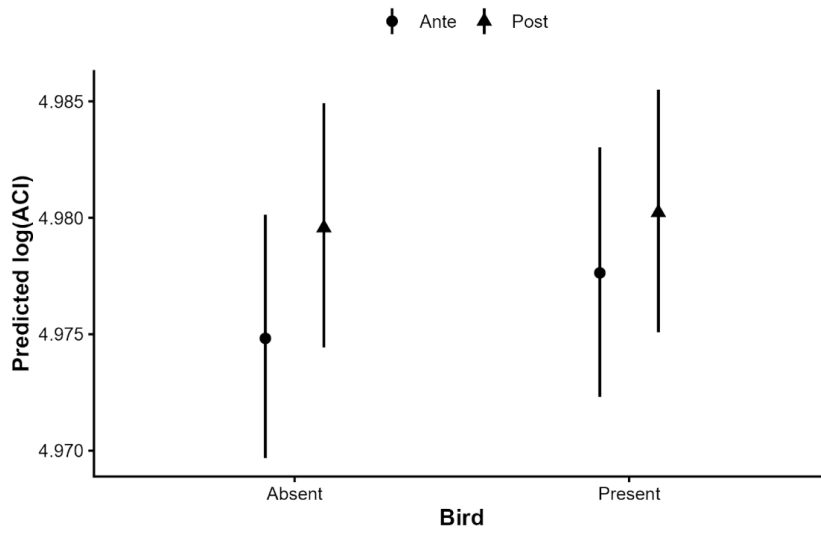


Figure 28. Effect of birds presence on ACI, ante and post-operam scenario.

Effect of human voices on acoustic complexity

Predicted at richness = 0 (fixed effects only), 95% bootstrap CI

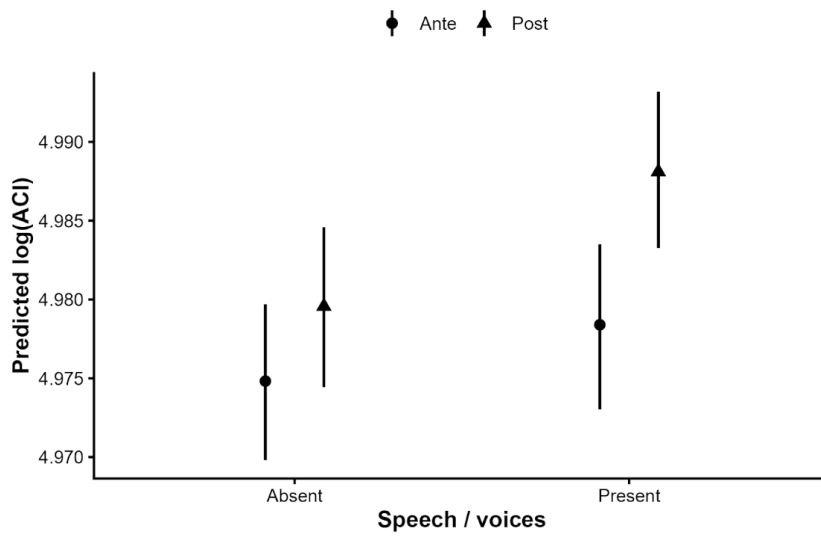


Figure 29. Effect of human speech on ACI, ante and post-operam scenario.

4.4 Discussion

In this study, the two main branches of ecoacoustics (ecoacoustic indices and avian vocalization detection) have been implemented alongside sound events classification to characterize the sonoscape of an urban square before and after being regenerated and assess potential changes comparing the square with two near-located urban green areas.

The methodology has been carefully defined to ensure correct data elaboration. Indeed, an equalization process has been carried out to linearize the frequency response of Song Meter Micros which present a peak at 6 kHz [63] limiting biases in ecoacoustic indices elaborations. Moreover, ecoacoustic indices' parameters have been carefully calculated as promoted in [50, 51, 64] as well as a modification of ADI, AEI, H and ZCR to account for minimum and maximum frequency threshold [50, 51]. Different indices have been used to better characterize the sonoscape [65] while some of them (i.e., BI and NDSI) have not been employed to avoid biases due to the urban context [33].

The implementation of machine learning algorithms to classify sound sources has grown exponentially in ecoacoustics since 2008 [66]. In a recent review on machine learning methods applied in ecoacoustics [66], three studies used a random forest classifier, focusing respectively on Furnariidae birds [67] (using MFCCs+functionals as input features getting a recall rate close to 0.9), frog choruses [68] (using ecoacoustic indices as input features) and dolphin whistles [69]. Other studies used MFCCs as input features focusing on whales [70], cicadas and rain [71] and on animals' syllable segmentation [72]. All these studies focused on a specific group of animals or geophony, but not on urban sound events in general; moreover, no study has been carried out in Italy to their knowledge. This may be due to a prevailing focus in ecoacoustics on the classification and detection of biophonies and certain geophonies. Regarding urban sound classification not focused on ecoacoustics, many studies have been conducted; however, the use of different methods prevents a direct comparison on results.

About avian community characterization, in literature there are studies employing BirdNET with accurate and good results [73, 74].

In this study, the ecoacoustic indices analysis carried out on the square highlighted intra-scenario differences. In the boxplot analysis, sites 3 and 5 Hnew ante-operam present

greater median values and boxplot width compared to the other sites, reflecting greater acoustic heterogeneity possibly due to bird vocalizations, speech and tram passages. The same sites present higher boxplots for ZCRnew, which highlight the sites as noisier. Finally, site 5 DSC ante-dawn and day boxplot are wider which means there are shifts in the sounds present from high frequency ones (i.e., birds, carts, speech) to low ones (i.e., ventilation). This correspondence could have influenced their grouping in the ante-operam clusterization. Similarly, site 8's ADI, AEI, ZCRnew and NP ante-operam boxes are similar to the ones of site 1 and 2, and could have played a role in grouping them together; lower ADI means concentrated sounds on specific frequency bands (i.e., ventilation systems), while lower ZCRnew identify them as less noisier sites. Instead, in the post-operam scenario, the wider ACI of site 1 day-period and ADI and AEI boxplots of sites 1, 2 and 3 drove them in forming a cluster, as well as for sites 7 and 8 higher values for ADI, Hnew, DSC and ZCRnew. Wider ACI and ADI boxplots in the post-opera mean a greater variability in sound events. Greater values in Hnew and DSC in sites 7 and 8 reflect higher heterogeneity in sound signals in terms of temporal and spectral distribution such as more bird vocalization and speech and possibly cart passages. Finally, site 8 also presents higher median values for ADI which means more energy distribution along the spectrum which can be associated with the impulsive sounds of the cart passages.

The interpretations on the boxplot analysis are consistent with the sound sources present in the square and BirdNET. In the ante-operam, sites 1, 2 and 5 all present similar amounts of Speech, Tram, Complex and Motorbike sounds. Similarly, it can be seen in the post-operam scenario, with a similar events distribution for the two clusters. Moreover, site 8 presents more cart passages in the post-opera, while in site 7 are less present but bird vocalizations increased. Finally, in sites 1, 2 and 3, the sound sources are more temporally distributed as indicated by ACI and ADI.

BirdNET results do not show evident clusterization, probably due to the more distributed and mobile characteristics of birds instead of fixed technophonies like trams and traffic (motorbike and road) and the relatively small Piazza's surface and the obstruction caused by the university buildings.

Comparing the ante-operam with the post-operam scenarios, a first difference has been confirmed through the boxplot analysis where all indices presented variation in median values or box width. These changes have been confirmed by the PCA exhibiting differences

in scenarios and day periods, like wider post-operam ellipses which mirror the wider post-operam boxplots. Finally, a confirmation derived from the dissimilarity index calculations which showed that, even if site stability was present (because the highest values of dissimilarity were not reached) there is indeed a dissimilarity between the ante and post-operam sites especially for sites 2-5-7-8.

In literature, ecoacoustics have been rarely used to assess changes in regeneration processes and the majority are linked to non-urban regeneration actions such as forest restorations [15, 79]. To our knowledge, there are no other studies assessing the efficacy of an urban regeneration process by means of ecoacoustics.

This research confirmed that ecoacoustic indices are also sensitive to urban changes and thus can be used to verify the effects of urban interventions.

The differences in Piazza's scenarios assessed by ecoacoustic indices are validated by the sound events classification and BirdNET results as we described before. The classifier underlined a difference in sound sources repartition and presence, with Road and Insect contribution drastically reduced in post-operam while other sources like Birds emerged. Birds' presence and richness changes have been confirmed by BirdNET with a positive improvement of both parameters in the post-operam scenario. This result suggests the efficacy of the regeneration project in attracting birds, potentially increasing both the biodiversity of the Piazza and the pleasantness of its soundscape. Finally, the linear mixed-effects model further validated the relationship between indices (ACI in this case) and sound sources, and the sonoscape increased in sound complexity. The difference between scenarios is once again highlighted by the change in associations between ACI and birds, richness, speech and Cart_Trolley in the two phases.

The relationship between ACI and "Speech" is consistent with another study carried out in Piazza della Scienza aimed at linking ecoacoustic indices to people's soundscape perception by means of questionnaires; in it, ACI resulted to be linked to perceived people's sounds as speech [78]. This relation is also confirmed by [79] where the recreational behaviors of people were analyzed and those in which speech is involved (such as social interactions and sport activities) are correlated with ACI.

In literature, the interactions and regressions between ecoacoustic indices and avian richness and sound sources are widely explored but there are contrastive results. The

relationship between ACI and avian richness and vocalizations' presence is consistent with studies carried out in temperate regions [43, 75, 47] even if [80] did not find ACI or other indices to be strongly correlated to avian richness in a university context. The comparative study [76] assesses the greater number of studies which prove a lack in correlation compared to the ones demonstrating correlation. Finally, [77] analyzed four ecoacoustic datasets and avian point counts worldwide showing rare consistency between indices and richness correlation. For these reasons, other studies must be conducted, standardizing problems such as device differences, ecoacoustic indices calculation methods and sampling methods, to spread ecoacoustics outside academia and into environmental protection and monitoring actions.

Differences between the three areas have been assessed by means of principal components analysis (PCA) applied separately to the areas. Indeed, the relative contribution of ecoacoustic indices to the principal components differed among areas, with the Piazza datasets explaining a lower proportion of variance in the first components compared to the two park areas. Moreover, the first ecoacoustic indices in explaining the PCs varied between areas but still maintained their contribution role, as observed in [30]. Another similarity with [30] lies in H index being the first contributor in PC1 in the green areas (Parco Nord and Vivaio). Finally, PCA carried out on the all-areas dataset showed ellipses and centroides with different orientations strengthening the different contribution of indices between the green areas and the square. Focusing on the square, the post-operam wider ellipse shows a sonoscape shifting to the parks' ones.

The dissimilarity between the park sites and the post-intervention Piazza sites 5, 6, 7 and 8 (ground level and courtyards), relative to the ante-intervention Piazza sites, is clearly reflected by the separation observed in the NMDS ordination space. The same happens for the dissimilarity between Piazza pre-intervention site 7 against site 8 which is shown as the greatest distance between pre-intervention sites in the NMDS plot. Finally, the non-dissimilarity between sites 1,2,3 ante and post-operam is shown by their grouping in the NMDS. All these differences can be seen at areas' scale in the areas' heatmap where the parks against Piazza post-operam present lower dissimilarity than parks against Piazza ante-operam.

The differences between Piazza ante-operam and post-operam can be explained by the greater avian richness and a more spread vocalization rate throughout the day of the latter,

even if the top five species remain the same. However, avian richness alone is insufficient to account for the similarity between the post-intervention Piazza and the Vivarium and Parco Nord sites.

Avian richness and the common top 5 vocalizing species between Parco Nord and Vivarium can explain their similarity. Also the equal distribution between vocalizing dawn peaks and during the day can explain their short grouping in the NMDS plot. The common equally distributed vocalizing rate of Piazza post-operam and Vivarium can explain the closeness of site 9 (Vivarium) with sites 5, 7, 8 post-operam; this reasoning works also for the difference with the Piazza ante-operam.

Surely, other sound sources in the parks contribute to the ecoacoustic indices values and thus similarity/dissimilarity. These differences cannot be attributed solely to specific anthropogenic sources such as train traffic near the Vivarium or tram passages in the Piazza, as trams were already present during the ante-intervention phase. Nor the sampling year can be addressed since Vivarium recordings were carried out in 2022 and Piazza after-intervention and Parco Nord in 2025. Nevertheless, the post-intervention sonoscape of the Piazza appears more similar to that of an urban park than in the ante-intervention condition. It is important to note that the observed convergence does not imply ecological equivalence. Rather, it indicates a measurable improvement in acoustic structure and variability within a highly anthropized context, without replacing the ecological functions provided by larger and less disturbed green areas.

In any case, this similarity outcome was not self-evident, as the regeneration did not include direct interventions on major acoustic sources such as ventilation systems. From an urban regeneration perspective, these findings suggest that relatively low-impact interventions, such as flooring removal, vegetation increase and changes in space usability, can significantly influence urban sonoscapes. Even in the absence of direct noise-mitigation measures, modifications of land cover and public use patterns appear sufficient to alter the acoustic structure of the environment. This highlights the potential role of ecoacoustic monitoring as a complementary tool for evaluating the environmental effectiveness of urban regeneration projects. In particular, ecoacoustic indices here used can reflect ecological wellness and restoring processes [39-41] even in highly anthropized urban environments where overlapping sounds poses challenges to the monitoring.

4.5 Conclusions

In this study, two urban parks and a recently renovated university square in Milan have been monitored with passive acoustic recorders and their sonoscapes have been characterized by calculating 5 ecoacoustic indices and using BirdNET. The square has been monitored before and after the intervention and a machine learning sound classifier has been developed to better assess its sonoscape changes.

Before these computations, an equalization procedure has been carried out to uniformize the frequency responses of Song Meter Micros and Audiomoth which are not similar nor linear. This reduced interpretative biases in the analysis alongside the careful definition of ecoacoustic indices' hyperparameters.

Differences between the square intervention phases were detected in terms of absolute values changes, increment in data variance and changes of PCA ellipses orientation. Moreover, the dissimilarity index distinguishes between ante-operam and post-operam measurement sites. The trained random forest classifier highlighted sound sources repartition changes while BirdNET investigation demonstrated an increase in avian species richness and change in vocalization rates. Finally the relationship between ACI, sound events and avian richness have been analyzed using linear mixed-effects models. ACI showed a relationship with avian richness, speech presence and cart passages. In addition, the model assessed a significant increase in acoustic complexity in the post-operam scenario.

Differences between the three areas (the square and the urban parks) have been assessed by the PCA, the calculation of the dissimilarity index and by BirdNET avian richness and vocalization rates. Generally, the post-operam square ecoacoustic dataset resulted to be more similar to the ones of the two parks demonstrating the efficacy of flooring removal and greening in changing the sonoscape towards an urban park one. Moreover, BirdNET assessment showed an improvement in avian richness in the square and the change in vocalization rates can explain the increased similarity with the parks.

Thus, this study demonstrated the positive effects of an urban regeneration project on its sonoscape even in the absence of measures aimed at directly addressing the sources of noise. Moreover, ecoacoustic indices proved efficacy on detecting these changes. In the

future, the Piazza's sonoscape will be monitored using fixed recorders to better assess the role of vegetation and plants growth. Finally, this study hopes to spark interest in the assessment of urban regeneration interventions which are a hot-topic nowadays to better understand their effect on the city's sonoscapes.

References

1. Hänninen, O., Knol, A. B., Jantunen, M., Lim, T. A., Conrad, A., Rappolder, M., ... & EBoDE Working Group. (2014). Environmental burden of disease in Europe: assessing nine risk factors in six countries. *Environmental health perspectives*, 122(5), 439.
2. Lutz, W., Amran, G., Bélanger, A., Conte, A., Gailey, N., Ghio, D., ... & Stonawski, M. (2019). *Demographic scenarios for the EU: Migration, population and education*. Publications Office of the European Union.
3. Francis, C. D., & Barber, J. R. (2013). A framework for understanding noise impacts on wildlife: an urgent conservation priority. *Frontiers in Ecology and the Environment*, 11(6), 305-313.
4. Pijanowski, B. C., Farina, A., Gage, S. H., Dumyahn, S. L., & Krause, B. L. (2011). What is soundscape ecology? An introduction and overview of an emerging new science. *Landscape ecology*, 26(9), 1213-1232.
5. Francis, C. D., Newman, P., Taff, B. D., White, C., Monz, C. A., Levenhagen, M., ... & Barber, J. R. (2017). Acoustic environments matter: Synergistic benefits to humans and ecological communities. *Journal of environmental management*, 203, 245-254.
6. Bowler, D. E. (2010). Green spaces affect emotional wellbeing more than physiology. *Nursing Standard*, 25(4), 17.
7. Lachowycz, K., & Jones, A. P. (2013). Towards a better understanding of the relationship between greenspace and health: Development of a theoretical framework. *Landscape and urban planning*, 118, 62-69.
8. McMahan, E. A., & Estes, D. (2015). The effect of contact with natural environments on positive and negative affect: A meta-analysis. *The journal of positive psychology*, 10(6), 507-519.
9. Zhao, H., & Wang, S. (2025). Rethinking concrete reuse workflow in Hong Kong: A comparative study with Swiss models. In *Structures and Architecture* (pp. 42-50). CRC Press.
10. Donnelly, R., & Marzluff, J. M. (2006). Relative importance of habitat quantity, structure, and spatial pattern to birds in urbanizing environments. *Urban Ecosystems*, 9(2), 99-117.
11. Alvey, A. A. (2006). Promoting and preserving biodiversity in the urban forest. *Urban forestry & urban greening*, 5(4), 195-201.
12. Sanesi, G., Gallis, C., & Kasperidus, H. D. (2010). Urban forests and their ecosystem services in relation to human health. In *Forests, trees and human health* (pp. 23-40). Dordrecht: Springer Netherlands.
13. Faeth, S. H., Bang, C., & Saari, S. (2011). Urban biodiversity: patterns and mechanisms. *Annals of the new York Academy of Sciences*, 1223(1), 69-81.

14. Farina, A., Krause, B., & Mullet, T. C. (2024). An exploration of ecoacoustics and its applications in conservation ecology. *BioSystems*, 245, 105296.
15. Gitau, C., Kettel, E., Abrahams, C., Webala, P. W., & Uzal, A. (2025). The role of ecoacoustics in monitoring ecosystem degradation and restoration. *Restoration Ecology*, 33(8), e70168.
16. Gibb, R., Browning, E., Glover-Kapfer, P., & Jones, K. E. (2019). Emerging opportunities and challenges for passive acoustics in ecological assessment and monitoring. *Methods in Ecology and Evolution*, 10(2), 169-185.
17. Benocci, R., Brambilla, G., Bisceglie, A., & Zambon, G. (2020). Eco-acoustic indices to evaluate soundscape degradation due to human intrusion. *Sustainability*, 12(24), 10455.
18. Bradfer-Lawrence, T., Gardner, N., Bunnefeld, L., Bunnefeld, N., Willis, S. G., & Dent, D. H. (2019). Guidelines for the use of acoustic indices in environmental research. *Methods in Ecology and Evolution*, 10(10), 1796-1807.
19. Sueur, J., & Farina, A. (2015). Ecoacoustics: the ecological investigation and interpretation of environmental sound. *Biosemiotics*, 8(3), 493-502.
20. Llusia, D. (2024). The limits of acoustic indices. *Nature Ecology & Evolution*, 8(4), 606-607.
21. Dröge, S., Martin, D. A., Andriafanomezantsoa, R., Burivalova, Z., Fulgence, T. R., Osen, K., ... & Kreft, H. (2021). Listening to a changing landscape: Acoustic indices reflect bird species richness and plot-scale vegetation structure across different land-use types in north-eastern Madagascar. *Ecological Indicators*, 120, 106929.
22. Luna-Naranjo, D., Martinez-Vargas, J. D., Sánchez-Giraldo, C., Daza, J. M., & López, J. D. (2024). Quantifying and mitigating recorder-induced variability in ecological acoustic indices. *Ecological Informatics*, 82, 102668.
23. Eldesoky, A. H., Gil, J., Kindvall, O., Stavroulaki, I., Jonasson, L., Bennett, D., ... & Pont, M. B. (2025). A bird species occurrence dataset from passive audio recordings across dense urban areas in Gothenburg, Sweden. *Scientific Data*, 12(1), 1180.
24. Bick, I. A., Bakkestuen, V., Cretois, B., Hillier, B., Kålås, J. A., Pedersen, M., ... & Sethi, S. S. (2024). National-scale acoustic monitoring of avian biodiversity and phenology. *bioRxiv*, 2024-05.
25. Vidaña-Vila, E., Navarro, J., Stowell, D., & Alsina-Pagès, R. M. (2021). Multilabel acoustic event classification using real-world urban data and physical redundancy of sensors. *Sensors*, 21(22), 7470.
26. Durán-Paredes, C. A., Grijalba-Obando, J. A., Cajas-Ordóñez, S. A., & Sánchez-Ferreira, C. (2025). Urbanphony-3-CNN: A Convolutional Neural Network for Identifying the Urban Soundscape Taxonomy in Spectrograms Generated from Audios of Historic Cities. *Ingeniería e Investigación*, 45(2), e116327.
27. Wood, C. M., & Kahl, S. (2024). Guidelines for appropriate use of BirdNET scores and other detector outputs. *Journal of Ornithology*, 165(3), 777-782.

28. Tseng, S., Hodder, D. P., & Otter, K. A. (2025). Setting BirdNET confidence thresholds: species-specific vs. universal approaches. *Journal of Ornithology*, 1-13.
29. Navine, A. K., Denton, T., Weldy, M. J., & Hart, P. J. (2024). All thresholds barred: direct estimation of call density in bioacoustic data. *Frontiers in Bird Science*, 3, 1380636.
30. Marques, T. A., Thomas, L., Martin, S. W., Mellinger, D. K., Ward, J. A., Moretti, D. J., ... & Tyack, P. L. (2013). Estimating animal population density using passive acoustics. *Biological reviews*, 88(2), 287-309.
31. Darras, K. F., Rountree, R. A., Van Wilgenburg, S. L., Cord, A. F., Pitz, F., Chen, Y., ... & Mammides, C. (2025). Worldwide Soundscapes: a synthesis of passive acoustic monitoring across realms. *Global Ecology and Biogeography*, 34(5), e70021.
32. Bradfer-Lawrence, T., Duthie, B., Abrahams, C., Adam, M., Barnett, R. J., Beeston, A., ... & Froidevaux, J. S. (2025). The Acoustic Index User's Guide: A practical manual for defining, generating and understanding current and future acoustic indices. *Methods in Ecology and Evolution*, 16(6), 1040-1050.
33. Fairbrass, A. J., Rennert, P., Williams, C., Titheridge, H., & Jones, K. E. (2017). Biases of acoustic indices measuring biodiversity in urban areas. *Ecological Indicators*, 83, 169-177.
34. Zheng, H. W., Shen, G. Q., & Wang, H. (2014). A review of recent studies on sustainable urban renewal. *Habitat international*, 41, 272-279.
35. Lee, G. K., & Chan, E. H. (2008). The analytic hierarchy process (AHP) approach for assessment of urban renewal proposals. *Social indicators research*, 89(1), 155-168.
36. Chan, E. H., & Yung, E. H. (2004). Is the development control legal framework conducive to a sustainable dense urban development in Hong Kong?. *Habitat international*, 28(3), 409-426.
37. Vieillard, C., Vidal-Beaudet, L., Dagois, R., Lothode, M., Vade pied, F., Gontier, M., ... & Ouvrard, S. (2024). Impacts of soil de-sealing practices on urban land-uses, soil functions and ecosystem services in French cities. *Geoderma Regional*, 38, e00854.
38. Maienza, A., Ungaro, F., Baronti, S., Colzi, I., Giagnoni, L., Gonnelli, C., ... & Calzolari, C. (2021). Biological restoration of urban soils after de-sealing interventions. *Agriculture*, 11(3), 190.
39. Trono, A., & Zerbi, M.C. (2002) Milan: the city of constant renewal. *GeoJournal* 58(1):65–72
40. Municipality of Milan. (2025). *Piazze Aperte*. Retrieved January 29, 2026, from <https://www.comune.milano.it/aree-tematiche/quartieri/piano-quartieri/piazze-aperte>
41. Municipality of Milan. (2025). Mappa dei progetti di Rigenerazione urbana. Retrieved January 29, 2026, from <https://www.comune.milano.it/argomenti/rigenerazione-urbana/mappa-dei-progetti-di-rigenerazione-urbana>
42. Acoustic Indices for Biodiversity Assessment and Landscape Investigation, Jérôme Sueur, Almo Farina, Amandine Gasc, Nadia Pieretti and Sandrine Pavoine, *Acta Acustica* vol. 100 (Number 4), 2014, pp. 772-781

43. Pieretti, N., Farina, A., & Morri, D. (2011). A new methodology to infer the singing activity of an avian community: The Acoustic Complexity Index (ACI). *Ecological indicators*, 11(3), 868-873.
44. Boelman, N. T., Asner, G. P., Hart, P. J., & Martin, R. E. (2007). Multi-trophic invasion resistance in Hawaii: bioacoustics, field surveys, and airborne remote sensing. *Ecological Applications*, 17(8), 2137-2144.
45. Sueur, J., Pavoine, S., Hamerlynck, O., & Duvail, S. (2008). Rapid acoustic survey for biodiversity appraisal. *PloS one*, 3(12), e4065.
46. Quinn, C. A., Burns, P., Hakkenberg, C. R., Salas, L., Pasch, B., Goetz, S. J., & Clark, M. L. (2023). Soundscape components inform acoustic index patterns and refine estimates of bird species richness. *Frontiers in Remote Sensing*, 4, 1156837.
47. Eldridge, A., Guyot, P., Moscoso, P., Johnston, A., Eyre-Walker, Y., & Peck, M. (2018). Sounding out ecoacoustic metrics: Avian species richness is predicted by acoustic indices in temperate but not tropical habitats. *Ecological Indicators*, 95, 939-952.
48. Lawrence, B. T., Hornberg, J., Haselhoff, T., Sutcliffe, R., Ahmed, S., Moebus, S., & Gruehn, D. (2022). A widened array of metrics (WAM) approach to characterize the urban acoustic environment; a case comparison of urban mixed-use and forest. *Applied Acoustics*, 185, 108387.
49. Ulloa, J. S., Hauptert, S., Latorre, J. F., Aubin, T., & Sueur, J. (2021). Scikit-maad: An open-source and modular toolbox for quantitative soundscape analysis in python. *Methods in Ecology and Evolution*, 12(12), 2334-2340.
50. Guagliumi, G., Canedoli, C., Potenza, A., Zaffaroni-Caorsi, V., Benocci, R., Padoa-Schioppa, E., & Zambon, G. (2025). Unraveling Soundscape Dynamics: The Interaction Between Vegetation Structure and Acoustic Patterns. *Sustainability*, 17(9), 4204.
51. Guagliumi, G., Benocci, R., Angelini, F., Zaffaroni-Caorsi, V., & Potenza, A. (2024). Ottimizzazione dei parametri di calcolo degli indici eco-acustici: applicazione al Parco Regionale della Valle del Ticino. *Rivista italiana di acustica: 2, 2024*, 19-31.
52. Benocci, R., Potenza, A., Bisceglie, A., Roman, H. E., & Zambon, G. (2022). Mapping of the acoustic environment at an urban park in the city area of Milan, Italy, using very low-cost sensors. *Sensors*, 22(9), 3528.
53. Benocci, R., Afify, A., Potenza, A., Roman, H. E., & Zambon, G. (2023). Toward the Definition of a Soundscape Ranking Index (SRI) in an Urban Park Using Machine Learning Techniques. *Sensors*, 23(10), 4797.
54. Potenza, A., Vidana-Vila, E., Afify, A., Benocci, R., Alsina-Pages, R. M., & Zambon, G. (2025, June). Preliminary Results on Audio Event Classification Applied to a University Square in Milan (Italy) Before an Urban Regeneration Project. In *PROCEEDINGS OF FORUM ACUSTICUM* (pp. 2171-2178). European Acoustics Association.

55. Swaminathan, B., Jagadeesh, M., & Vairavasundaram, S. (2024). Multi-label classification for acoustic bird species detection using transfer learning approach. *Ecological Informatics*, *80*, 102471.
56. Kahl, S., Wood, C. M., Eibl, M., & Klinck, H. (2021). BirdNET: A deep learning solution for avian diversity monitoring. *Ecological Informatics*, *61*, 101236.
57. Pérez-Granados, C. (2023). BirdNET: applications, performance, pitfalls and future opportunities. *Ibis*, *165*(3), 1068-1075.
58. Abdi, H., & Williams, L. J. (2010). Principal component analysis. *Wiley interdisciplinary reviews: computational statistics*, *2*(4), 433-459.
59. Ward Jr, J. H. (1963). Hierarchical grouping to optimize an objective function. *Journal of the American statistical association*, *58*(301), 236-244.
60. Ja, H. (1979). A k-means clustering algorithm. *JR Stat. Soc. Ser. C-Appl. Stat.*, *28*, 100-108.
61. Kaufman, L. (1990). Rousseeuw, PJ: Finding Groups in Data: An Introduction to Cluster Analysis. *Applied Probability and Statistics, New York, Wiley Series in Probability and Mathematical Statistics*.
62. Benocci, R., Afify, A., Potenza, A., Roman, H. E., & Zambon, G. (2023). Self-consistent soundscape ranking index: the case of an urban park. *Sensors*, *23*(7), 3401.
63. Potenza, A., Zaffaroni-Caorsi, V., Benocci, R., Guagliumi, G., Fouani, J. M., Bisceglie, A., & Zambon, G. (2024). Biases in Ecoacoustics Analysis: A Protocol to Equalize Audio Recorders. *Sensors (Basel, Switzerland)*, *24*(14), 4642.
64. Kemp, J., Azofeifa-Solano, J. C., Barneche, D. R., Brooker, R., Arévalo, J. E., Erbe, C., & Parsons, M. (2025). Impact of acoustic index parameters on soundscape comparisons. *Methods in Ecology and Evolution*, *16*(5), 872-885.
65. Dröge, S., Fulgence, T. R., Osen, K., Rakotomalala, A. A. N. A., Raveloaritiana, E., Schwab, D., ... & Martin, D. A. (2024). Understanding acoustic indices as multi-taxa biodiversity and habitat quality indicators. *Ecological Indicators*, *169*, 112909.
66. Nieto-Mora, D. A., Rodriguez-Buritica, S., Rodriguez-Marin, P., Martínez-Vargaz, J. D., & Isaza-Narvaez, C. (2023). Systematic review of machine learning methods applied to ecoacoustics and soundscape monitoring. *Heliyon*, *9*(10).
67. Albornoz, E. M., Vignolo, L. D., Sarquis, J. A., & Leon, E. (2017). Automatic classification of Furnariidae species from the Paranaense Littoral region using speech-related features and machine learning. *Ecological informatics*, *38*, 39-49.
68. Brodie, S., Allen-Ankins, S., Towsey, M., Roe, P., & Schwarzkopf, L. (2020). Automated species identification of frog choruses in environmental recordings using acoustic indices. *Ecological Indicators*, *119*, 106852.
69. Serra, O. M., Martins, F. P. R., & Padovese, L. R. (2020). Active contour-based detection of estuarine dolphin whistles in spectrogram images. *Ecological Informatics*, *55*, 101036.

70. Trawicki, M. B. (2021). Multispecies discrimination of whales (cetaceans) using Hidden Markov Models (HMMS). *Ecological Informatics*, 61, 101223.
71. Brown, A., Garg, S., & Montgomery, J. (2019). Automatic rain and cicada chorus filtering of bird acoustic data. *Applied Soft Computing*, 81, 105501.
72. Ramli, D. A., & Jaafar, H. (2016). Peak finding algorithm to improve syllable segmentation for noisy bioacoustic sound signal. *Procedia Computer Science*, 96, 100-109.
73. Fairbairn, A. J., Burmeister, J. S., Weisser, W. W., & Meyer, S. T. (2025). BirdNET can be as good as experts for acoustic bird monitoring in a European city. *Plos one*, 20(9), e0330836.
74. Sethi, S. S., Bick, A., Chen, M. Y., Crouzeilles, R., Hillier, B. V., Lawson, J., ... & Banks-Leite, C. (2024). Large-scale avian vocalization detection delivers reliable global biodiversity insights. *Proceedings of the National Academy of Sciences*, 121(33), e2315933121.
75. Farina, A., & Salutari, P. (2016). Applying the ecoacoustic event detection and identification (EEDI) model to the analysis of acoustic complexity. *Journal of Mediterranean Ecology*, 14(14), 13-42.
76. Alcocer, I., Lima, H., Sugai, L. S. M., & Llusia, D. (2022). Acoustic indices as proxies for biodiversity: a meta-analysis. *Biological Reviews*, 97(6), 2209-2236.
77. Sethi, S. S., Bick, A., Ewers, R. M., Klinck, H., Ramesh, V., Tuanmu, M. N., & Coomes, D. A. (2023). Limits to the accurate and generalizable use of soundscapes to monitor biodiversity. *Nature Ecology & Evolution*, 7(9), 1373-1378.
78. Zaffaroni-Caorsi, V., Azzimonti, O., Potenza, A., Angelini, F., Grecchi, I., Brambilla, G., ... & Zambon, G. (2025). Exploring the soundscape in a university campus: Students' perceptions and eco-acoustic indices. *Sustainability*, 17(8), 3526.
79. Fu, W., Ran, C., Huang, J., Chen, Z., Fan, S., Fang, W., ... & Chen, Z. (2023). Can acoustic indices reflect the characteristics of public recreational behavioral in urban green spaces?. *Ecological Indicators*, 154, 110729.
80. Levik, A., Dobromyslov, I., Goretskaia, M., Matasov, V., & Filyushkina, A. (2025). Ecoacoustic methods application for urban biodiversity monitoring. *Urban Ecosystems*, 28(2), 4.

Thesis conclusions

Conclusions

Ecoacoustic studies have bloomed in the last twenty years across the globe, investigating the terrestrial and marine sonoscapes to answer questions about the acoustic world we live in, from quality assessment to biodiversity monitoring and anthropogenic impacts evaluation. These questions have been addressed through the development of ecoacoustic indices to summarize the acoustic information contained in field recordings, as well as machine learning tools to detect specific vocalizations. Nowadays, the ecoacoustic literature is debating the interpretability and reliability of ecoacoustic indices which still rely on aural or machine learning classification validation and behave differently according to the studies, methodology applied, ecosystem and climate region. This uncertainty translates in the lack of a common and standardized methodology even if steps ahead are being taken also thanks to international studies and the increase of connection in the community.

In this prolific and alive environment, urban settlements are understudied probably because of their tendential homogeneous structure and scarce faunal richness, presence of numerous anthropogenic impacts and various noise sources which increase the difficulty of studies due to signal overlaps and masking. However, the urban environment's richness in acoustic signals constitutes a thriving challenge and opportunity to test the robustness of techniques and methods.

Linked to the urban context, in the last decade cities and metropolises have carried out regeneration and renewal projects to address the increase in temperatures and frequent heatwaves by de-sealing and greening areas to reduce the heat island effect and offer climate refuges for the population. These actions can also improve the ecological connectivity between cities' green areas and rural core areas outside the urban matrices. These interventions could be monitored using ecoacoustics to assess possible improvements in biodiversity and in quality of the sonic environment, which could lead to a more diverse and richer sonoscape and pleasant soundscape for citizens.

In this thesis work, the urban regeneration of a university square in Milan has been studied using ecoacoustic indices, machine learning algorithms to classify sound sources and BirdNET to detect avian vocalizations. To quantify the quality of the new square's

sonoscape, it has been compared to the sonoscape of two green areas, the peri-urban Regional Park Parco Nord and the pocket park Vivarium-Bicocca.

A preliminary study regarded the equalization of audio files to linearize the frequency response of passive acoustic recorders. This procedure reduces biases in ecoacoustic indices which are introduced by sensitivity peaks and valleys along the frequency spectrum. Indeed, sensitivity changes are reflected in indices values which could be wrongly interpreted leading to erroneous conclusions. This bias could partially explain the incongruency in literature of studies predicting avian richness using ecoacoustic indices. Moreover, the use of different devices' models to compare sonoscape measuring sites (as discussed in Chapter 5) can be wrongly executed because of the devices' different frequency response which produce biases on the indices. This issue is also reflected in the results' comparison between research studies. Finally, non-equalization biases can potentially be present in machine learning studies or in the use of BirdNET and similar softwares that rely on external libraries. In fact, sensitivity peaks or valleys can distort the recording, potentially reducing the models' capacity of classifying sound events.

In the thesis, the equalization procedure developed and tested in Chapter 2 has been applied to all the next performed studies guaranteeing consistency throughout the research outline.

In Chapter 3 a preliminary study on the machine learning classification of the Piazza's sonoscape has been carried out. It defined the classification algorithm and input features used in the investigation of Piazza's sonoscape.

The complete investigation of Piazza della Scienza has been presented in Chapter 4. The use of seven ecoacoustic indices (ACI, ADI, AEI, H, DSC, ZCR, NP), machine learning classifier and BirdNET allowed for a comprehensive and complete sonoscape picture. A linear mixed-effects model was employed to address the effect of species richness, birds' and five sound classes' presence on ACI. During the analysis, the indices ADI, AEI, H and ZCR were carefully calculated, considering a dB_threshold value consistent with the Piazza's background noise, and introducing the minimum frequency for ADI and AEI and the maximum frequency for H and ZCR (which are absent in the R packages). The Random Forest classifier has been trained using 10-fold cross-validation and default hyperparameters values; precision, recall and F1-score were calculated to validate the

model. Finally, BirdNET parameters were tested to get the best precision and recall possible. The sonoscape of the post-operam Piazza resulted to be dissimilar to the ante-operam. In fact, it is more complex and acoustically variate, with a changed contribution of sound sources (such as speech, birds, insects and road traffic) and an increased avian richness and more temporal distributed vocalization rates. The linear-regression model confirmed the change in ACI after the intervention and a relationship between ACI and avian richness, birds' and human speech presence.

Finally, to understand the magnitude of these changes, the Piazza's sonoscape has been compared to the one of Parco Nord and Vivarium-Bicocca in Chapter 5. Five ecoacoustic indices were used (ACI, ADI, AEI, H, ZCR) alongside BirdNET; the dissimilarity index and non-parametric multidimensional scaling were computed. The same preprocessing on indices performed in Chapter 5 was carried out for these analyses. Different BirdNET settings were tested and the final set reflected the background noise and overlapping sounds difference between the areas. The results highlighted a high similarity between the post-operam square sonoscape and the urban parks' sonoscape. In particular, the Piazza measurement sites located on the ground floor and courtyards where the depaving and greening took place were similar to the parks' site while the sites located at the first floor of the buildings did not change. Indeed, the sonoscape of the first-floor sites is more influenced by the ventilation systems located on the building roofs, while they are less capable of acquiring the changed signals produced in the square. This finding is particularly interesting because no mitigation actions were taken on the ventilation systems during the regeneration project; nonetheless, modifications of land cover and public use patterns appear sufficient to improve the acoustic structure of the near sonic environment. From an urban regeneration perspective, it proves that relatively low-impact interventions, such as pigmentation removal, vegetation increases and changes in space usability, can significantly influence urban sonoscapes. In this perspective, ecoacoustics emerges not only as a monitoring tool, but also as a potential decision-support instrument for urban planning and climate adaptation policies, fostering an evidence-based dialogue between environmental science, urban design, and public governance.

To sum up, this thesis work produced a protocol to reduce the biases in ecoacoustic indices calculation, demonstrated the improvement of Piazza della Scienza sonoscape thanks to the MUSA regeneration project and the potential role of ecoacoustics as a tool for monitoring and evaluating the environmental effectiveness of urban regeneration actions.

While these results are inherently linked to a specific urban context and regeneration intervention, the proposed methodological framework is transferable and replicable across different urban environments, offering a scalable approach for ecoacoustic-based assessment of urban transformation processes.

These findings trigger new research lines, such as:

- A. Testing the efficacy of the equalization protocol in overcoming interpretative and correlational biases in ecoacoustics: in ecoacoustics, various studies are trying to use ecoacoustic indices as proxies for biodiversity; this protocol could help overcome some biases linked to the non-linear frequency response of the devices;
- B. Applying the thesis' methodology to assess the efficacy of other urban regeneration strategies and interventions;
- C. Investigate how ecoacoustics can contribute to the identification and characterization of urban quiet areas, another hot topic in the urban environment.

Finally, there is the hope of seeing integrated these and the other studies carried out during the thesis work with the ecoacoustics national and international community. By providing a structured and reproducible methodological framework, this work contributes to ongoing efforts to improve comparability, robustness, and interpretability in ecoacoustic research. Participation in initiatives such as the Worldwide Soundscapes project represents a concrete pathway to expand terrestrial soundscape knowledge. In parallel, the development of an Italian ecoacoustic network could foster methodological exchange, strengthen collaborations, and support ongoing efforts toward standardization, ultimately enhancing the role of ecoacoustics in the protection of both ecological and human acoustic wellbeing. In this perspective, ecoacoustics emerges not only as a monitoring tool, but also as a common language to connect ecological processes, urban transformation, and human experience of the acoustic environment.

Tesi di dottorato realizzata nell'ambito del progetto MUSA finanziato dal PNRR Missione 4
Componente 2 Investimento 1.5, finanziato dall'Unione Europea - NextGenerationEU - CUP
H43C22000550001